MANUFACTURING LOW-DENSITY PARTICLEBOARDS FROM WHEAT STRAW AND DISTILLER'S DRIED GRAINS WITH SOLUBLES

A Thesis
Submitted to the Graduate Faculty
of the
North Dakota State University
of Agriculture and Applied Science

By

Sagar Regmi

In Partial Fulfillment of the Requirements
for the Degree of
MASTER OF SCIENCE

Major Department:
Agricultural and Biosystems Engineering

April 2021

Fargo, North Dakota

North Dakota State University
Graduate School

Title

MANUFACTURING LOW-DENSITY PARTICLEBOARDS FROM WHEAT STRAW AND DISTILLER'S DRIED GRAINS WITH SOLUBLES

By

Sagar Regmi

The Supervisory Committee certifies that this ***disquisition*** complies with North Dakota State University's regulations and meets the accepted standards for the degree of

MASTER OF SCIENCE

SUPERVISORY COMMITTEE:

Dr. Nurun Nahar
Chair

Dr. Dilpreet Bajwa

Dr. Igathinathane Cannayen

Approved:

July 6, 2021
Date

Dr. Kenneth J. Hellevang
Department Chair

ABSTRACT

Agricultural byproducts like wheat straw and distillers dried grains with solubles (DDGS) have not found a good market in the wood composite industry. Utilizing DDGS for particleboard in addition to using it as feed will add economic value. This study investigated the potential of using DDGS and wheat straw at different proportions in low-density particleboard with phenol-formaldehyde binder. The effect of alkaline pretreatment of DDGS and wheat straw on the properties of board was also studied. Particleboards were tested for physical and mechanical properties, including density, water absorption, thickness swelling, flexural, internal bond, screw withdrawal, and hardness properties. Particleboards with 25% DDGS loading and 75% wheat straw met most of the mechanical properties requirement for low-density particleboards. Alkaline pretreatment did not improve the properties of manufactured particleboards. This study suggests that a higher fiber fraction DDGS and wheat straw can be used in low-density particleboards with reduced synthetic resins.

ACKNOWLEDGMENTS

I would like to acknowledge all the people who helped me during my MS at NDSU. Dr. Nurun Nahar, my advisor, always kept me motivated in my research. I also acknowledge my supervisory committee members Dr. Dilpreet Bajwa and Dr. Igathinathane Cannayen, for dedicating their time and patience to this research. I also like to thank Dr. Ewumbua Monono, and my lab peer Mr. Sanaul Huda for helping me to drive this project forward. I appreciate the assistance from undergraduate research assistant, Max Salzer. I like to thank Shashi Bhusan, Ph.D. student at ABEN, for helping me with the scanning of DDGS samples. I will also like to thank the NDSU center for writers, especially Andrew Taylor, for his assistance in improving my writing. I acknowledge Dr. Richard Horsley for his excellent Field Design class and SAS programming, which was useful for the statistical analysis of my research. I like to thank James Moos, maintenance mechanic from ABEN, for helping with machinery issues. Finally, I would like to thank the North Dakota Corn Council for financial support of this research.

TABLE OF CONTENTS

LIST OF TABLES

LIST OF FIGURES

LIST OF ABBREVIATIONS

CDS.....Condensed Distillers Solubles

Db.....Dry Basis

DDG.....Distillers Dried Grains

DDGS.....Distillers Dried Grain with Soluble

DOE .....Department of Energy

IB.....Internal Bond

LD .....Low Density

LE.....Linear Expansion

MDI.....Methylene Diphenyl Di-isocyanate

MOE.....Modulus of Elasticity

MOR .....Modulus of Rupture

NDF.....Neutral Detergent Fiber

PF .....Phenol Formaldehyde

PSD ……Particle Size Distribution

SW.....Screw Withdrawal

UF .....Urea Formaldehyde

USDA.....United States Department of Agriculture

WDG.....Wet Distiller's Grains

LIST OF SYMBOLS

S#20	Sieved DDGS with US sieve size 20
S#40	Sieved DDGS with US sieve size 40
SA#20 – H	Heavier fraction of the #20 sieved DDGS when aspirated through the air aspirator
SA#20 – L	Lighter fraction of the #20 sieved DDGS when aspirated through the air aspirator
SA#40 – H	Heavier fraction of the #40 sieved DDGS when aspirated through the air aspirator
SA#40 – L	Lighter fraction of the #40 sieved DDGS when aspirated through the air aspirator
Original DDGS	DDGS obtained from ethanol industry and NDF value of 44.56%
Fractionated DDGS	SA#20 – L" fraction DDGS with NDF value of 55.90%
Conwood	Control boards made from wood as filler and 6% PF (% solid)
Conwhst	Control boards made from wheat straw as filler and 6% PF (db)

LIST OF APPENDIX FIGURES

1. INTRODUCTION

Wood-based particleboards are the largest constituents of housing and furniture product. Overall, about 69.0% of the softwood lumber consumed in 2017 was used for housing (Howard and Liang, 2019). Increasing demand for wood, its associated cost, and the use of urea-formaldehyde (UF) or phenol-formaldehyde (PF) resins with potential health issues have resulted in the necessity of using renewable agricultural fibers to replace the wood particles in the particleboards industry. A recent growing tendency is observed toward reducing the density and increasing the thickness of particleboards for furniture manufacture which is applicable to door cores, sound absorption, and thermal insulation (Kawasaki and Kawai, 2006). Low-density particleboards are defined as a particleboard with a density of less than 640 kg/m^3 (ASTM, 2012). Using agricultural byproducts and agricultural residues as alternative materials to wood-based low-density particleboards can be a potential solution.

Particleboards developed from two or more components combine benefit using locally available feedstock and new product development with better properties. The use of wheat straw enables the particleboards production over a range of densities (200 to 800 kg/m^3) (Luo and Yang, 2010; Zhang et al., 2010) as compared to wood panels where panels with a density lower than 400 kg/m^3 are almost impossible (Boquillon et al., 2004). Wheat is the second most cultivated plant in the world for agriculture production, and hence wheat straw is one of the widely available lignocellulosic materials in the world. Currently, wheat straw is not used as efficiently as possible (Palmieri et al., 2017). Burning fuel, cattle feed, mulch, and bedding materials for animals are common uses of wheat straw. Wheat straw contains cellulose, hemicellulose, and lignin, making it suitable for manufacturing lingo-cellulosic particleboards (Karr et al., 2000; Kundu et al., 2014; Rowell et al., 1995; Wang and Sun, 2002).

The steady increase in corn-based ethanol fuel production has dramatically increased the supply of its major co-product known as distiller's dried grain with soluble (DDGS). In a typical dry-grind ethanol production plant, approximately one-third of ethanol, one-third of carbon dioxide, and one-third of DDGS are obtained from every kilogram of corn processed (Chatzifragkou et al., 2015; Cheesbrough et al., 2008; CIGI, 2013; Davis, 2001). The amount of DDGS produced is steadily increasing since 1990, with 44 million tons of DDGS generated in the USA in 2019 (Council, 2021). The majority of DDGS is utilized as animal feed, though the high fiber content of DDGS limits its uses mainly for ruminants. However, any biorefinery's economic viability depends on the effective use of all the components by attaining a profitable revenue. Therefore, finding other avenues to use DDGS or making value-added products from DDGS would benefit the ethanol industry.

There have been recent efforts to utilize DDGS as a feedstock to produce value-added products. Fractionation of DDGS into high protein and high fiber to enhance the value of DDGS has been investigated by Srinivasan et al., (2005) that could contribute to an additional economic benefit (Srinivasan et al., 2006). DDGS were fractionated using an aspiration process into two categories: one with higher protein and low fiber fraction and the other with higher neutral detergent fiber (NDF) content (Srinivasan et al., 2005). Higher protein and lower fiber fraction will have a greater value as feed for non-ruminants (swine, poultry, and fish), or could be a potential source for additional oil extraction (Srinivasan et al., 2009). On the other hand, a high fiber fraction can be converted to fermentable sugar or the potential to be used in manufacturing composite materials, thus making bio-refineries competitive and sustainable.

The fibers extracted from DDGS and corn grain have shown promising potential as a filler in polymer composites (Julson et al., 2004). DDGS can act as both filler and natural

adhesive because of the adhesive nature of zein protein, which constitutes about 30-40% of corn protein (Shukla and Cheryan, 2001). The adhesive properties of DDGS can be increased by denaturation of the native protein (Rowell, 2012). Zein protein from DDGS has been used as a multifunctional binder in low-density particleboards (Sundquist and Bajwa, 2016). Besides, the zein protein of the DDGS can decouple and react with the resin increasing mechanical properties. DDGS has been used recently as a multifunctional filler in synthetic resin bonded wood particleboards to improve their physical and mechanical properties (Sundquist and Bajwa, 2016).

Resin plays an important role in the properties of particleboards. High formaldehyde emission and their associated health issues have led manufacturers to look for alternatives to reduce formaldehyde usage. The drive to lower emissions has influenced research into alternative binders, including natural proteins. Current research shows that plant proteins can be a useful supplement or replacement to petroleum-based resins (Mo et al., 2001). Though there have been several studies on the application of DDGS, both as a natural adhesive and filler material on particleboards (Liaw et al., 2019; Sundquist and Bajwa, 2016; Tatara et al., 2007, 2009), to our knowledge, there was no study on the combined application of DDGS and wheat straw on low-density particleboards. Also, there has been no research in applying high fiber fraction of DDGS on making low-density particleboards.

1.1. Objectives

Previous studies on lignocellulosic panels investigated the potential of single crop residue. This research aimed to integrate DDGS and wheat straw into the manufacturing of particleboards as both DDGS fiber and wheat straw have shown potential in particleboard processing. The objective of this research is to optimize the amount of DDGS fiber to be mixed

with wheat straw for the manufacturing of low-density particleboards. It is hypothesized that the DDGS contain fiber and protein molecules suitable for binding; therefore, a high proportion of DDGS fibers can be used as functional material in composites. The specific objectives of this research are:

1. To simplify the elusieve process for fractionation of DDGS to separate DDGS into two fractions - one with higher protein content and another with higher NDF content,
2. To compare the physical and mechanical properties of the particleboards made from fractionated DDGS to that from original DDGS,
3. To study the effect of alkaline pretreatment of DDGS and wheat straw on the properties of particleboards,
4. To find the economic viability of making boards with DDGS and wheat straw.

2. LITERATURE REVIEW

This chapter discusses the basic definitions and terms related to corn and dried distillers' grains with solubles (DDGS), wheat straw, productboard manufacturing, and attempts to replace synthetic resins with natural protein fiber from agricultural residues. Some background information about corn-based DDGS, their fiber extraction process is presented. Research regarding DDGS, DDGS fiber, and wheat straw in particleboard production is also presented and discussed.

2.1. Composition panels

Composition panels are defined as a structural and decorative panels of variable density, and they are made from lignocellulosic particles (usually wood) and synthetic resins. Heating the cellulosic fibers with resin under high heat and pressure results in productboards. Productboards are traditionally produced from wood chips and wood flour, but all the composite panels made from any lignocellulosic materials from plants fall under productboards. These productboards are generally categorized into two broad categories of fiberboards and particleboards. While fiberboards are made from the fibrous portion of the woody materials, specific lignocellulosic particles or pieces define particleboards. Both fiberboards and particleboards require additional bonding agents to provide the required bond strength. They are further classified based on particle size and density.

2.1.1. Classification and usage of particleboards

Manufacturing of particleboards started around 1950 after the production companies started producing lumber and plywood using industrial wood residues (Puettmann et al., 2013). To satisfy the increasing wood demand, wood-based board product such as fiberboards are being employed which is manufactured under temperature and pressure using wood or other

lignocellulosic materials and binders. Depending upon density, fiberboards are further classified as particleboards (PB), medium density fiberboard (MDF), hardboard (HB), and oriented strand boards (OSB) (Hemmilä et al., 2017). Those with a density greater than 800 kg/m^3 are called hardboard. Fiberboard with a density of less than 640 kg/m^3 are low-density particleboards. Medium-density fiberboards are those having density in between high and low-density fiberboard. Low-density particleboards are commonly used for door cores. The properties requirement for the high, medium and low density particleboards are defined in ANSI standard A208.1-2009 update. Table 2.1 shows the selected minimum requirements of particleboards for different physical and mechanical properties.

Table 2.1: Properties of the selected particleboard grades from ANSI A208.1-2009

Density classification	Grade	Physical and mechanical properties				
		Modulus of rupture (MPa)	Modulus of elasticity (MPa)	Internal bond (MPa)	Screw withdrawal (N)	Linear expansion (max. %)
High density	H-1	14.90	2160	0.81	1600	N/A
	H-2	18.50	2160	0.81	1700	N/A
	H-3	21.10	2475	0.90	1800	N/A
Medium density	M-0	7.60	1380	0.31	N/A	N/A
	M-1	10.00	1550	0.36	N/A	0.40
	M-S	11.00	1700	0.36	800	0.40
Low density	LD-1	2.80	500	0.10	360	0.40
	LD-2	2.80	500	0.14	520	0.40

The American National Standards Institute (ANSI) maintains the standards for the particleboards. The standard's physical and mechanical properties are the modulus of rupture, modulus of elasticity, internal bond, hardness, screw withdrawal, and linear expansion properties.

2.1.2. Common binders used in particleboard industry

Particleboard manufacturing involves the utilization of filler or resin, which act as adhesive. Generally, there are three types of synthetic resins used in wood-based boards: urea-

formaldehyde (UF), phenol-formaldehyde (PF), and methylene diphenyl di-isocyanate (MDI). UF resins are utilized where low moisture exposure is possible since the cured resin degrades in a moist environment. Therefore, UF resin is usually applied in interior furniture and other similar products. For outdoor and bathroom applications, where there is excessive moisture, PF and MDI are commonly used. PF and MDI cost substantially greater than UF resins.

Formaldehyde has a carcinogenic effect and can also cause respiratory problems or cancer at low doses. Even though MDI is less toxic than formaldehyde, it is hazardous to workers and can cause respiratory issues. Because of health and sustainability issues, research has been shifted to find alternative fillers that can act as a natural binder. There has been a great surge from both academic institutions as well as by the composite industries to include natural fibers in place of synthetic fibers in polymer composites. The United States Department of Agriculture (USDA) and the Department of Energy (DOE) have set targets of having at least 10% of all basic chemical building blocks be created from renewable and plant-based sources in 2020 and increasing this contribution to 50% by 2050 (Mohanty et al., 2005). Soy flour and corn are renewable resource materials that could work as binders as alternative resin (Sundquist and Bajwa, 2016).

2.2. Natural fibers

There are two types of plants known as primary and secondary plants based on their utilization. Primary plants are grown for their fiber, which includes jute, hemp, kenaf, and sisal. Secondary plants are plants from which the fibers are produced as a byproduct. Examples of secondary plants are pineapple, oil palm, and coir. Fibers could be obtained from woody or non-woody plants. The plant fibers from non-woody plants can be categorized into six types which are bast fibers, leaf fibers, seed fibers, core fibers, grass, and reed fibers.

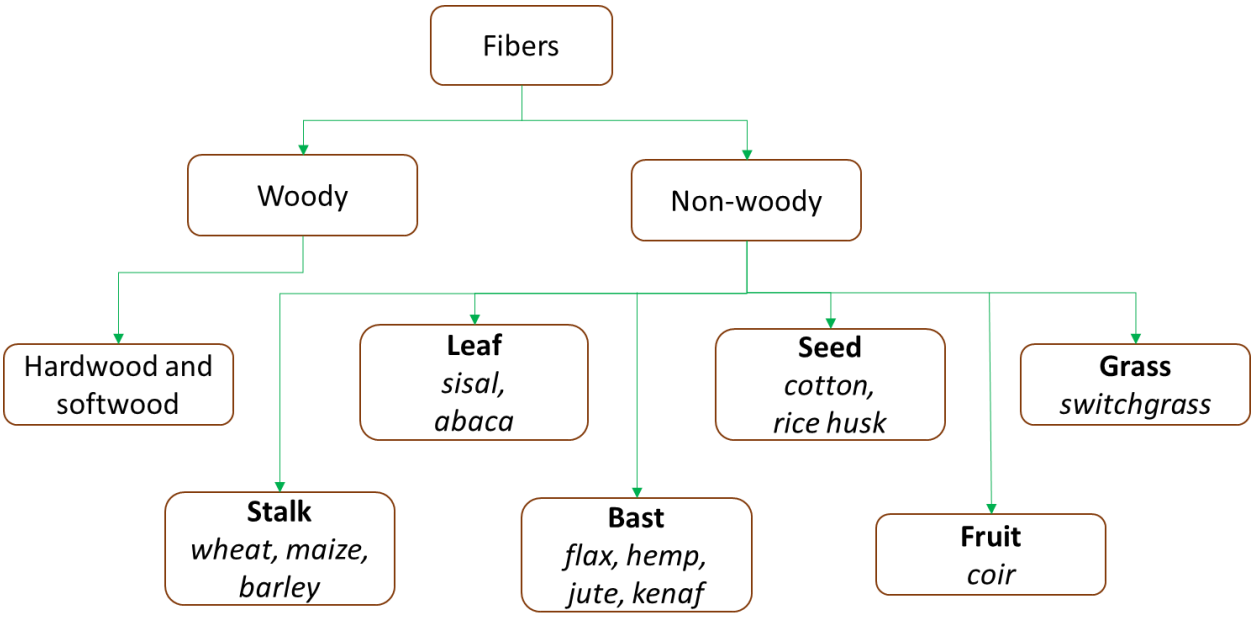

Figure 2.1: Different types of plant-based natural fibers
Adapted from (Biagiotti et al., 2004)

2.3. Corn production and corn kernel structure

In the US, corn grain is used both as a renewable feedstock for ethanol production as well as a major feed for animals. With 96,000,000 acres of land used for corn production, the US is the world's largest corn producer. In 2018, corn for grain production was estimated to be 14.4 billion bushels (USDA-NASS, 2019). In the transition from petroleum fuel to alternative fuel, the world is now shifting towards ethanol as an alternative fuel. The US has the largest contribution in ethanol production; in 2018, USA alone produced 16.06 billion gallons of ethanol, which is 56% of global ethanol production (RFA, 2019). Since ethanol production in the US is mainly from corn using dry or wet grind and fermentation plants, it has been a serious concern for utilizing corn by-products and their value addition.

Corn grain is a major feed source of livestock, swine, and poultry industries due to its high starch content (~70%). The fiber in corn is not easily digested by non-ruminants such as

poultry and swine. Also, during the corn ethanol production, only the starch fraction is utilized by the enzymes with fiber fraction remain unused.

2.3.1. Corn kernel structure

It is necessary to understand the structure of corn kernels because different kernel components have a differing composition of protein, starch, and fiber, which determines the physical and mechanical properties of manufactured particleboards. The corn kernel consists of three major components: the endosperm, hull, and germ, depicted in Figure 2.2. Each component has various concentrations of protein, fat, starch, and cellulose. The majority of the kernel is endosperm which contains high concentrations of protein and starch. The germ is comprised majorly of lipids and proteins, while cellulose and hemi-cellulose fibers comprise the hull of the kernel. Lignin is found throughout the kernel as it acts as a binding agent. There is a prolamine protein found in the endosperm region of the corn kernel called as zein. Zein contributes to about 45 to 50 percent of protein in corn (Shukla and Cheryan, 2001). Zein has been proved as a natural adhesive in different applications. This zein property makes it possible to use composite materials for better adhesion between fiber and matrix.

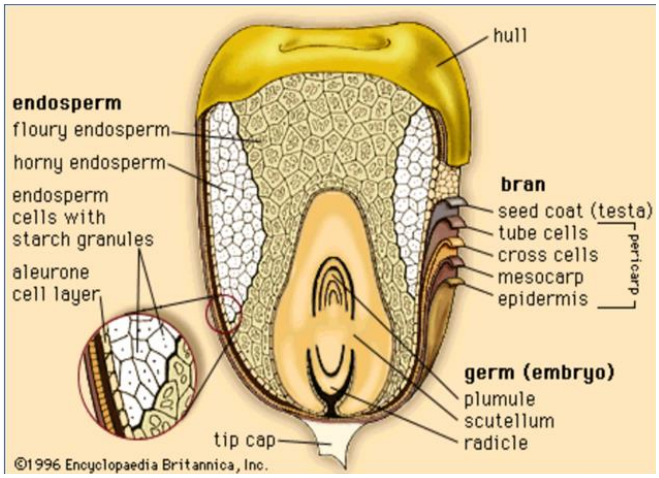

Figure 2.2: Corn kernel structure

2.4. DDGS as a byproduct of the ethanol industry

There are two different types of processing methods used in the production of ethanol: dry and wet. A general overview of the dry-grind ethanol process is illustrated in Figure 2.3.

Corn kernels are initially ground to expose the starch-containing endosperm. The ground corn is then cooked and fermented. During the fermentation process, starch is converted into ethanol and carbon dioxide.

$$C_6H_{12}O_6 \text{ (Starch)} \longrightarrow 2C_6H_5OH \text{ (Ethanol)} + 2CO_2 \text{ (Carbon dioxide)} \quad (1)$$

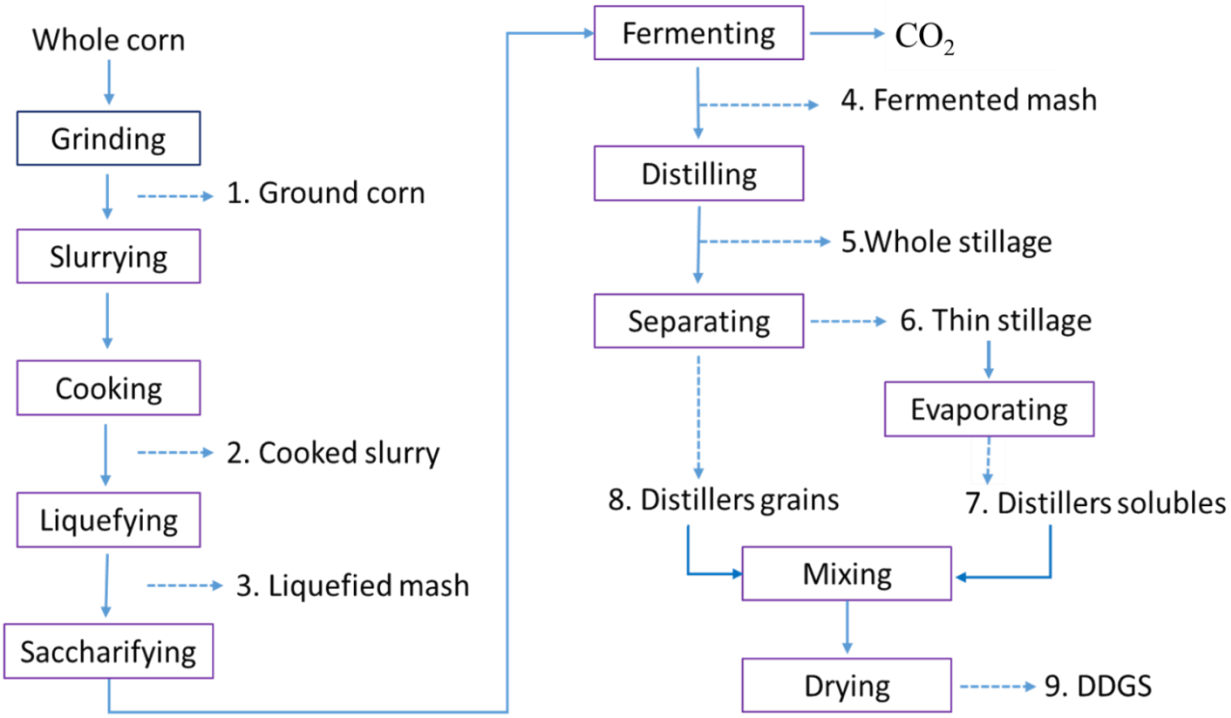

Figure 2.3: Different steps involved in the dry-grind ethanol process
Adapted from (Liu and Rosentrater, 2012)

After ethanol is distilled from the slurry, the remaining proteins, fats, and cellulosic materials are dried to form DDGS. The high protein, fat, and fiber contents in DDGS make this material a suitable animal feed and promising material as an alternative cellulosic material for particleboards. The corn ethanol production has seen a steady increase in the last few decades to 16.06 billion gallons of ethanol in 2018 (RFA, 2019). More than 90% of the corn ethanol

industries currently employ some variation of the dry grind process for ethanol production. The dry-grind ethanol process differs from the corn wet milling process, as it lacks the steeping step at the front end. Also, it uses little or no fractionation of the corn kernel components before saccharification of the starch and fermentation (Krueger et al., 1976). In this process, the whole grain is ground by a hammer mill into a coarse powder with a mean diameter of 1 mm. In the next step, the milled corn is liquefied with the addition of enzyme, followed by a saccharification step, where starch in corn is converted into simple sugars. These sugars are next fermented by yeast cells. The unfermented residuals from corn grain flour pass through a stripper where ethanol is recovered. The portion left after separating ethanol is called whole stillage. The whole stillage consists of fiber, oil, protein, other unfermented grains and yeast cells. The whole stillage is centrifuged to produce a liquid fraction called thin stillage and a solid fraction known as wet distiller's grain (WDG). A part of thin stillage is recycled to slurry the ground grain. The remaining thin stillage is concentrated through multiple-effect evaporators to produce a syrup called condensed distiller's solubles (CDS). The WDG is dried to obtain the distiller's dried grain (DDG). When CDS is mixed with WDG and dried, it is called distiller's dried grain with solubles (DDGS). The dry solid residue remaining after ethanol production is known as the DDGS.

DDGS is the coproduct of fuel ethanol production from corn, wheat, sorghum, and other cereal grains using the dry grind process. In the dry grind process, the starch in the cereal grains is converted to ethanol and the remaining components, which are protein, fiber, fat and ash, end up in DDGS. DDGS is a solid and has a color range of golden yellow to brown. Roughly for every bushel (25.4 Kg) of corn processed, 8.16 kg of DDGS and 11 liters of ethanol are produced (Davis, 2001). DDGS is mainly used as cattle feed, and because of its high fiber content, it is

also used at low inclusion levels in poultry and swine diets (Shurson, 2018). Since the ethanol plants are still in a low-profit margin, additional revenue from co-products is becoming more critical.

Currently, the majority of DDGS is utilized as feedstock. With the increasing production of DDGS, other markets have been explored so that the value of DDGS will not diminish. The residues from the corn-to-ethanol production process contain high fiber levels; they may be compatible with incorporation into polymers, which is an option that can gain good economic returns. The fiber component in DDGS is not easily digestible by poultry and swine. The separation of fiber makes the DDGS amenable to the non-ruminants and increases its nutritional characteristics due to higher protein and oil contents. Research has been done to separate fiber from DDGS to create different products for increasing economic values. DDGS with high protein and fat content can be fed to non-ruminant animals or used for extracting additional oil, a more value-added product. On the other hand, high fiber content can have different applications (Singh et al., 2001; Srinivasan et al., 2005).

DDGS fiber separation could result in different applications for both the high fiber and high protein fraction. However, removing fiber from DDGS using air aspiration alone resulted in limited success because fiber content was only slightly enriched in the aspirated DDGS fraction compared to the residual DDGS fractions. The reduction in fiber content of the residual DDGS is not large enough to make it a practical feedstuff for non– ruminants because the fiber levels are significantly above the levels typically found in non–ruminant diets (Singh et al., 2001). The separation of DDGS into two fractions, one with higher fiber content (eleusieved DDGS) and the other with high protein and fat content (enhanced DDGS) was effectively done by Srinivasan et al. (Srinivasan et al., 2005). Their method called ‘elusieved method’, a combination of sieving

and elutriation, was also used to separate fiber from DDG. When DDG is separated using elutriation followed by sieving, the amount of elusieved fiber and enhanced DDG were respectively 11.9% and 88.1% (Srinivasan et al., 2008). DDGS fiber separation has been proved economically feasible for both lab and pilot-scale manufacturing with a payback period of only 1.4 years (Srinivasan et al., 2009). Implementing elusieve process in 2030 metric tonnes/day, requires total capital investment to be $1.4M; the increase in revenue due to products from the process would be $0.4-0.7M/year, and the payback period would be 2.5-4.6 years (Srinivasan et al., 2006). These fibers can act as a natural filler in low-density particleboards.

2.4.1. Separation of DDGS fibers

DDGS contains various complex organic macromolecules, such as carbohydrates, proteins, and oils. Individual DDGS particles differ significantly in their chemical composition, shape, size, and density (Bhadra et al., 2009). To separate DDGS fibers, different experiments have been done with various methods of dry fractionation, including dry milling accompanied by sieving (Wu and Stringfellow, 1982), air aspiration (Singh et al., 2002), sieving alone (Liu, 2008), and a combination of sieving and elutriation (Srinivasan et al., 2005). All of the above methods have had their limitations. Some of these did not get improved nutrients, while others had to use complicated equipment. The elutriation or aspiration process was used to separate fiber fraction from DDGS (Srinivasan et al., 2008). DDGS particles under upward air-flow are separated with combined effects of density, shape, and size characteristics in this process. When a particle falls, it experiences a downward gravitational force balanced by the upward drag and buoyancy force known as its terminal velocity (Srinivasan et al., 2005). The air velocity must be greater than the terminal velocity of the DDGS fraction and lower than the terminal velocity of non-fiber fractions to separate the fiber fraction. The flat shape of DDGS fiber combined with

low mass would experience higher drag force, thus possessing lower terminal velocity than less flat non-fiber DDGS fraction (Srinivasan et al., 2008). The drawback of this process is that the less dense and bigger DDGS fiber particles can be easily mixed with more dense and smaller non-fiber particles under air-flow. To overcome this problem, a sieving step DDGS was added to the existing elutriation process.

By sieving DDGS into different sieve fractions and air classifying these sieve fractions separately, the mixing of small-sized non-fiber can be effectively eliminated. The DDGS particles are first sieved into four to five sieving fractions. Each fraction is elutriated to collect DDGS fibers except for the smallest sieve fraction with lower fiber and higher protein and oil contents. The combination of elutriation and sieving is known as elusieve (Figure 2.4) (Srinivasan et al., 2009). The elusieve method used on DDGS results in two products- DDGS fraction with enhanced oil and protein content, and elusieve fiber. The elusieved DDGS with increased protein and oil content and lower fiber has several advantages to offer such as improved digestibility in non-ruminants and increased nutritional value.

Elusieved DDGS fraction can be worth $5-20 per ton more than DDGS with lower fat and protein content (Srinivasan et al., 2005). Economic analysis for employing elusieve process for fiber separation in the dry-grind ethanol plant processing corn at 2030 metric tonnes/day estimated the payback period of 1.1 year (Srinivasan et al., 2009). The capital investment in this process was low due to simple equipment, sifters, and aspirators.

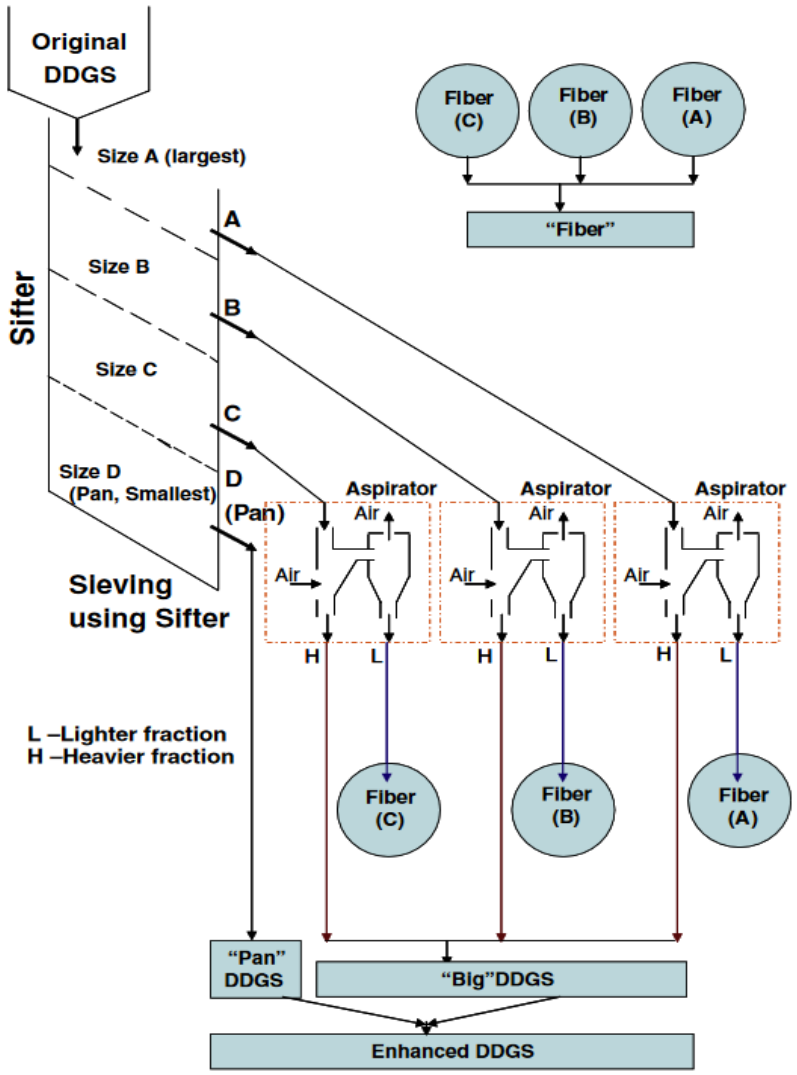

Figure 2.4: Schematic of elusieve processing
Source: (Srinivasan et al., 2009)

2.5. Processing effects and alternative resins for particleboards

Due to the large demand for wood products, many improvements and modifications of these products can occur. Wood and wood-based particles have been in long use to manufacture medium and high-density particleboards. It is theorized that the current wood usage comprises only four percent of the theoretical amount of products that can be formed from lignocellulosic materials (Maloney, 1977). Almost all wood-based fiberboards use synthetic resins for the bonding of particles. In recent years, biocomposites that use agricultural fibers as fillers or

reinforcement have gained attention as they add value to agriculture and use a renewable source of fiber (Thakur et al., 2013). These composites are light in weight, easy to process, have comparable specific properties with synthetic composites, and cost-effective. Current research not only focuses on the replacement of synthetic adhesive by natural adhesive but also on the reduction/replacement of wood by other binders. Efforts have been made to use DDGS and DDGS fiber as a natural binder along with wood flour. Agricultural residual fibers such as corn pith, plant stalk, and straw have been considered as alternative renewable sources for particleboard manufacturing. Various studies have been done on particleboards utilizing agricultural fiber, which include wheat straw (Tabarsa et al., 2011), kenaf core (Xu et al., 2006), sugar cane bagasse (Widyorini et al., 2005), rice husk (Melo et al., 2014) and more. Only a few research is available on low-density straw particleboards, which may have the potential for application in door core. Current research into the improvement of lignocellulosic boards focuses on how alternative lignocellulosic materials and the processing affect the mechanical properties.

2.5.1. Effects of different processing parameters

Several processing parameters have been identified with the implementation of alternative lignocellulosic materials that affect the mechanical properties. Among these, three parameters that are considered necessary include the pressing condition (press time and press temperature), particle drying, and particle size.

2.5.1.1. Press condition

Pressing time affects the strength of the binders. A shortened press time results in an insufficiently cured binder due to the limited heat penetration (Tabarsa et al., 2011), thus lowering the board's internal bond strength. An increased press time has also been shown to

negatively affect the tensile strength and bending strength of the synthetic resin-free or binderless boards due to the degradation of the strength-bearing fibers (Xu et al., 2006).

The press temperature also affects the properties of the panels. It has been shown that the various lignocellulosic binders' properties are temperature-dependent and characteristic of each binder (Khosravi et al., 2010). An increase in press temperature has been shown to improve binderless boards' water absorption properties (Ando and Sato, 2009) and reduce the required press time. The effect of temperature on dimensional and mechanical properties of wheat straw particleboards was found to significantly affect the strawboard dimensional stability than on mechanical properties (Karr et al., 2000). In addition to the press temperature, steam pressing will improve binderless boards' mechanical properties when compared simply to dry hot pressing (Widyorini et al., 2005). The addition of moisture increases the heat transfer and the hydrogen bonding between proteins (Xu et al., 2006). Rowell et al., (1995) studied the effect of pretreatment of aspen on properties of particleboards; three treatments were applied: untreated, steam treated, and acetylated boards. It was found that treatments have no effect or sometimes even reduced the MOE, MOR, and internal bond strength values as compared to untreated samples. This might be probably because of the breaking of lignin which holds the fibers together (Rowell et al., 1995).

2.5.1.2. Particle drying

Raw material should be sufficiently dry before starting the particleboard manufacturing. Particle drying is important as it improves the panels' mechanical properties compared to green particles (Khosravi et al., 2010). Some moisture is useful to the curing process as it increases the heat transfer, as observed in the addition of steam to the hot pressing (Widyorini et al., 2005; Xu et al., 2006). The drying temperature is also an important processing parameter. Increasing the

drying temperature increases the degradation of the hemicellulose content (Sari et al., 2013). The degradation of hemicellulose decreases the degree of polymerization that can be achieved, thus reducing the board's mechanical properties (Christiansen, 1991).

2.5.1.3. Particle size

The reduction of particle size largely influences the tensile strength, toughness, and stiffness (Fu et al., 2008). This effect is caused by the increase of the particle's surface area, improving the load transfer between the matrix and the fiber (Arzt, 1998; Fu et al., 2008). The increase in the surface area also increases the adhesion of the particles. The increase in the surface area creates more exposed functional groups on protein, lignin, and hemicellulose, thus improving board's bonding (Ando and Sato, 2009). The reduction of particle size with differing lignocellulosic fillers produces different properties because of chemical composition variations (Julson et al., 2004). The smaller size of particles helps in the dispersion of particles in particleboards. Well-dispersed particles also improve the adhesion of alternative binders. Liquid dispersions of proteins due to polymerization caused during hot pressing have exhibited better properties than a dry mixture of the same particle size. While studying the influence of particle size of wheat straw on mechanical properties of particle panels it was found that although modulus of elasticity (MOE) decreased from 3200 to 2600 MPa, when the size of wheat straw was reduced from 20 mm to 2 mm, the thermal swelling (TS) decreased from 25% to 15%, and internal bonding (IB) increased from 0.42 to 0.81 MPa. However, the MOR remained unchanged and the decrease of MOE was due to the decline of finer-form factor (length/diameter ratio) (Boquillon et al., 2004). It is assumed that a decrease in particle size causes an increase of contact surface area between the resin and wheat straw particle. Measurement of particle size and particle size distribution (PSD) is important to understand the relationship between particle size

and mechanical properties of particleboards. Particle size, PSD, and shape of particles are important parameters for many industrial processes because the chemical, optical, and mechanical properties and the mixing behavior of particles are affected by size and shape (Harr, 1977). Due to limited sieve availability, sieves fabrication limitations, and particle flow behavior in restricted space, mechanical sieving cannot classify very fine particles into many groups. The machine vision method to calculate PSD using ∑Volume approach eliminates these limitations (Igathinathane et al., 2012).

Liu (2008) found that it can be highly feasible to fractionate DDGS for compositional enrichment based on particle size. PSD of DDGS can be a quality parameter for measurement because the extent of PSD can serve as an index for potential of DDGS fractionation (Liu, 2008). An inexpensive machine vision approach was used by Igathinathane et al. (2012) for reliable and accurate measurement of particle size and PSD. Particle size is an important physical property of DDGS because particle size will influence the other physical properties such as the bulk density, angle of repose, compressibility, heat transfer characteristics, and flow-ability properties of DDGS (Bhadra et al., 2009). Generally, the particle size of DDGS ranges from less than 0.1 mm to more than 2 mm in diameter (Bhadra et al., 2009).

2.5.2. Alternative resins for particleboard manufacturing

Common binders used in the manufacturing of particleboards are urea-formaldehyde (UF), melamine formaldehyde (MF), phenol formaldehyde, or isocyanate based resins (Maloney, 1977). The cost and the health hazards of these resins create the fundamental drive to find renewable alternative resins. In the past, natural protein-based resins have been used to produce lignocellulosic materials. Current research shows that plant proteins can be an effective supplement or replacement to petroleum-based resins. Soy-protein-based resins have been

commonly used as a natural resin for particleboards in the past (Taylor & Francis Group, 2003). Besides soy protein, wheat gluten and cotton-seed protein can be used as an effective alternative in particleboards (Khosravi et al., 2010). Corn proteins are commonly used as an extension in resins. Corn protein extract and corn starch based binders have exhibited superior properties compared with commercially available alternatives (Ando and Sato, 2010; Moubarik et al., 2010). Corn meal extended PF resins exhibit properties suitable for plywood and fiberboards. Pure corn-based binders have also been developed. Zein has been used as the sole binder in biopolymer composites (Kim et al., 2010). Corn gluten meal has exhibited thermoplastic properties due to strong protein interactions, which have been utilized to produce wood-based composites (Beg et al., 2005).

Other forms of protein have also been investigated, including blood meal and peanut flour. The blood meal and peanut-based binders meet the exterior and interior MDF boards requirements, respectively (Yang et al., 2006). The effectiveness of these alternative resins is mainly dependent upon the plant's chemical composition affecting the adhesion in wood-based products (Khosravi et al., 2010; Nordqvist et al., 2013). The DDGS with higher protein and oil content attracts $5-20 more per ton because of the added nutritional value compared to the unprocessed DDGS containing hull fiber (Belyea et al., 2004b). The benefits of DDGS without the hull fiber include increased weight gain in birds, and a larger portion of the feed can be supplemented by elusieved DDGS (Amezcua et al., 2007). The hull fibers extracted from DDGS and corn grain have shown promising potential as a filler in polymer composites (Julson et al., 2004). DDGS fiber is a good fiber filler for outdoor applications where the material will be subjected to UV weathering (Pandey et al., 2017), and it has a low cost of 8-13 cents per kilogram, which is relatively cheaper than wood fibers and starch (Li and Sun, 2011).

All types of cellulosic fibers can be used as reinforcement or filler in plastics, including flax, hemp, jute, straw, wood fiber, rice husks, wheat barley, oats, rye, grass, kenaf, sisal, hyacinth, banana fiber, and pineapple leaf fiber (Belyea et al., 2004a). The main advantages of using lignocellulosic fibers are that they are neutral sources causing less net emission of carbon dioxide back to the environment at disposal, readily available at a much lower cost than synthetic fiber, and can be recycled easily. Though synthetic fibers have found extensive usage in composite materials for a long time, their severe environmental effects cannot be ignored. The lignocellulosic fibers are renewable, widespread, and readily available in comparison to glass or carbon fibers (Belyea et al., 2004b).

2.5.3. Binderless boards

Research has also been performed to replace the petroleum-based resin completely. Starch has been used to create a binder for medium-density fiberboards (Abbott et al., 2012). Lignocellulosic materials have also been used to produce binderless boards. Sugi-heart and sapwood have also been used to produce binderless boards in Japan (Ando and Sato, 2010). Kenaf core-powder-based binderless boards are currently being developed with further research focused on improving the water absorption properties (Ando and Sato, 2009; Xu et al., 2006). Bagasse, the remnant of sugarcane processing, is one of the most promising lignocellulosic materials (Widyorini et al., 2005). The bagasse-based binderless particleboards perform similarly to their resin-based counterparts (Nonaka et al., 2013). The various attempts at creating binderless boards show the potential of using the functional chemical components of plants as binders. Still, future research needs to be performed to improve the water absorption of the binderless boards. Various types of lignocellulosic materials can be combined with wood for a mixture of new properties. Post-processed lignocellulosic materials are in abundance and have

great potential to be supplemented into particleboards. Bagasse and hemp have been supplemented up to 50 wt. % and either outperform the reference wood particleboards or meet the standard properties (Nikvash et al., 2010). Canola particles also exhibit adequate properties up to 30 wt. % loading (Nikvash et al., 2010). DDGS is an additional lignocellulosic waste material that may have potential for use in particleboards. In a comparative study between wheat straw and soy straw fiberboards, it was found that wheat straw fiberboards have better mechanical and physical properties than soy straw fiberboards (Sitz, 2016).

2.6. DDGS in particleboard production

This section considers the properties of the DDGS and discusses relevant research involving DDGS as a filler for composites. The properties of DDGS vary due to how it is processed and the growing conditions of the harvested year (Liu and Rosentrater, 2012). The particle size of the DDGS is an important classification of the grains. The particle sizes vary greatly depending upon the processing but the distribution generally falls between 0.1 and 4 mm, with the majority of the particles approximately 0.5 mm in diameter (Liu, 2008). The structure of how the protein, fats, and carbohydrates arrange themselves in the individual particles affects how the material can bond with itself.

As previously discussed, corn protein shows promise as an alternative resin. Minimal research has been conducted regarding DDGS filled composites. Composites are the materials made of two or more components combined to obtain a new material with properties better than those of the individual components. The advancements in fiber-reinforced polymer and cement materials have led to them being used as the preferred building materials over the traditional concrete and steel materials.

The natural fiber polymer composites offer numerous advantages: availability in abundance, light-weight, non-abrasiveness, renewability, biodegradability, and high specific stiffness. As a filler for thermoplastics, DDGS thermoplastics generally exhibit a decrease in mechanical properties (Julson et al., 2004). Superior properties can be achieved by incorporating a coupling agent (Tisserat et al., 2013). DDGS incorporation into thermosets shows promise. It has been shown that DDGS can be incorporated into phenolic resin at 25% loading while maintaining mechanical properties (Tatara et al., 2009). Design properties for molded, corn-based DDGS-filled phenolic resin to produce a biomaterial were barely affected by mold pressure and temperature. However, DDGS level has a significant effect on all mechanical properties studied (Tatara et al., 2009). Further testing showed an increase to 50% with only a slight reduction of properties (Tatara et al., 2007). Pandey et al. (2018) have recently pointed that corn and DDGS fiber can replace oak as potential fillers at 30% and 50% loading to obtain the same flexural stiffness value. In all cases, the filler's predominant downfall is increased water absorption (Pandey, 2017; Tatara et al., 2007, 2009). While more research needs to be completed, DDGS shows promise as a filler for thermosets and thermoplastics. Moreover, it has great potential to be incorporated into lignocellulosic boards as supplemental material.

Most research has been carried out with hot press temperature of 150-195 ℃ due to the degradation of raw material starting above those temperature (Melo et al., 2014; Tisserat et al., 2018; Widyorini et al., 2005). A few research (Nonaka et al., 2013) have been done considering the higher temperature up to 280 ℃ to investigate if the polymerization of lignin and extractives are more advantageous than the heat degradation effect. The results were excellent concerning water absorption and thickness swelling with higher temperature. With NaOH pretreatment of DDGS, medium density particleboards were manufactured with 50% loading of DDGS in wood

particles, which replaced the synthetic resins (Liaw et al., 2019). This was because the alkaline pretreatment was able to denature the zein protein present in DDGS, making it a natural adhesive and a multifunctional filler in wood particleboard (Liaw et al., 2019).

2.7. Wheat straw for particleboards

Wheat is the second most cultivated cereal plant worldwide, and hence wheat straw is one of the widely available lignocellulosic materials in the world. Currently, wheat straw is not used as efficiently as it should be, and land-filling or open burning are common practices for this resource that create significant environmental problems. The bulk density of straw particles is one-third lower than typical wood particles. Wheat straw is an annually renewable agricultural byproduct and can be used in a different application. Among these, the production of particleboard panels, which are almost exclusively produced from timber or timber by-products like saw dust, seems feasible. They can be used in particleboard because of their salient features as built-in insulation, sound suppression characteristics, and low cost (Boquillon et al., 2004). Wheat straw contains cellulose (35-40%), hemicellulose (25-30%), and lignin (10-15%) and is suitable for manufacturing lingo-cellulosic particleboards (Karr et al., 2000; Kundu et al., 20014; Rowell et al., 1995; Wang and Sun, 2002). Wheat straw particles have a high aspect ratio (ratio of fiber length to diameter), which gives good strength properties.

Several studies have been done on the use of wheat straw for making biocomposites. Bekhta et al. (2013) studied the effect of pretreatment of raw material on particleboard properties. They suggested that wheat straw has the potential to be used as a raw material for manufacturing particleboards. In another research, wheat straw was bonded with poly-isocyanate resin and was hot-pressed at 190 ℃ and 3.6 MPa for 5 minutes to get properties that are higher than the requirements of JIS A 5908 (Luo and Yang, 2010). Although, urea-formaldehyde (UF)

is the most commonly used resin in wood-based panels, straw particles have high compatibility with oil-based resins due to their straw surface-free energy. This parameter (straw surface-free energy) in straw exhibits very low polar component than wood species leading to high compatibility with oil-based resins than UF (Boquillon et al., 2004). Since DDGS also acts like an oil based natural resin, the use of wheat straw with DDGS in low-density particleboard can play an essential role in the value addition of both materials. In addition to that, the use of wheat straw allows the production of panels over a larger range of densities (200 to 800 kg/m^3) as compared to wood panels, where panels with density lower than 400 kg/m^3 is almost impossible (Boquillon et al., 2004). It suggests that wheat straw are particularly suitable for low-density applications.

Fine particles are generated during the hammer milling of wheat straw. Fines have been reported to wear milling tools and degrade the mechanical properties of manufactured particleboards (Halvarsson et al., 2010). Because of the increased surface area and decreased aspect ratio on the wheat straw particles due to the presence of fines, a higher resin fraction would be required to maintain the particleboard properties (Halvarsson et al., 2010). A screening is required to remove the fines from the wheat straw particles before further processing. Particles smaller than US sieve mesh size 80 have been identified as significant inhibitor on mechanical properties of agricultural fiber based composites (Lee et al., 2006). So it is important to remove the fines before processing with the raw materials.

2.8. Pretreatment of biomass for particleboards

The introduction of surface modification to enhance weak adhesion between natural fibers is an effective way to improve the physical and mechanical properties of particleboards. Surface modification aims to reduce the hydrophilic nature of cellulose-rich fibers by replacing

hydroxyl groups of cellulose with less hydrophilic or hydrophobic chemical groups. Thermal pretreatment, hot-water pretreatment, acidic pretreatment (Liaw et al., 2019), enzymes pretreatments (Zhang et al., 2003), oxalic acid and steam (Li et al., 2011), and alkaline pretreatment (Bekhta et al., 2013; Liaw et al., 2019) are some of the pretreatment methods studied. Out of these pretreatment methods, alkaline pretreatment has been studied for both DDGS based particleboards and for wheat straw-based particleboards.

Many studies have reported that lignin can act as a natural binder in particleboards by hot-pressing high-lignin lignocellulosic materials (Araújo et al., 2018; Fahmy and Mobarak, 2013; Mobarak et al., 1982). Some pretreatment methods, such as steam explosion and thermal pretreatment, are used to expose lignin to the surface so that enhanced interlocking adhesion could be achieved for making binderless boards (Anglès et al., 1999; Mancera et al., 2011; Quintana et al., 2009). Sodium hydroxide treatment is used to break the internal hydrogen bonds of the coiled protein molecules, extensively unfold them and expose the abundant available polar groups for adhesion (Wang and Sun, 2002). Alharbi et al., (2020) studied the effect of 1 wt. and 3 wt. % alkaline pretreatment in activating efficient lignin condensation. They found that optimum mechanical and thermal properties were obtained for hot-pressed biopolymers pretreated with 1 wt. % NaOH (Alharbi et al., 2020). With NaOH pretreatment of DDGS, medium density particleboards were manufactured with 50% loading of DDGS in wood particles, which replaced the synthetic resins (Liaw et al., 2019). This was because the alkaline pretreatment was able to denature the zein protein present in DDGS, making it a natural adhesive and a multifunctional filler in wood particleboard (Liaw et al., 2019).

While NaOH pretreatment has shown better performance with particleboards from DDGS, contradicting results have been reported in wheat straw-based particleboards.

Pretreatment using NaOH solution to wash wheatgrass reduced the qualities of finished particleboards bonded with p-MDI and urea-formaldehyde (UF) resins (Zheng et al., 2007). On the other hand, improved mechanical properties of wheat straw particleboards bonded with UF by removing wax and ash from the wheat straw surface through bleaching with alkali (NaOH) has been reported (Wu and Gatewood, 1998).

The combination of alkaline treatment and hydrogen peroxide in the paper-making industry is an environmentally friendly, easy-to-operate process (Salam et al., 2007). This strategy was also adopted by Mo et al., where they found that particleboards made from wheat straw treated with 1M NaOH and 0.2% H_2O_2 solution gave a better performance than their untreated counterparts (Mo et al., 2001). It has been reported that the effect of alkaline and alkaline peroxide treatments on rice husk was the removal of hemicelluloses (Ciannamea et al., 2010), which increased the ratio of cellulose (C) and lignin (L) to hemicellulose (H), extractives (E), and ash (A). They have used $((C + L)/(H + E + A))$ – a factor which determines the ability of any biomass to perform well in particleboards, the higher the better (Alharbi et al., 2020). But these methods involved washing and drying after treatment with alkaline. However, Cao et al., (2017) used different wt. % of NaOH and sprayed to wheat straw for alkaline pretreatment before manufacturing particleboards with p-MDI resin. Boards with pretreated wheat straw had better mechanical properties than untreated wheat straw at all the loadings (Cao et al., 2017). Studies on pretreatment of both DDGS and wheat straw for their application on particleboards has not yet been found with PF resin as synthetic resin. NaOH can break internal hydrogen bonds that exist in coiled protein molecules. This NaOH is expected to unfold protein molecules and expose them to available polar groups for stronger adhesion (Cheng et al., 2004).

3. MATERIALS AND METHODS

This chapter discusses the materials used in these experiments, methods used to produce the particleboard panels, and various analytical methods used for testing.

3.1. Materials

Wheat straw was first ground to small size using the hammer mill (SchutteBuffalo Model W6H, Buffalo, New York, USA) (Figure 3.1) and then by Wiley mill (Thomas Wiley Laboratory mill, Model 4; Arthur N. Thomas Company, Philadelphia, PA, USA) (Figure 3.2) with 2 mm screen. After grinding, wheat straw particles were sieved, and particles below US sieve size #60 (also termed as fines) were removed. Pine wood flour of 2020-grade from American Wood Fibers (Wausau, WI, USA) was used to make control boards. The average particle size of the wood flour was determined to be 425 μm.

Figure 3.1: Hammer mill used for initial grinding of wheat straw

Figure 3.2: Wiley mill for the grinding of wheat straw

DDGS produced from Tharaldson Ethanol (Casselton, ND) and collected from NDSU Dairy Unit under the Animal Science Department, was used to fractionate DDGS at the pilot plant lab at NDSU. For the fractionation of DDGS, the DDGS was first sieved into different sieve size of US sieve size number 10 (equivalent 2 mm), 20 (~0.841 mm), 40 (~0.420 mm), 60 (~0.250 mm), 80 (~0.177 mm), and pan using a testing sieve shaker (Ro-Tap W.S. Tyler, Mentor, Ohio) as shown in Figure 3.3. The sieving was done for five minutes. This sieving process was conducted based on the American Society of Agricultural Engineers (ASAE) standard method. These sieved DDGS were then aspirated using an aspirator (Model 6DT4-01, Kice Metal Products Co. Inc., Wichita, Kansas, USA) shown in Figure 3.4. DDGS was fed manually and two different density fractions were collected from the original DDGS at two different parts of the machine. The outlet opening was adjusted to 75^0 angles at the inlet (~0.25 inches of water column) using manual gear to control the vacuum pressure for fractionation of DDGS. The discharge of the feed hopper was equipped with an adjustable slide gate to regulate product flow.

Figure 3.3: Sieving machine used for sieving DDGS and wheat straw

Figure 3.4: Air aspirator for fractionation of DDGS into heavier and lighter fractions

All DDGS samples collected were analyzed for chemical composition at the Nutrition Laboratory, Department of Animal Science, North Dakota State University. Acid detergent fiber

(ADF), neutral detergent fiber (NDF), nitrogen (N), protein, and ash were determined. Moisture content was determined by heating the samples to 105 ℃ for 24 hour period (overnight) and then taking the weight. The oven dried samples were put back to a furnace and heated to 575 ℃ for 24 hour to calculate the ash content. Two replicates were taken from all samples for moisture content analysis.

Phenol formaldehyde used for making particleboards was obtained from Georgia Pacific LLC, and it contained nearly 48% solid residue on the resin. 2M NaOH solution was prepared from reagent grade NaOH. The initial moisture content (MC) of original DDGS, SA#20-lighter DDGS (or fractionated DDGS), wheat straw, and wood particles were 14.17%, 14.17%, 6.70%, and 4.61% (db), respectively. SA#20-lighter fraction of DDGS was selected for making particleboards because of the high NDF (55%) content on this fraction. This SA#20-lighter fraction DDGS is referred to as 'fractionated DDGS' hereafter. Regardless of the initial MC, the MC of the sample mix before the hot press was targeted below 10 %.

3.2. Image acquisition and processing

Cone and quartering technique, as used by Igathinathane et al. (2012), was used for deriving samples for image processing, wherein an appropriate small quantity (adequate for necessary replications) of well mixed particles was poured into a heap on a clear sheet of paper. The heap was then spread using a strong-thin cardboard by gentle vertical chopping motion, first along one direction and then in the direction perpendicular to the previous. Cardboard was used as it did not cause electrostatic attraction among dust particles. Using the cardboard, three thin sectors of the spread material were marked and spilt as the selected samples (replication) for image processing.

A flatbed document scanner (CanoScan LIDE 300, 48-bit, Canon USA. Inc., Lake Success, NY, USA) was used to acquire color images of the particles. Care was taken to spread the individual particles so that they did not touch or overlap with the other particles.

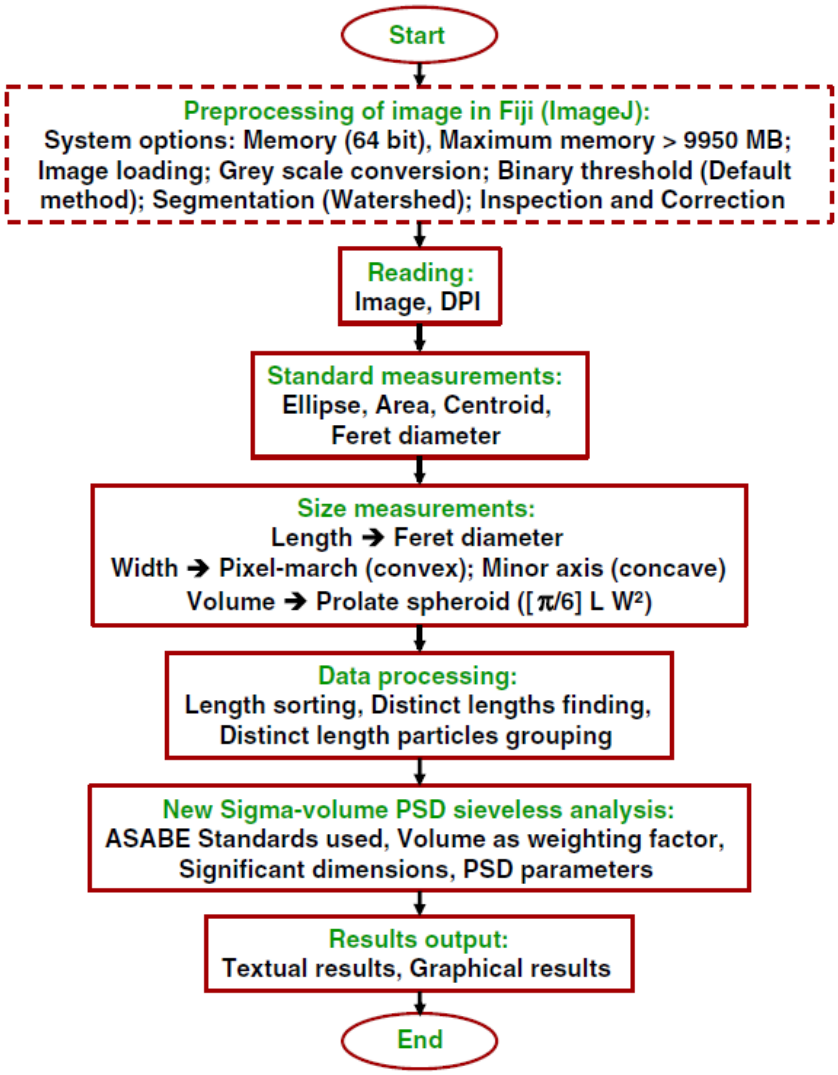

Figure 3.5: Flowchart of the ∑Volume machine vision plugin for particle size distribution (PSD) sieveless analysis of different particles
(Igathinathane et al., 2012)

The actual transfer of samples to the scanner bed was performed by picking the particles using a flat paint brush and stroking the brush gently with the cardboard. This action caused the sample particles to fly down and get deposited on the scanner bed. A transparent sheet was used

on the scanner bed for easy loading and removal of particles from the bed. After depositing, the layout was inspected using a magnifier and touching particles were separated using the tip of a knife. The scanning was done by leaving the scanner lid completely open and turning off the lights of the room. All the images were scanned at 600 DPI on both horizontal and vertical direction. A built in ImageJ plugin developed by Igathinathane et al. (2012) was used to process the images to acquire the PSD parameters for all scanned samples (Figure 3.5).

3.3. Panel processing

The term fractionated DDGS used in this research means 'lighter fraction of aspirated and #20 sieved DDGS'. Weighted amount of filler material based on the treatment (DGGS, wheat straw, or wood) was mixed by continuous rotation of cement mixture (1-1/4 cu. ft. cement mixture, Central Machinery, CA, USA). Water and phenol-formaldehyde were first mixed and then sprayed (at the air pressure 50 psi) on the filler material contained in the rotating cement mixture using the paint spray gun (WIMMER H-2000G H.V.L.P. Air Gravity Paint Sprayer) as shown in Figure 3.7. For the manufacturing of particleboards with NaOH pretreated DDGS samples, NaOH solution was sprayed on the DDGS using the same cement mixture and spray gun.

Figure 3.6: Cement mixture for mixing the raw materials with resin

Figure 3.7: Paint spray gun for mixing resin

The blend of different material composition is as shown in Table 3.1;

Table 3.1: Composition of DDGS, wheat straw, and wood used to make particleboards

Formulation (DDGS: Wheat straw)	Composition (wt. %)				
	DDGS (dry weight)	Wheat straw (dry weight)	Wood (dry weight)	Phenol - formaldehyde (solid %)	Added water to phenol-formaldehyde (as is basis)
25:75	24.25	72.75	X	3	1/3rd of PF
50:50	48.5	48.5	X	3	1/3rd of PF
75:25	72.75	24.25	X	3	1/3rd of PF
Control wheat straw	X	94	X	6	1/3rd of PF
Control wood	X	X	94	6	1/3rd of PF

After blending, the mixture was put into a mold (6”x12”) for panel pressing to get a targeted thickness of 6 mm (Figure 3.8). Sheets of Teflon were also used on the two halves of mold to prevent fibers from sticking to the mold surface during pressing. The mold with fibers was then pressed via a preheated Carver Hot Press Model 4122 (Wabash, IN). Step-wise pressure was increased every four minutes. When the final pressure reached to 18 Mton, it was pressed at that pressure for 4 minutes. The intermediate pressures were 6 Mton and 12 Mton. The following table depicts the processing conditions for the press;

Table 3.2: Process conditions for hot pressing of panels

Press parameters	Values
Upper platen temperature	195 ℃
Lower platen temperature	195 ℃
Press time	12 minutes
Pressure	6, 12, &18 Metric Ton (=3.8 MPa)
Time to maximum pressure	4 minutes

After the panel was hot-pressed, it was removed from the mold and allowed to cool for a minimum of 24 hours before testing for physical and mechanical properties.

Figure 3.8: Mold for manufacturing particleboards

Figure 3.9: Carver hot press for pressing the boards

3.4. Design of experiment

A three factor factorial design was used where parameters being used were (1) the loading concentrations of DDGS and wheat straw, (2) fractionated DDGS vs. original DDGS,

and (3) alkaline pretreatment or not. Loading concentrations of DDGS are 25%, 50%, and 75% and the rest wheat straw to make 100%. Eight panels (6”x12”) were produced for each blend, and all samples were cut from them for testing purposes. Since a single board was not sufficient to make all different testing samples needed, two particleboards were used so that single reading of all tests can be obtained with two boards (Figure 3.11). It means that, with eight boards manufactured for each treatment, we could get only four replications for each testing. Each sample was produced with a target density of 600 kg/m^3, the criterion for low-density particleboards is less than 640 kg/m^3.

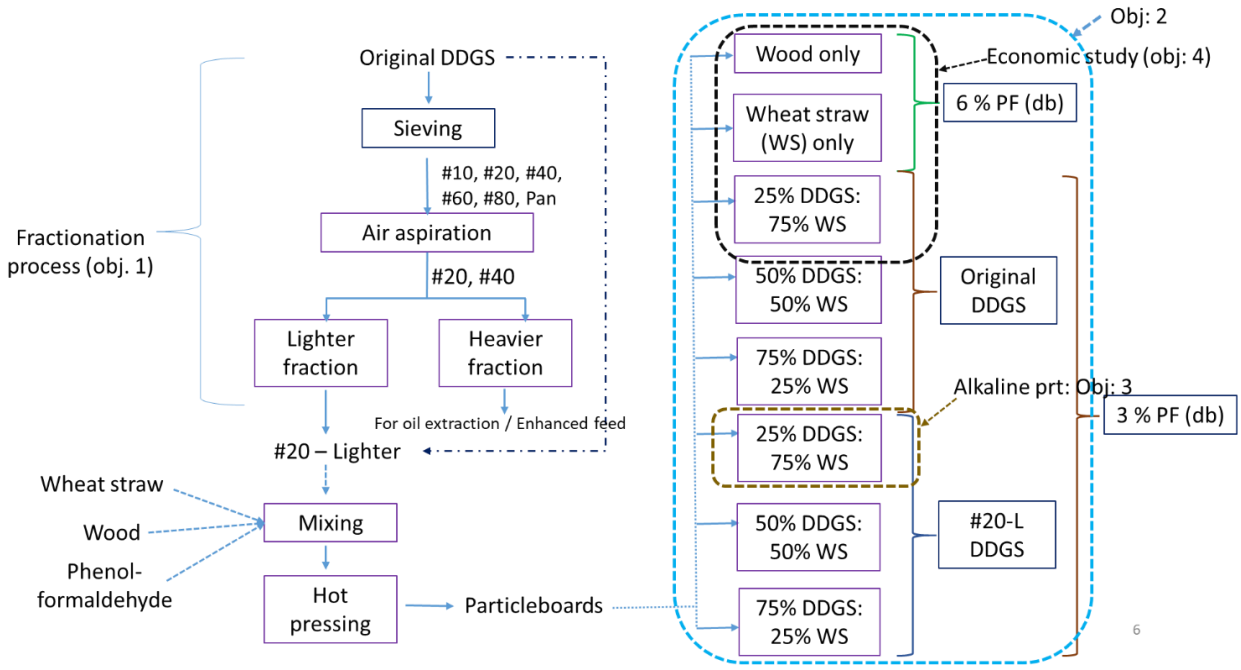

Figure 3.10: Overall experimental design for fractionation of DDGS and manufacturing of boards

3.5. Fourier transform infrared spectroscopy analysis

Fourier transform infrared spectroscopy (FTIR) was performed on untreated as well as 2.0 M sodium hydroxide treated particles from different DDGS samples to determine the difference in functionality between chemically treated DDGS and untreated DDGS. The analysis

was conducted using a Thermo Scientific Nicolet 8700 FTIR spectrometer (Waltman, MA, USA). All of the samples were mixed with KBr (potassium bromide) and pressed at 2 tons using a Specac Mini-Pellet Press (Limited, UK) to form disc-shaped specimens. Spectra were collected in absorption mode in the region of 4000 to 500 cm^{-1}. The spectra were corrected for the surrounding air as the background spectrum.

3.6. Scanning electron microscopy analysis

Morphology of surfaces of different raw biomass materials before manufacturing of boards was observed via scanning electron microscopy (SEM) at an accelerating voltage of 15kV. To find the chemical composition and to see if silica is present at significant amount in the wheat straw fibers, SEM and energy-dispersive X-ray analysis was done at USDA Electron Microscopy laboratory at NDSU.

3.7. Physical and mechanical testing

Physical and mechanical tests were performed to evaluate the changes and minimum requirements. Density, linear expansion, and water absorption tests were done for physical testing. For mechanical properties of boards, static bending, internal bond strength, screw withdrawal, and hardness tests were done. Samples for these tests were cut in accordance with ASTM D1037- Standard Test Methods for Evaluating Properties of Wood-Based Fiber and Particle Panel Materials with some modification. Figure 3.11 below shows the initial cut pattern used to obtain the samples from the particleboards for different testing.

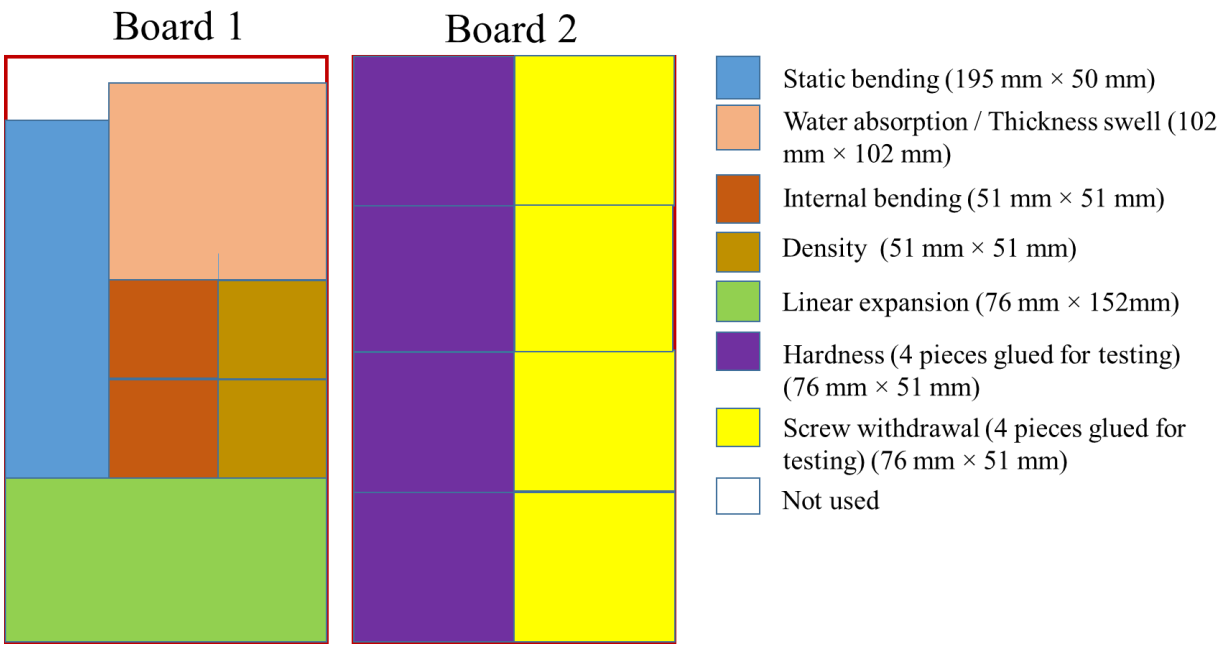

Figure 3.11: Board samples cut for physical and mechanical testing

3.7.1. Density measurement

The density of each particle board was measured using mass and length measurement in accordance with ASTM D2395.

$$\text{Density} = \frac{\text{Mass}}{L*W*T} \quad (2)$$

Where, L is the length of sample (meters), W is the width of the sample (meters), and T is the thickness of the sample (meters). Mass was measured in kilograms and density in kg/m^3. Two values from parallel edges were measured and averaged for length and width. However, for thickness, four values from the center of four sides were measured and then averaged. A digital Vernier caliper was used for measuring the dimensions.

3.7.2. Linear expansion testing

ASTM D1037-12 Section 24 was followed for testing the linear expansion with a change in moisture content. This testing evaluates the boards for their dimensional stability as the ambient moisture content changes. Linear expansion test measures the response of a material to

the presence of humidity. The response of material under the exposure of heat is measured in linear thermal expansion. Low expansion is desired as it indicates the resilience of material to humidity, preventing dimensions from fluctuating with climatic conditions.

Linear expansion tests were performed using a Binder Humidity Chamber Model (KBF 115-UL, Tutlingen, Germany) located at the Pilot Plant, NDSU. Samples were in dry condition and had dimensions of 76 mm × 152 mm and manufactured thickness as according to ASTM D1037. Samples were first conditioned to an equilibrium weight with the conditioning chamber that was set at a temperature of 20 ± 3 ℃ and 50% humidity. Weights of samples were taken every day (24 hour) until practical equilibrium was reached. Practical equilibrium is defined as the condition where the boards do not have a mass change of more than 0.05% in 24-hour. Once the samples reached practical equilibrium, initial length was noted from the longer edge of the board with two measurements from two edges and the values averaged. The length was measured with an accuracy of 0.02 mm. The samples were then exposed to 80% humidity at a temperature of 20 ± 3 ℃ for a couple of days till the samples reached practical equilibrium. The sample lengths were then measured from the two edges and the values averaged, and the linear expansion was calculated using the following equation.

$$\%\ \text{change in length} = \frac{L_f - L_i}{L_i} x100 \quad (3)$$

Where, L_i is the initial length at 50% humidity (i.e., lab condition), and L_f is the final length at 80% humidity. Four (4) samples for each formulation were tested for linear expansion. The arrangement of samples inside the humidity chamber is shown in Figure 3.12.

Figure 3.12: Linear expansion test samples arrangement

3.7.3. Water absorption testing

Water absorption test was carried out to measure the resistance of a particleboard to water absorption. An increase in weight and volume during this test signifies that the particleboard has absorbed water. Lesser water absorption is desired.

Dry panels of size 102 mm × 102 mm were submerged horizontally in tap water according to ASTM D1037. The temperature inside the tank was maintained at 20 ± 1 ℃. Testing followed 2-hour and 24-hour test method meaning that samples were removed from the water bath at 2 hour and then allowed to drain for 15 minutes before their weight and thickness were measured. After 24 hour also the same process was repeated. Multiple samples were tested in the same bath, and fresh tap water was used for each test. The percent change of mass and volume were calculated based upon their dry condition using the following equations.

$$\% \text{ change in mass} = \frac{M_f - M_i}{M_i} x\ 100 \quad (4)$$

$$\% \text{ change in thickness} = \frac{T_f - T_i}{T_i} x\ 100 \quad (5)$$

Where M_i and T_i are the initial mass and initial thickness, respectively, and M_f and T_f are the final mass and final thickness.

3.7.4. Static bending testing

Three-point static bend testing method is employed in accordance with ASTM D1037-12 Section 9 to measure the stiffness of particleboard samples. Higher stiffness means that the sample has adequate load bearing capacity and is desired. The fixtures and loading conditions are as shown in Figure 3.13 below.

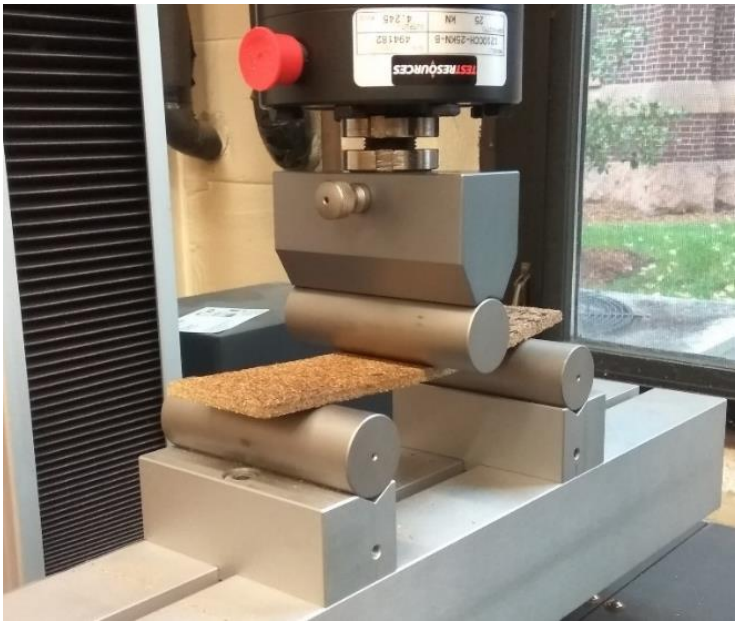

Figure 3.13: Three point flexural test setup using Instron universal testing machine

TestResources model 312 (Shakopee, MN, USA) was used to perform three-point static bend testing in accordance with the ASTM D1037 to measure both the modulus of elasticity (MOE) and modulus of rupture (MOR). The sample was 195 mm long, 50 mm wide as according to ASTM D1037. The load was applied at the distance of 97 mm from one free end of the sample.

The cross head speed for testing was calculated by the following equation.

$$N = \frac{33.3}{t} \quad (6)$$

Where *t* is the thickness of the sample, and N is the crosshead speed.

The modulus of elasticity (*E*) and modulus of rupture (R_b) were calculated using the following equation:

$$R_b = 3\frac{P_{max}L}{2w\,t^2} \tag{7}$$

$$E = \frac{2e6\Delta P}{wt^3\Delta l} \tag{8}$$

Where, *w* is the width of the sample (meter), *L* is the length (meter), *t* is the thickness (meter), P_{max} is the maximum load in Newton, and ΔP/Δl is the slope of the linear portion of the deflection curve.

3.7.5. Internal bond testing

Internal bond testing measures the cohesive strength of a panel. High internal bond strength signifies that the samples are well bonded. Square samples were cut to a length and width of 51 mm × 51 mm according to ASTM D1037 and glued to the loading blocks. The glue used was a hot melt adhesive bought from Minards. The loading blocks were heated on a hot plate and glue was applied to the surface. The sample was placed on the melted glue and the blocks were allowed to cool for a minimum of one hour. Then the process was repeated for the second surface. Minimum 6 hour was allowed to effectively adhering the loading blocks before the samples were tested.

Testing was performed on a TestResources model 312 (Shakopee, MN, USA) load frame at a rate of 1 mm/min rather than keeping the speed of testing at a rate of 0.08 cm/cm as was specified in ASTM D1037. This was done because of the unavailability of a suitable extensometer to measure and maintain strain rate. Adhesive failures between the glue and loading block were discarded and not included in the analysis. The fixture and loading blocks can be observed in Figure 3.14. The maximum stress was calculated by

$$\sigma_{max} = \frac{P_{max}}{wl} \quad (9)$$

Where P_{max} is the maximum load in Newton, w is the width of the sample (meter), and l is the length of the sample (meter). Six internal bond samples were tested for each particleboard formulation, two from the same boards as shown in figure 3.11 for cutting samples.

Figure 3.14: Internal bond test setup

3.7.6. Screw withdrawal test

Screw withdrawal tests measure how well a panel will support a fastener. A high screw withdrawal force indicates a material can easily support a screw. Screw withdrawal tests were performed on 76 mm × 76 mm samples, with four samples stacked together with weld-wood contact cement to get the desired thickness of 1 inch, width modified from ASTM D1037. The screw used was a Number 10 type AB with a pitch of 16 threads per inch following ASTM D1037. All samples were predrilled in the face using a 3.2 mm drill bit. Samples were tested in the dry condition on the aforementioned TestResources® Load Frame machine within 15 minutes of application of the screw. The strain rate used was 1.5 mm/min, and the sample was housed in internally produced fixtures as shown in Figure 3.15. The maximum load required to

remove the screw from the panel face was recorded for each sample. Three (3) samples were tested for each formulation.

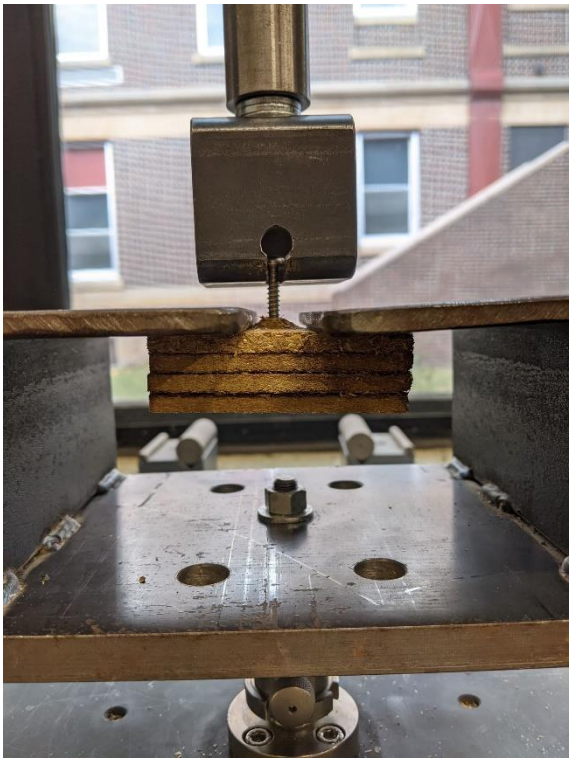

Figure 3.15: Screw withdrawal test setup

3.7.7. Hardness testing

Hardness test measures the ability of a substrate to resist deformation. A large hardness is desirable, which would prevent a particleboard-based material from denting under normal circumstances. Hardness testing was performed on 76 mm × 76 mm samples and four times the manufactured thickness to get 1-inch thickness. Again, as in case of screw withdrawal sample, the width has been modified from ASTM D1037 for hardness testing. The thickness of 1 inch was achieved by gluing four samples together using weld-wood contact cement following the ASTM standard. The Janka ball method was used to test hardness with a 9.5 mm diameter ‘ball’ shown in Figure 3.16. Testing was performed on the TestResources® Load Frame. The strain rate used was 6 mm/min in accordance with ASTM D1037. The test was stopped when the ‘ball’

penetrated 4.75 mm, and the maximum force was recorded as the hardness value. Three (3) samples were tested for each formulation. The average value was taken after performing the hardness test on two opposite corners of the same face of the same testing sample.

Figure 3.16: Hardness test setup

3.8. Statistical methods

Statistical analysis was conducted on the data obtained in this research to gain objective results on the effect that each of the studied variables had on manufactured boards according to the objective presented in chapter one. Each experiment was treated as an individual trial with a completely randomized treatment design. The SAS programming (version SAS 9.1, Cary, NC, USA) and general linear model (glm) process was used for analysis. Boxplot of data was made to get a clear picture of the distribution of results. Student t-test was carried out to test the least significant difference (LSD) for pairwise comparison of one treatment compared to other at a significance level of $p < 0.05$ based on ANOVA. The values are presented in the form of mean ±

standard deviation followed by a letter in the summary table. The results with different letters implies that the values of the means are statistically significantly different.

3.8.1. ANOVA of a factorial design

Analysis of variance or ANOVA is a statistical model that can estimate experimental errors and the effect of changing variables within a design on a single response value for a specified confidence level. For this thesis paper, the commonly used 95% confidence interval was implemented for all ANOVA analyses, which indicates that the estimated bounds of data for a particular set of variables include 95% of the data that would be produced looking at the entire population of data for that set of variables.

4. RESULTS AND DISCUSSION

This chapter includes the results from the fractionation process as well as the results from the manufactured particleboards. The first section will discuss the results of the fractionation process done by sieving and air aspiration of the DDGS. The second section will discuss results of PSD using machine vision approach. The third section discuss the properties of manufactured particleboards from the fractionated DDGS and original DDGS. The fourth section will discuss the effect of sodium hydroxide pretreatment of wheat straw and DDGS on particleboard properties. And the final section will discuss the economic analysis of the project.

4.1. Result of the fractionation process

This section contains the results from the sieving process and the air aspiration of the sieved DDGS in terms of both the yield of different fractions and the protein and NDF composition of all DDGS fractions.

4.1.1. Yield of sieving and aspiration

Standard sieving and a laboratory aspirator were used to make the fractionation process. The yield of different DDGS fractions and the composition of different yielding fractions is important in choosing the right fraction of DDGS for particleboard manufacturing. Figure 4.1 represents the yield percentage of DDGS in different sieves. The DDGS was divided into five different particle size samples using the US sieve no. 10 (~2.00 mm), 20 (~0.84 mm), 40 (~0.42 mm), 60 (~0.25 mm), and 80 (0.177 mm) mesh. Most of the DDGS fell in the sieve size of 20 and 40 mesh, with the highest fraction retained on US sieve size number 20. Similar trend on yield of DDGS on these sieve size was observed by Rausch et al. (2005). This sieve size (#20 and #40) has a yield of more than 60%, meaning that the average size of DDGS was around 0.81 mm – 2 mm. This result is similar to Cheng et al.'s findings, where the highest yield was found

in the particle size with 0.84 mm - 2.00 mm sieve (Cheng et al., 2014). Using a different batch of DDGS from a different source, Huda et al. found the average DDGS size to be 0.34 mm (Huda, 2020), contradicting our findings. This is because of the variability of DDGS particle size from plant to plant and process.

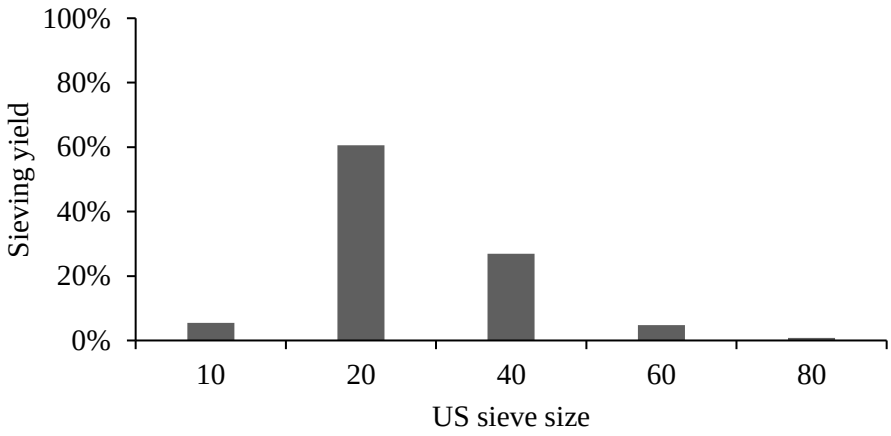

Figure 4.1: Basic particle size distribution of DDGS using mechanical sieves

Each sieve size of DDGS was air aspirated to get a heavier and lighter fraction of each sieve size. Since the yield of number 20 and number 40 sieve size altogether constituted more than 87% of total DDGS, the air aspiration results discussed only these two samples. Figure 4.2 shows the yield of heavier and lighter fraction of number 20 and number 40 sieve size obtained with the aspirator's air baffle set at 75° angle (i.e., 0.25 inches of water column). A good yield of heavy and lighter fractions was found in the number 20 sieved aspirated DDGS sample, with the yield being 38.25 % and 58.07 % for heavier and lighter fractions, respectively. The number 40 sieve size heavy fraction had the lowest yield. This is because the number 40 sieve size had a small size, and hence little weight, which made it easier for all the particles to be sucked by air pressure into lighter fractions during the aspiration process. The same trend was followed with the aspiration of numbers 60 and 80 mesh size, which is not documented here because of their minimal yield.

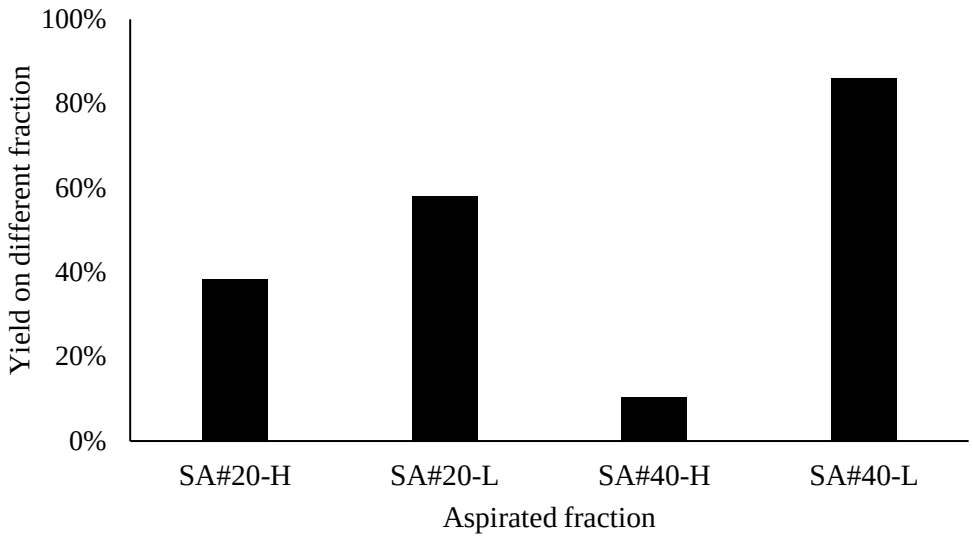

Figure 4.2: Yield of air aspiration of sieved DDGS
SA = Sieved and Air aspirated, #20 = US Sieve size 20, #40 = US Sieve size 40, L = Lighter fraction, H = Heavier fraction

Changing this pressure value had an impact on the yield and composition of different fractions of the DDGS. The pressure value at 0.25 inches of the water column was selected because with this pressure, two distinct fractions were obtained with a significant difference in oil content and fiber content, which will be useful for oil extraction and particleboard manufacturing. This pressure value was selected based on our preliminary experimental results, which showed that the heavy fraction had rich oil content while the lighter fraction had high fiber content. This experiment was conducted on a single batch to obtain enough sample for further work. Srinivasan et al. (2009) also reported that a large sample of DDGS was required to have the right amount of fiber increase, where they reported that only 4-15 % of fiber could be separated from the whole sample. With the increase in mesh size, the particle-size of DDGS decreases, making the particles very light, which ultimately lowers their yield on the heavier fraction. This can be seen by the yield of air aspiration of #40-heavier fraction as compared to the yield of #20-heavier fraction. However, a considerable yield of heavy and lighter fractions was found in the #20-heavier and #20-lighter fractions (38% and 58%, respectively).

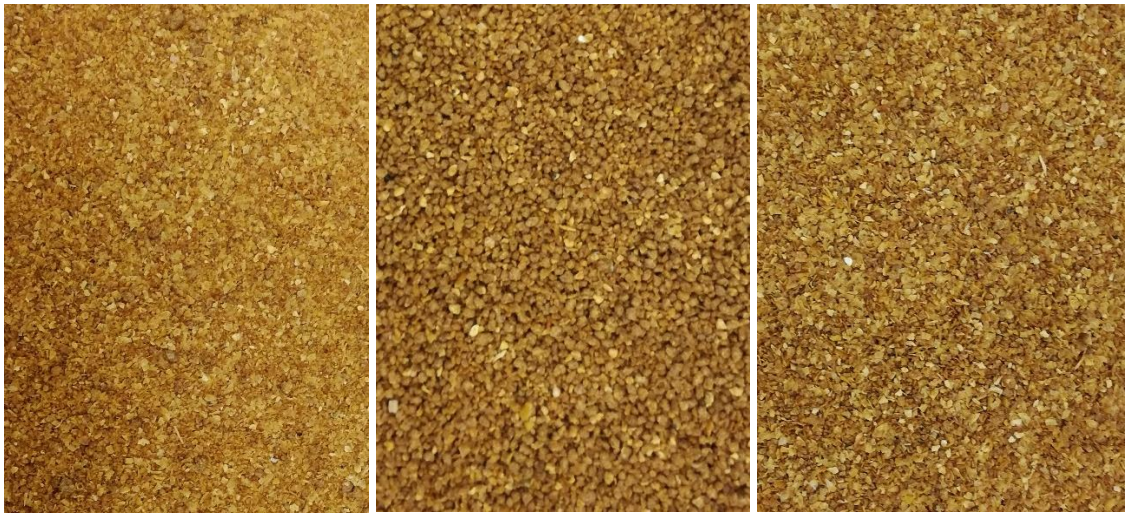

a) Original DDGS b) #20 Heavier fraction c) #20 Lighter fraction

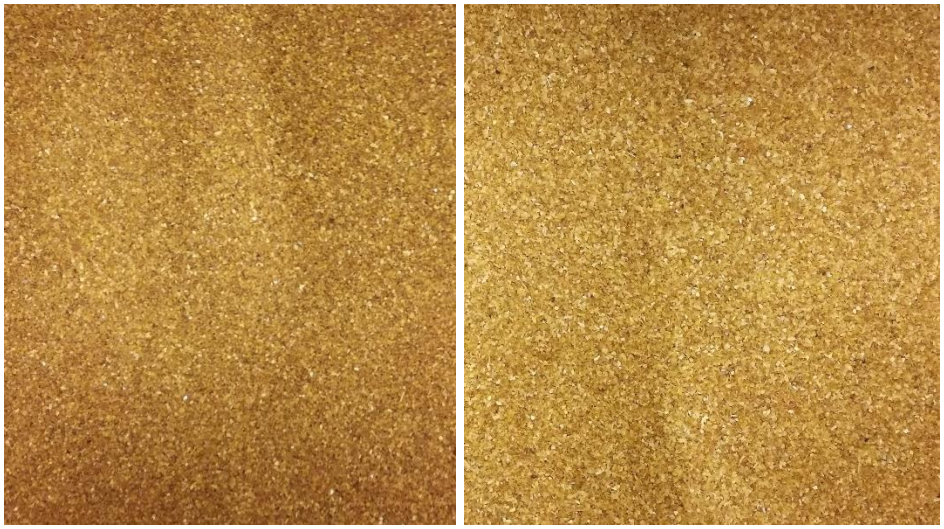

d) #40 Heavier fraction e) #40 Lighter fraction

Figure 4.3: Particle morphology of DDGS fractions

4.1.2. Chemical composition of different DDGS fraction

After aspiration, all the sample from sieving and aspiration works were analyzed for the chemical composition to study the change of protein and neutral detergent fiber. The results of the chemical composition show that the heavier fraction has increased protein content as compared to the original DDGS for both the number 20 as well as number 40 mesh size. In contrast to this, the lighter fraction of #20 and #40 sieve size has decreased protein content.

However, the neutral detergent fiber (NDF) content, was significantly increased on both the #20 and #40 lighter fraction. The highest increase in NDF content was found on the #20 lighter fraction, with an increase in NDF content by 25.44% compared to the original DDGS. This result is even higher than the work done by Srinivasan et al. (2009) where they were able to get fiber fraction of DDGS with a 12.4% increase in NDF values compared to the original DDGS. With sieving only (without further air aspiration), the NDF values of #20 sieved DDGS were around 19% higher than that of the original DDGS. The crude protein for #20 heavier fraction and #40 heavier fraction were 8.3% and 17.49 % higher than the original DDGS, respectively. These values are even higher than Srinivasan et al., where they reported 8.0% and 6.3% higher protein content than original DDGS for two different batches of DDGS (Srinivasan et al., 2006).

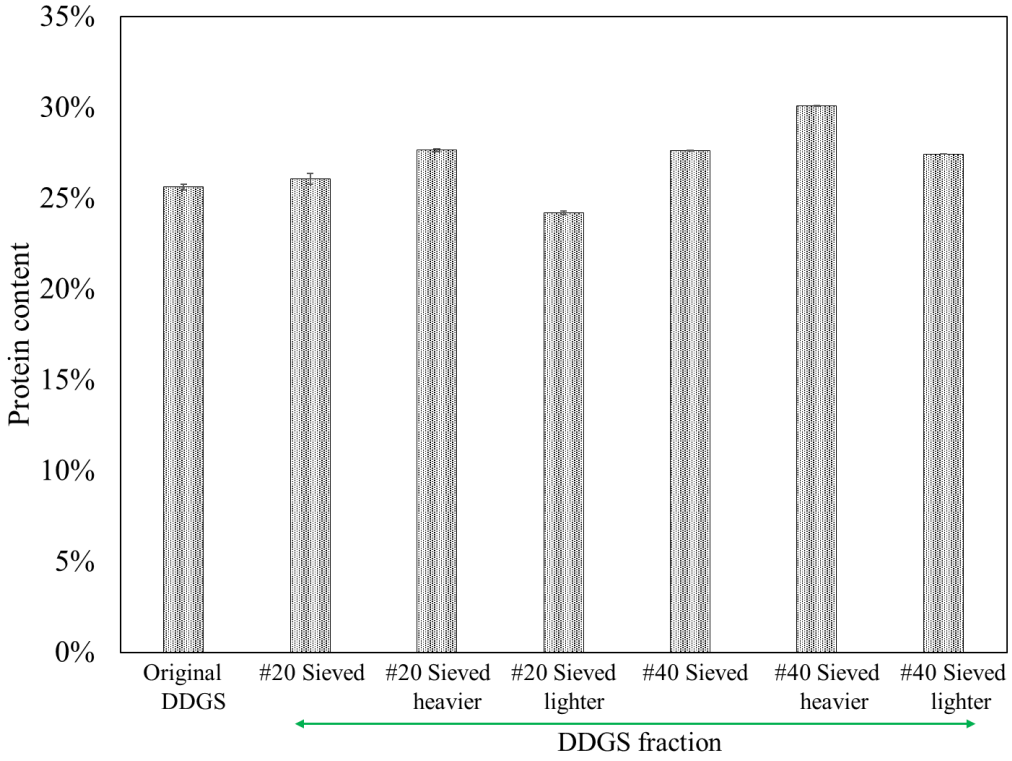

Figure 4.4: Protein content of different fractionated DDGS samples

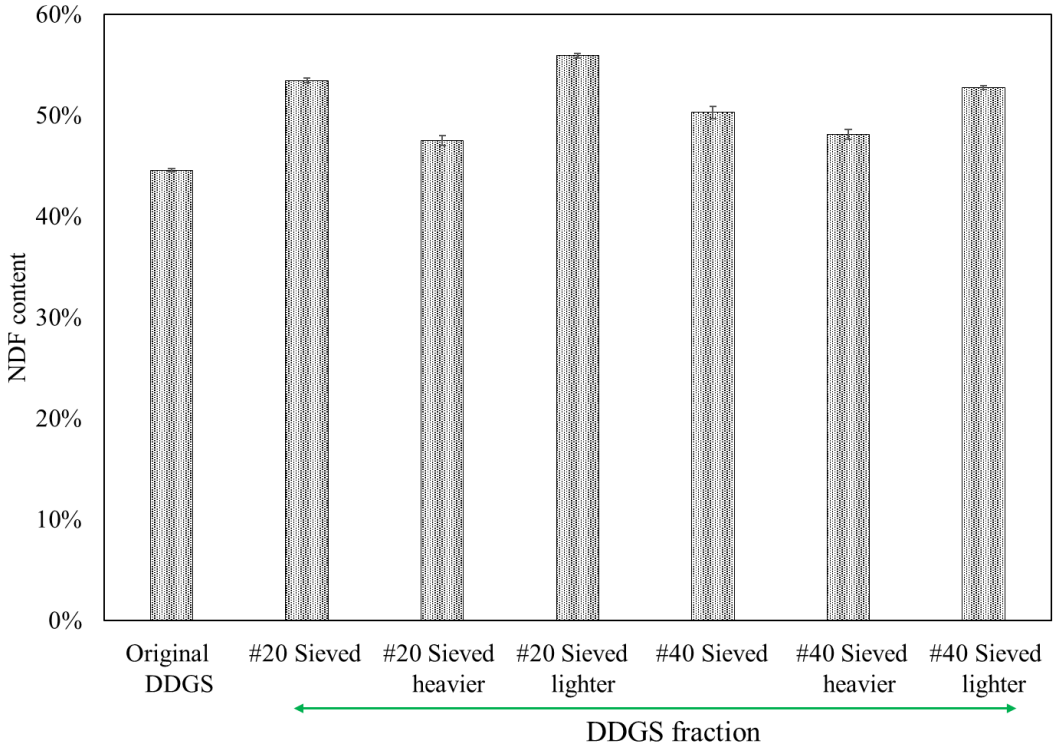

Figure 4.5: Neutral detergent fiber (NDF) content of different fractionated DDGS samples

With the increase in mesh size (i.e., decrease in DDGS particle size), the protein content has increased, and the NDF content has decreased. This is in line with the work done by Liu et al., where protein and ash contents increased and total CHO content decreased in all samples with the increase in mesh size (Liu, 2009).

4.2. ∑Volume method machine vision PSD results

The PSD for all materials was calculated using the ∑Volume method and the image processing plugin developed by Igathinathane et al. (2012). Using this user-developed ImageJ plugin, the PSD of all the fractionated particles as well as wood and wheat straw particles was analzed for all scanned images of the sample (Figure 4.6). Table 4.1 summarizes the mean and corresponding standard deviation (STD) of selected dimension-based PSD descriptors. This analysis results were derived from the three replications of all the raw materials after fractionation process that were used in manufacturing particleboards as well as for wood and

wheat straw particles used in control boards. The high standard deviation in the arithmetic mean length and arithmetic mean width for all the DDGS fractions (Table 4.1) suggests that particle size of DDGS varied greatly within a sample and PSD varied greatly among samples (Liu, 2008).

Figure 4.6 shows the selected area of the scanned images of the raw materials actually used in this experiment for manufacturing particleboards as well as all the remaining DDGS fractions from the fractionation work. One can easily distinguish visually the difference in size and shape of these raw materials. Wood particles have long length and short width as compared to DDGS particles. However wheat straw has the longest fibers which are assumed to provide high elastic properties for the manufactured particleboards. It can also be noticed that original DDGS (Figure 4.6C) has a range of particle size, however in case of SA#20-L DDGS (Figure 4.6F), the particle size is pretty consistent.

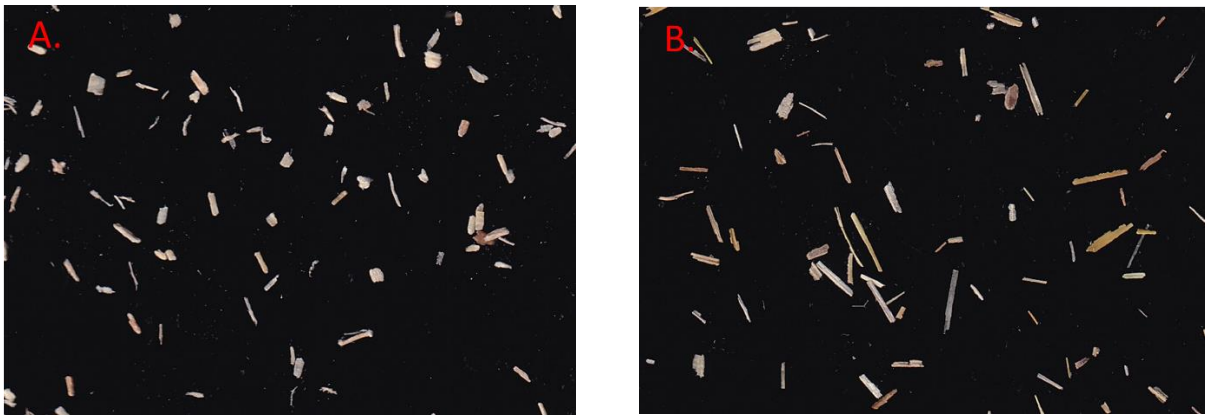

Figure 4.6: A portion of scanned image of particles
A. Wood particles, B. Wheat straw particles, C. Original DDGS, D. Number 20 sieved DDGS, E. Heavier fraction of number 20 sieved DDGS, F. Lighter fraction of number 20 sieved DDGS, G. Number 40 sieved DDGS, H. Heavier fraction of number 40 sieved DDGS, I. Lighter fraction of number 40 sieved DDGS

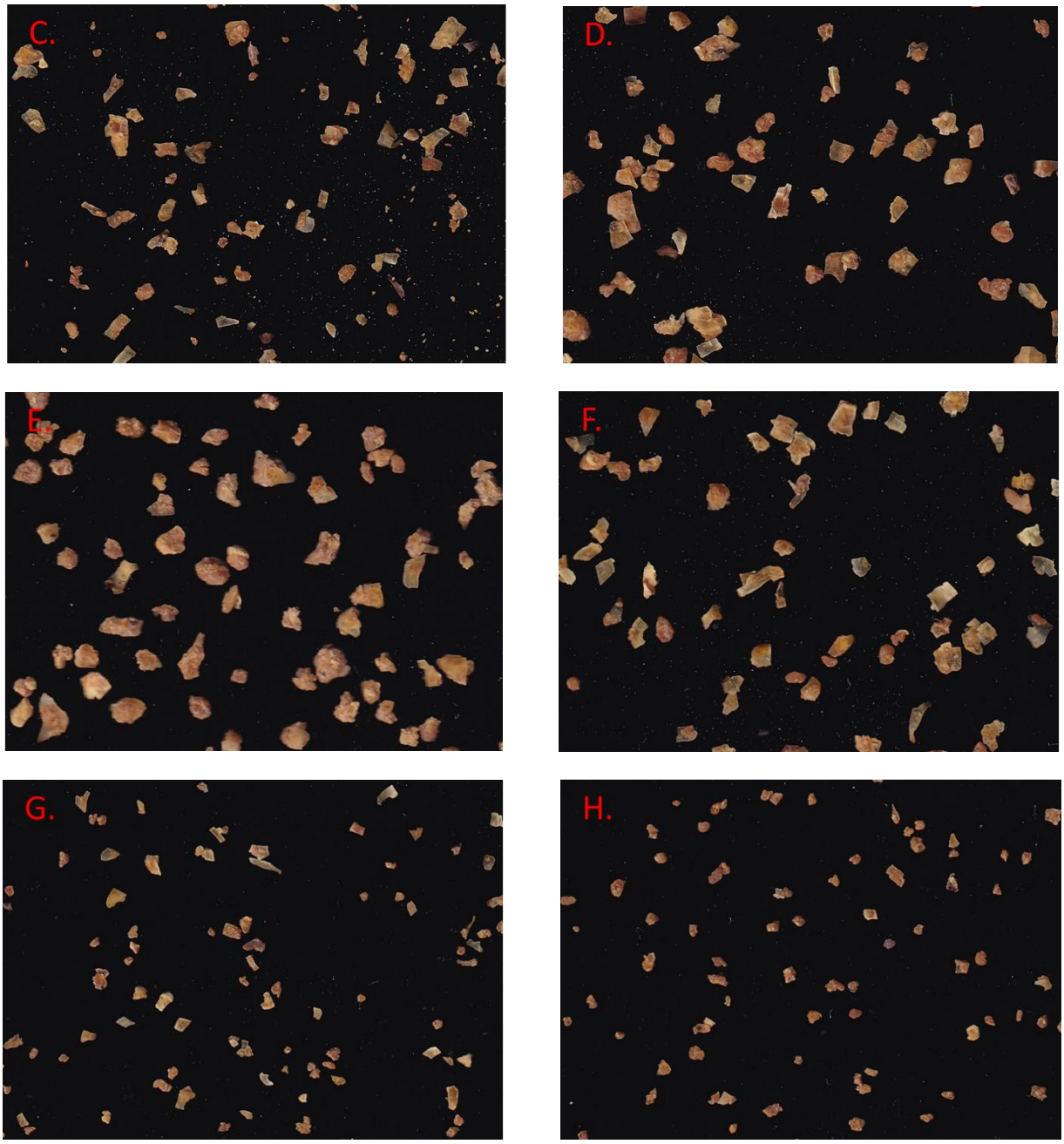

Figure 4.6: A portion of scanned image of particles (continued)
A. Wood particles, B. Wheat straw particles, C. Original DDGS, D. Number 20 sieved DDGS, E. Heavier fraction of number 20 sieved DDGS, F. Lighter fraction of number 20 sieved DDGS, G. Number 40 sieved DDGS, H. Heavier fraction of number 40 sieved DDGS, I. Lighter fraction of number 40 sieved DDGS

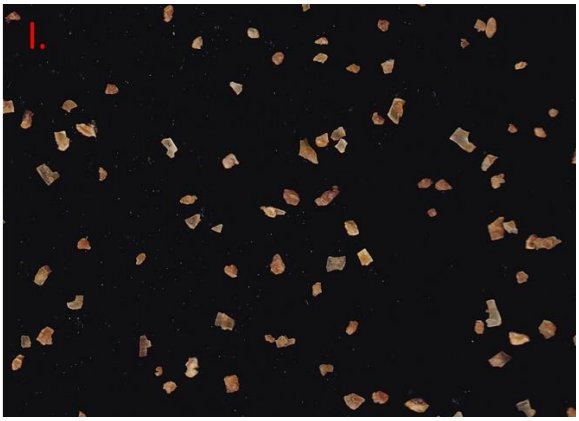

Figure 4.6: A portion of scanned image of particles (continued)
A. Wood particles, B. Wheat straw particles, C. Original DDGS, D. Number 20 sieved DDGS, E. Heavier fraction of number 20 sieved DDGS, F. Lighter fraction of number 20 sieved DDGS, G. Number 40 sieved DDGS, H. Heavier fraction of number 40 sieved DDGS, I. Lighter fraction of number 40 sieved DDGS

The normalized cumulative undersize distribution on Figure 4.7 also supports this statement. An overall linear trend was observed from the plots of cumulative size distribution, which indicates that the size distribution is log-normal. The cumulative under size curve for number 40 mesh sieved DDGS showed steep increase because the spread of length was relatively small (Figure 4.7 H).

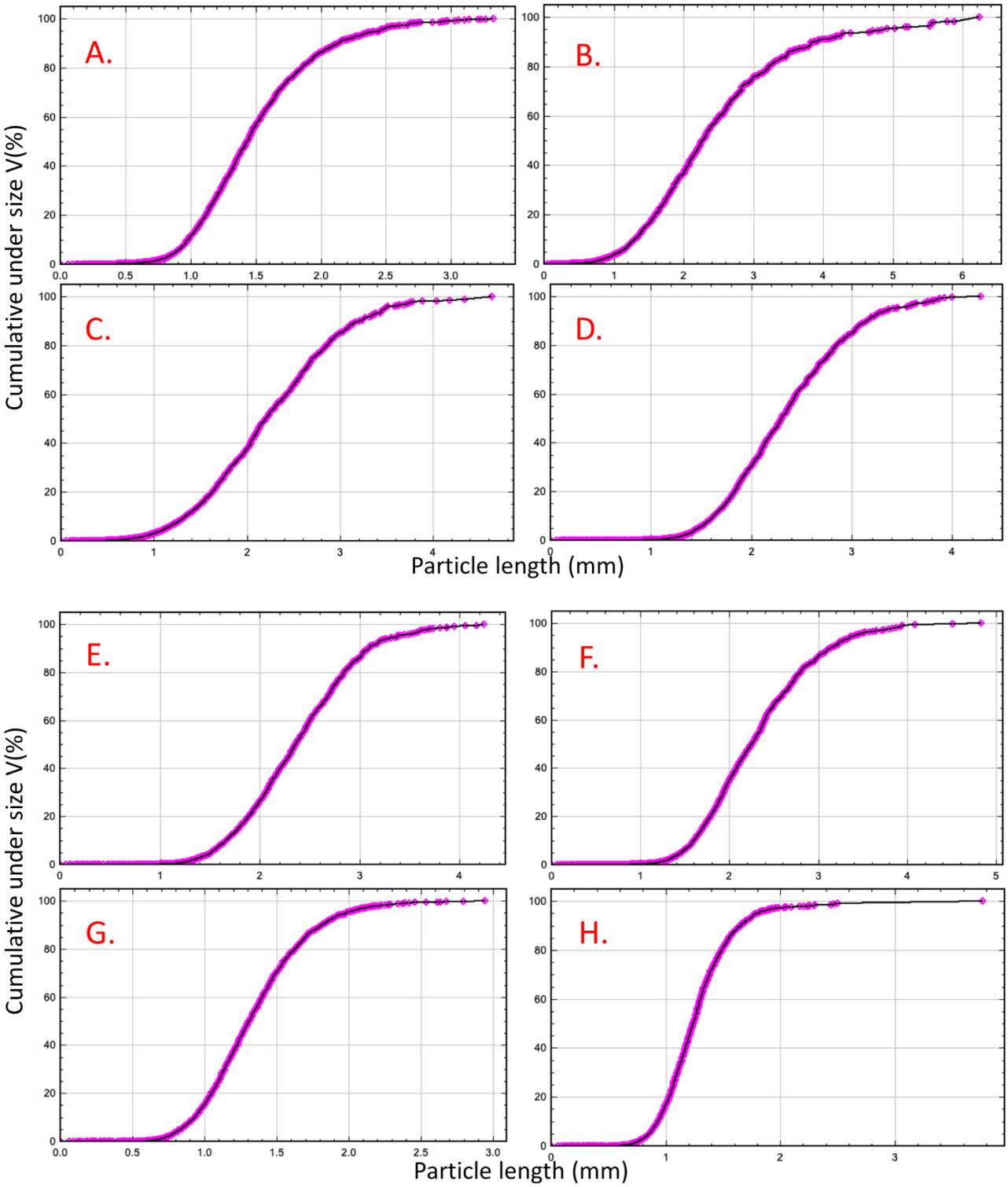

Figure 4.7: Cumulative size distribution of particles

A. Wood particles, B. Wheat straw particles, C. Original DDGS, D. Number 20 sieved DDGS, E. Heavier fraction of number 20 sieved DDGS, F. Lighter fraction of number 20 sieved DDGS, G. Number 40 sieved DDGS, H. Heavier fraction of number 40 sieved DDGS, I. Lighter fraction of number 40 sieved DDGS

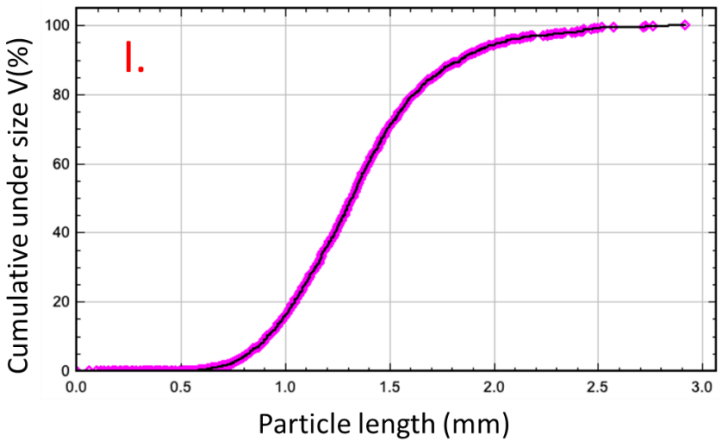

Figure 4.7: Cumulative size distribution of particles (continued)
A. Wood particles, B. Wheat straw particles, C. Original DDGS, D. Number 20 sieved DDGS, E. Heavier fraction of number 20 sieved DDGS, F. Lighter fraction of number 20 sieved DDGS, G. Number 40 sieved DDGS, H. Heavier fraction of number 40 sieved DDGS, I. Lighter fraction of number 40 sieved DDGS

Aspect ratio is defined in this analysis as the ratio of Feret's minimum length to the Feret's maximum length. Thus, as the length and width of the shape approach the same value, the aspect ratio approaches one. This does not necessarily mean the shape is circular, though a perfect circle does have an aspect ratio of 1.0. The aspect ratio of wheat straw particles was highest with a value of 3.85, followed by wood (2.60), #40 DDGS (1.56), original DDGS (1.52), and #20 DDGS (1.48), respectively (Table 4.1).

Table 4.1: Dimension-based particle size descriptors section results through ∑volume machine vision analysis

Dimension descriptor	Wheat straw	Wood	Original DDGS	#20 DDGS	#20-Ligther DDGS	#20-Heavier DDGS	#40 DDGS	#40-Lighter DDGS	#40-Heavier DDGS
Dimensional properties – length (mm)									
Minimum length	0.060±0.000	0.060± 0.000	0.060± 0.000	0.060± 0.000	0.060± 0.000	0.060± 0.000	0.060± 0.000	0.060± 0.000	0.060± 0.000
Maximum length	6.640±0.323	3.323± 0.005	4.355± 0.275	4.460± 0.588	4.747± 0.177	4.450± 0.356	2.913± 0.250	2.877± 0.033	3.087± 0.489
Arithmetic mean length	1.293±0.009	1.183± 0.024	1.145± 0.035	1.827± 0.009	1.747± 0.009	1.917± 0.061	1.103± 0.012	1.120± 0.014	1.117± 0.025
Arithmetic mean length STD	0.987±0.017	0.487± 0.012	0.780± 0.000	0.680± 0.024	0.707± 0.033	0.613± 0.041	0.360± 0.008	0.367± 0.005	0.330± 0.008
Dimensional properties - width (mm)									
Minimum width	0.040±0.000	0.040± 0.000	0.040± 0.000	0.040± 0.000	0.040± 0.000	0.040± 0.000	0.040± 0.000	0.040± 0.000	0.040± 0.000
Maximum width	1.907±0.168	1.620± 0.070	2.925± 0.315	2.580± 0.024	2.573± 0.068	2.597± 0.012	1.490± 0.107	1.657± 0.062	1.763± 0.185
Arithmetic mean width	0.323±0.005	0.447± 0.012	0.685± 0.015	1.123± 0.005	1.053± 0.005	1.243± 0.037	0.643± 0.005	0.657± 0.009	0.703± 0.012
Arithmetic mean width STD	0.257±0.005	0.220± 0.000	0.485± 0.005	0.437± 0.012	0.437± 0.019	0.417± 0.021	0.200± 0.000	0.203± 0.005	0.200± 0.008
Volume Properties (mm^3)									
Minimum volume (× 10^-5)	5.620±0.000	5.620± 0.000	5.620± 0.000	5.62± 0.000	5.620± 0.000	5.62± 0.000	5.62± 0.000	5.62± 0.000	5.62± 0.000
Maximum volume	8.530±0.909	3.220± 0.639	18.00± 5.850	14.50± 2.860	12.6± 0.883	13.4± 0.403	2.82± 0.417	3.67± 0.528	5.02± 2.170
Arithmetic mean volume	0.180±0.008	0.181± 0.0090	0.717± 0.010	1.660± 0.045	1.430± 0.046	1.980± 0.177	0.293± 0.0089	0.318± 0.013	0.345± 0.0184
Arithmetic mean STD (× 10^-5)	1.360±0.061	1.370± 0.070	5.440± 0.080	12.60± 0.350	10.90± 0.340	15.00± 1.32	2.22± 0.068	2.41± 0.099	2.62± 0.139
Shape factors analysis									
Aspect ratio :									
Maximum aspect ratio	27.990±3.270	10.350± 0.416	6.815± 0.125	6.507± 2.676	6.243± 0.817	4.830± 0.216	6.923± 0.640	8.953± 2.861	6.070± 0.115
Average aspect ratio	3.850±0.036	2.603± 0.024	1.525± 0.005	1.483± 0.005	1.513± 0.005	1.420± 0.008	1.560± 0.008	1.553± 0.005	1.457± 0.005
Average aspect ratio STD	3.173±0.117	1.307± 0.026	0.445± 0.005	0.400± 0.036	0.437± 0.039	0.317± 0.012	0.463± 0.021	0.450± 0.016	0.327± 0.012
Circularity :									
Minimum circularity	0.060±0.016	0.177± 0.009	0.295± 0.005	0.270± 0.064	0.297± 0.033	0.390± 0.022	0.273± 0.029	0.250± 0.062	0.350± 0.008
Average circularity	0.600±0.000	0.660± 0.000	0.815± 0.005	0.757± 0.005	0.757± 0.005	0.770± 0.008	0.797± 0.005	0.800± 0.000	0.820± 0.000
Average circularity STD	0.267±0.005	0.173± 0.005	0.130± 0.000	0.100± 0.000	0.107± 0.005	0.080± 0.000	0.100± 0.000	0.097± 0.005	0.080± 0.000
Rectangularity :									
Minimum rectangularity	0.050±0.008	0.153± 0.017	0.275± 0.045	0.300± 0.036	0.287± 0.017	0.363± 0.042	0.220± 0.024	0.257± 0.071	0.290± 0.008
Average rectangularity	0.573±0.005	0.610± 0.000	0.720± 0.000	0.683± 0.005	0.680± 0.000	0.697± 0.005	0.693± 0.005	0.700± 0.000	0.717± 0.005
Average rectangularity STD	0.240±0.000	0.157± 0.005	0.110± 0.000	0.090± 0.000	0.093± 0.005	0.070± 0.000	0.090± 0.000	0.083± 0.005	0.070± 0.000
Hollowness index:									
Maximum hollowness	0.770±0.037	0.580± 0.024	0.440± 0.040	0.487± 0.082	0.410± 0.041	0.350± 0.073	0.400± 0.041	0.403± 0.025	0.363± 0.029
Average hollowness	0.170±0.000	0.130± 0.000	0.100± 0.000	0.093± 0.005	0.100± 0.000	0.087± 0.005	0.093± 0.005	0.090± 0.000	0.080± 0.000
Average hollowness STD	0.120±0.000	0.073± 0.005	0.050± 0.000	0.040± 0.000	0.040± 0.000	0.030± 0.000	0.033± 0.005	0.037± 0.005	0.030± 0.000

Note: Mean - arithmetic mean, and STD - standard deviation of three replications used; Aspect ratio -[major/minor axes], Circularity - [4*PI*area/perimeter^2], Rectangularity - [area/(bound rect. height*width)], Hollowness index - [(convex_area-area)/convex_area]; the values for minimum aspect ratio, maximum circularity, and maximum rectangularity are 1 and minimum hollowness values are 0 for all samples because of the nature of the formulas used in their calculation.

In mechanics, the flexural modulus (MOE) measures the tendency of the material to bend. Since large bonded area resist deformation, higher aspect ratio is important consideration for attaining a high flexural modulus. It has been found that high aspect ratio gives better flexural properties for manufactured particleboards (Juliana et al., 2012). Keskin et al. (2015) found that particleboards manufactured from poppy husk with aspect ratio of 2.5 had low MOR, MOE, and IB values than those manufactured from pine wood with aspect ratio of 4.2. Similar results were also found by Iswanto et al., (2017), where better contact area and mechanical properties were observed for particleboards manufactured from mahogany wood (aspect ratio 8.5) than that from sengon wood (aspect ratio 6.1). In case of DDGS samples, the spread of length values were slightly greater than that of width, however, for wheat straw and wood, the length values were significantly larger than that of width. It suggests that, the particles were more of round or elliptical shape for DDGS samples.

In mechanical sieving, classification of particlesize is based on particle width. Sometimes particles with small width but long length can pass through the sieve diameter. In PSD determination using image analysis, however, can give other dimensions and geometry related parameters for those particles, such as length-based analysis for PSD. Circularity, rectangularity, and hollowness index are some of the geometry based parameters that has been also analysed using this machine vision method of sieveless PSD determination.

Circularity is a function of the area divided by the square of the perimeter, and is a measure of both the particle form and roughness. Round particles flow better (e.g., during compression molding to press particleboards), thus they have good tendency to give better bonding properties. This might be one of the reasons for particleboards made with original DDGS having better internal bond properties as compared to those from fractionated #20-L

DDGS particles, as original DDGS particles had higher circularity as compared to sieved and aspirated #20 – ligther particles (circularity values of 0.815 vs 0.757, repectively) (Table 4.1). Schneider and Conway (1969) also reported that semi-circular end shaped particles gave low strength while rectangular-shaped particles gave superior strength. Although wood and wheat straw, because of high aspect ratio might provide better flexural strength, DDGS-based boards can have better adhesive strength because of their higher rectangularity (Table 4.1). This might be one reason that incorporation of 25% DDGS produced comparable IB values to control wheat straw boards even with a 50% reduction in use of phenol formaldehyde resin.

4.3. Physical and mechanical properties of particleboards

This section discusses the results for physical and mechanical testing of the particleboards made from the fractionated DDGS and compares with control wood and control wheat straw samples. This fractionated DDGS means the #20 sieved lighter fraction of DDGS obtained from the fractionation process, which has a NDF value of 55.90%. Particleboards made from the original DDGS having a NDF value of 44.56% were also tested to compare the effect of the increased fiber content of DDGS on the properties of the particleboards. Tests performed and results found were for density, linear expansion, water absorption, thickness swelling, static bending, internal bonding, screw withdrawal, and hardness. ANOVA was performed to check the significant difference on the means of treatments at 95% confidence interval. A student-t test was performed to calculate the LSD (least significant difference) values and hence differentiate the means, which can be found in the summary below which summarize the physical and mechanical properties of the manufactured particleboards.

Table 4.2: Summary of physical properties of particleboards

Treatment	DDGS: wheat straw loading (%)	PF (dry basis) conc. (%)	Density (kg/m3)	Water Absorption (%)		Thickness Swelling (%)	
				2 Hour	24 Hour	2 Hour	24 Hour
Control-Wheat straw	0:100	6	573.05±4.31	124.29±2.20b	134.28±3.31bc	34.09±2.52b	35.50±1.62b
Control-Wood	X (only wood)	6	613.92±12.72	100.32±0.81a	109.75±1.16e	19.59±1.35d	19.60±1.92d
Original DDGS	25:75	3	627.70±22.72	134.18±3.56a	142.54±3.54a	39.68±4.26a	40.41±4.23a
Original DDGS	50:50	3	629.01±24.14	121.24±5.96c	124.59±5.73d	28.78±1.53bc	31.21±1.26c
Original DDGS	75:25	3	611.59±28.46	115.96±7.40d	117.40±7.02e	22.30±1.33c	23.03±2.52c
'SA#20-L' DDGS	25:75	3	614.92±17.57	122.96±1.62ab	136.10±3.94ab	37.04±1.39bc	37.30±1.65ab
'SA#20-L' DDGS	50:50	3	608.26±12.76	118.30±3.61a	124.30±2.89ab	38.65±3.50bc	39.09±5.05c
'SA#20-L' DDGS	75:25	3	587.78±31.92	120.58±4.29c	123.79±5.14cd	28.70±1.09bc	32.95±1.83c

Table 4.3: Summary of mechanical properties of particleboards

Treatment	DDGS: wheat straw loading (%)	PF (dry basis) conc. (%)	IB (MPa)	Screw Withdraw (N)	MOE (MPa)	MOR (MPa)	Hardness (N)
'SA#20-L' DDGS	25:75	3	0.12±0.01d	224.05±11.68b	831.53±46.52a	3.27±0.07c	1309.67±98.97b
'SA#20-L' DDGS	50:50	3	0.15±0.01a,d	194.70±11.80c	539.30±40.12c	2.21±0.16d	1004.34±62.91c
'SA#20-L' DDGS	75:25	3	0.15±0.02a,c,d	133.59±4.18d	292.07±32.35d	1.19±0.05e	689.09±137.03d
Original DDGS	25:75	3	0.12±0.01d	247.01±1.97b	720.16±42.81b	3.65±0.10b	1649.51±29.13a
Original DDGS	50:50	3	0.24±0.02c	242.47±4.14b	479.97±39.06c	2.15±0.15d	1413.60±84.26b
Original DDGS	75:25	3	0.23±0.01a,c	133.74±10.64d	289.83±19.80d	1.30±0.03e	939.60±102.90c
Control-Wheat straw	0:100	6	0.15±0.05a,d	236.76±17.48b	902.60±83.74a	4.76±0.27a	1683.21±74.88a
Control-Wood	X (only wood)	6	0.63±0.12b	532.05±24.84a	542.94±53.56c	3.76±0.30b	1787.18±82.34a

4.3.1. Density measurement results

The targeted density was 600 kg/m^3 and the ANSI 208.1 defines low-density particleboards as those having a density less than 640 kg/m^3. The boxplot shows that most formulations were able to confirm to the ANSI 208.1 standard for low-density particleboard.

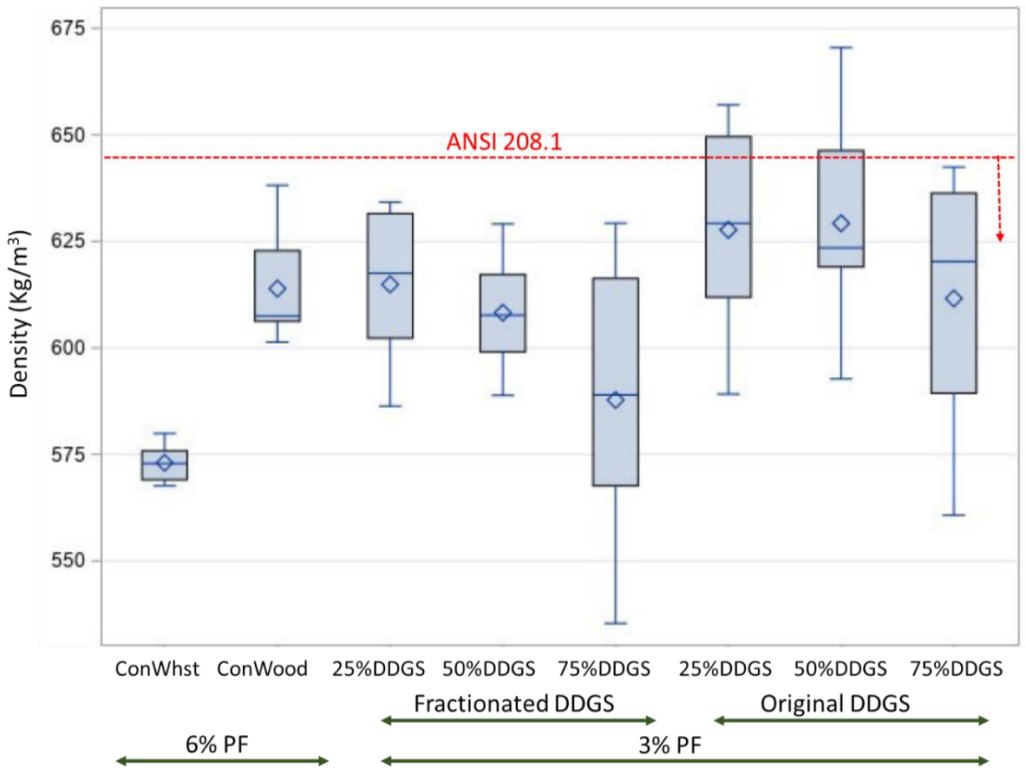

Figure 4.8: Boxplot of density of particleboards
PF = Phenol Formaldehyde, ANSI 208.1 for low-density particleboards is below 640 kg/m^3, and the direction of arrow shows the acceptable quality standards

The slight difference on density between treatments are likely due to compressibility issues or issues with maintaining consistent mass or moisture content for all treatments. Since the variations are not huge (and not statistically significantly different at p = 0.05), no considerations were made to adjust other properties of the boards based on density.

4.3.2. Water absorption results

Four samples from each formulation were used for water absorption test. This test shows the boards' resistance to water absorption. Both the change in mass and thickness were reported for 2 hour as well as for 24 hour. ANOVA analysis was done to determine the significant difference between the treatment means with a 95% confidence level.

4.3.2.1. Two hour water absorption results

The water absorbed by the boards was measured by taking the weight of particleboard samples after two hours of submersion in water. A boxplot of the two hour water absorption test can be seen in Figure 4.9. The boxplot shows significant changes between the formulations, with control wood formulation showing great performance. All the other boards, which had wheat straw content, had significantly higher water absorption. All the board formulations made with fractionated DDGS were in the same grouping as the control wheat straw samples. The model accuracy was given by R^2 = 82.90%, indicating a good estimator of the variability in the mass absorption properties at 2 hours. The relatively lower water absorption of particleboards with original DDGS as compared to fractionated DDGS is most likely because of the smaller particle sizes of DDGS in original DDGS. The smaller particle size goes into the spaces between the wheat straw particles and reduces the void spaces which can absorb more water.

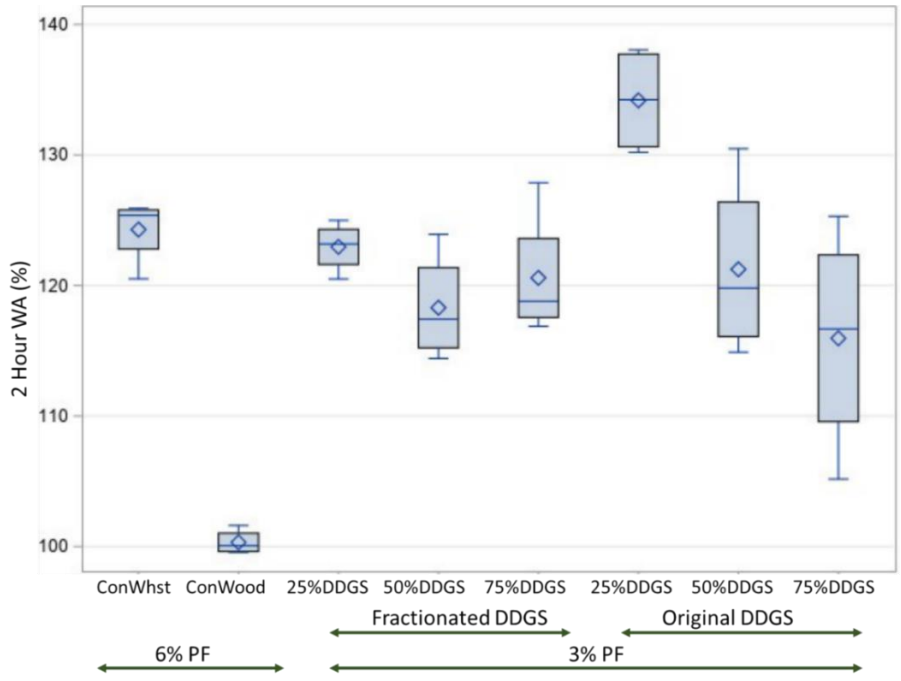

Figure 4.9: Boxplot of 2 hour water absorption
PF = Phenol Formaldehyde, There is no ANSI 208.1 standard for low-density particleboards for water absorption

4.3.2.2. Twenty-four hour water absorption results

Water absorption test for the 24 hour period was also done for each formulation. A boxplot of collected data can be seen in Figure 4.10. Again, as in the case of 2 hour water absorption, control wood had significantly lower water absorption than any other treatments. The students' t-test grouping based on the LSD of the means (Table 4.2) shows that there are several groupings due to performance changes with increasing DDGS concentration, both in case of the fractionated DDGS as well as the original DDGS. The water absorption properties were significantly improved when the DDGS concentration was increased from 25% to 50%, with original DDGS having even better properties than fractionated DDGS because of higher oil content in original DDGS, which helped in repelling water. The model accuracy was given by R^2 = 85.83%, indicating a good estimator of the variability in the mass absorption properties at 24 hours.

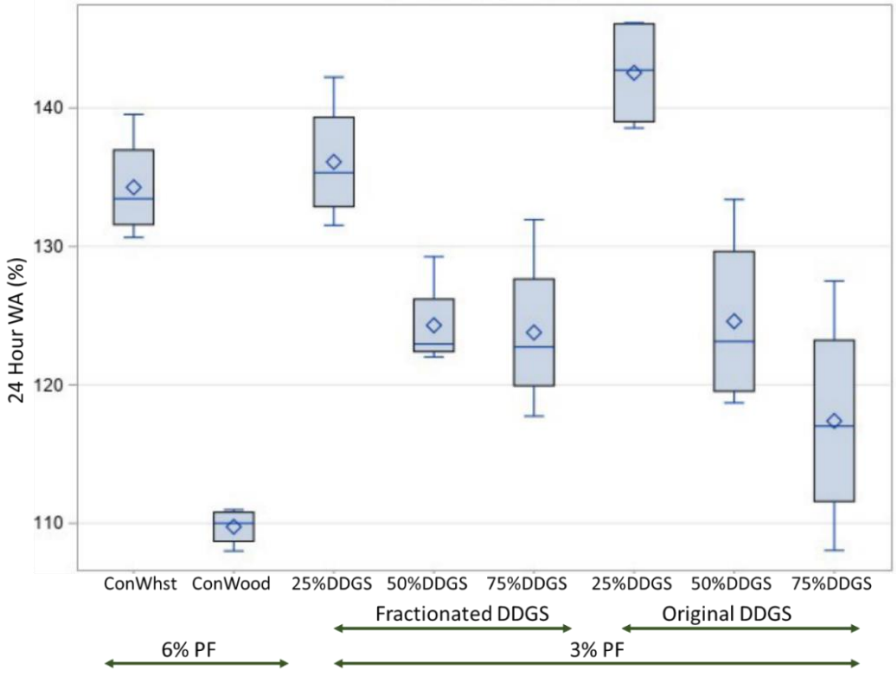

Figure 4.10: Boxplot of 24 hour water absorption
PF = Phenol Formaldehyde, There is no ANSI 208.1 standard for low-density particleboards for water absorption

4.3.2.3. Two-hour thickness swelling results

Thickness swelling test for the 2 hour period was done for each formulation. A boxplot of collected data can be seen in Figure 4.11. The students' t-test grouping based on the LSD of the means (as can be seen on Table 4.2) shows that treatments are significantly different among each other due to performance changes with increasing DDGS concentration, both in case of fractionated DDGS as well as original DDGS. The thickness swelling properties were significantly improved when the DDGS concentration was increased from 25% to 50% because of increase in fat and protein of DDGS. The high thickness swelling with higher wheat straw content is also related to the high content of silica on wheat straw (Melo et al., 2014). At alpha = 0.05, the means for boards with fractionated DDGS were significantly different than that with original DDGS at all DDGS concentrations. The model accuracy was given by R^2 = 93.05%, indicating a good estimator of the variability in the 2 hours thickness swelling properties.

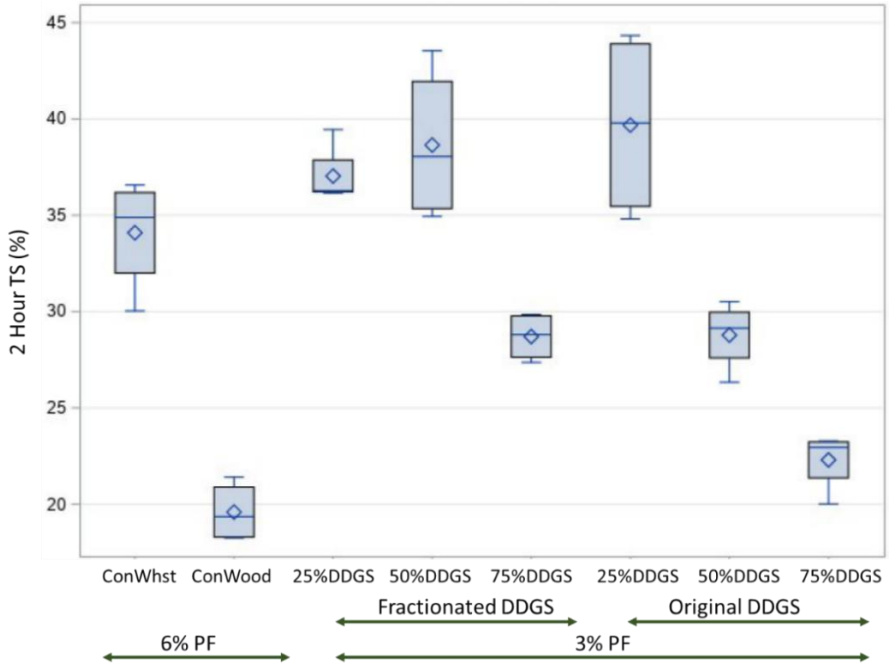

Figure 4.11: Boxplot for 2 hour thickness swelling
PF = Phenol Formaldehyde, There is no ANSI 208.1 standard for low-density particleboards for thickness swelling

4.3.2.4. Twenty-four hour thickness swelling results

Thickness swelling test for the 24 hour period was also done for each formulation. A boxplot of collected data can be seen in Figure 4.12. The students' t-test grouping based on the LSD of the means (as can be seen on Table 4.2) shows that there are several groupings due to performance changes with increasing DDGS concentration, both in case of fractionated DDGS as well as original DDGS. The thickness swelling properties were not significantly different for boards with 25% and 50% fractionated DDGS to that of control wheat straw boards. The high thickness swelling with higher wheat straw content is also related to the high content of silica on wheat straw (Melo et al., 2014). At alpha = 0.05, the means for boards with fractionated DDGS were significantly different than that with original DDGS at 50 and 75% DDGS concentrations. The model accuracy was given by R^2 = 91.96%, indicating a good estimator of the variability in the 24 hours thickness swelling properties. The thickness swelling values of boards with original DDGS at higher loading (50% and 75%) tended to be lower than those made from coarse particles of #20-Lighter fraction. This may be caused by the closer structure of the board, where the contact among the fine particles is better (Han et al., 1998). Higher IB strength at these loadings for original DDGS may also contribute to the reduction in water penetration.

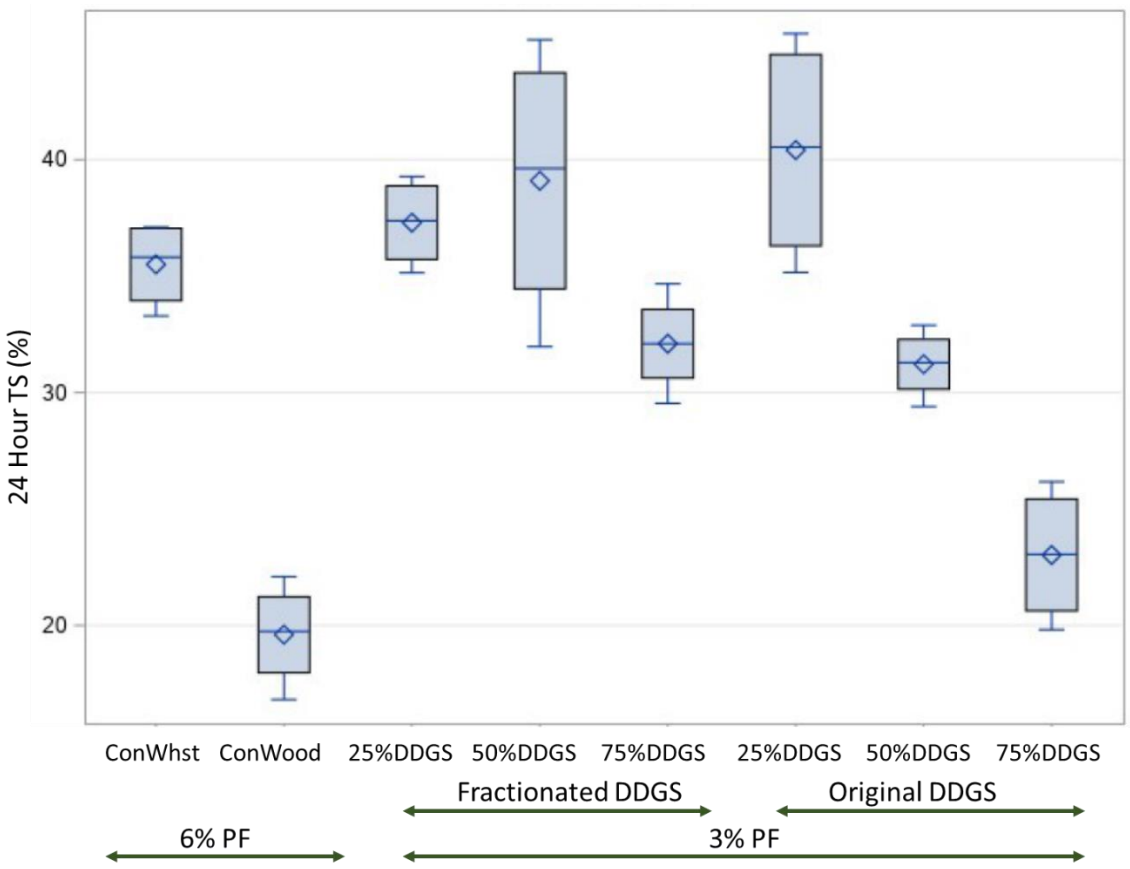

Figure 4.12: Boxplot of 24 hour thickness swelling
PF = Phenol Formaldehyde, There is no ANSI 208.1 standard for low-density particleboards for thickness swelling

4.3.3. Linear expansion results

Linear expansion testing was done to determine the effect of DDGS loading and DDGS fiber concentration on the relative expansion of the boards in the linear dimension. Linear expansion testing shows the resistance to linear expansion under high humidity. Four samples from each board were tested for the linear expansion with an average linear expansion value determined for each formulation. ANOVA analysis was used to determine significant factors influencing the linear expansion with a 95% confidence interval. Figure 4.13 shows the boxplot for linear expansion.

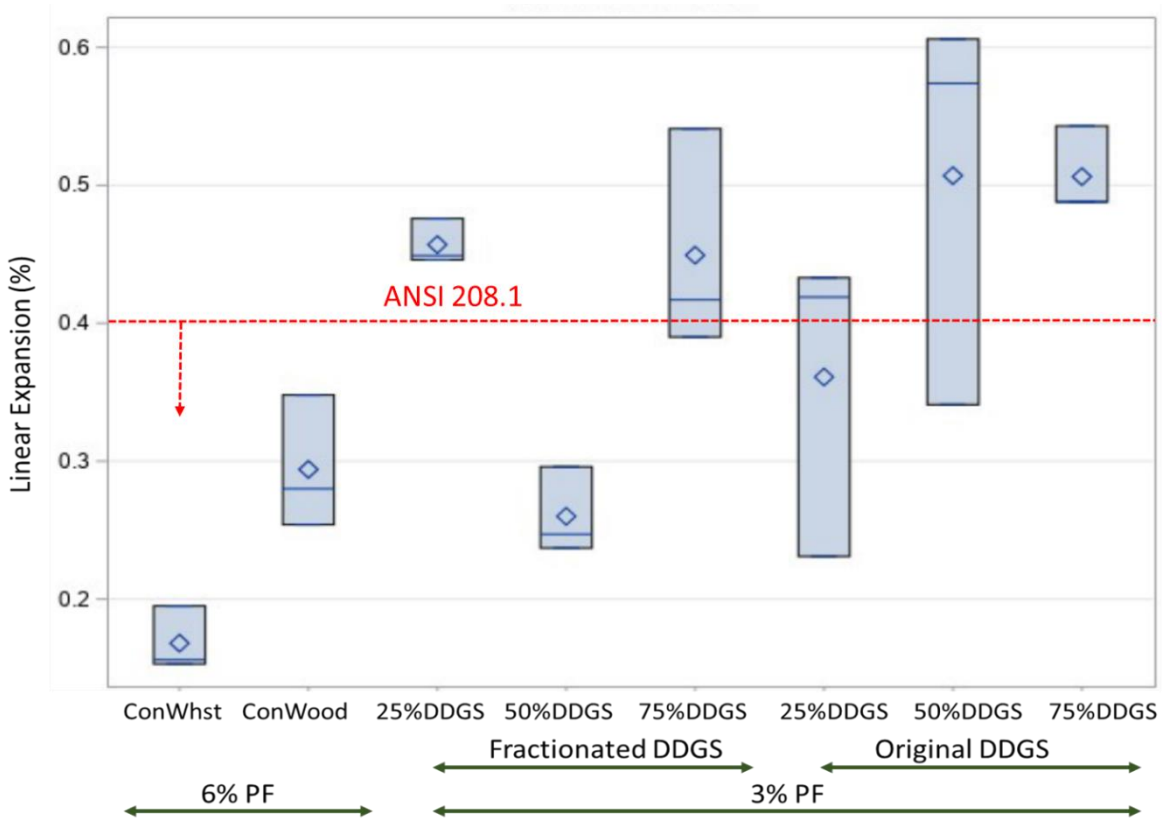

Figure 4.13: Boxplot of linear expansion
PF = Phenol Formaldehyde, ANSI 208.1 standard for low-density particleboards for linear expansion is 0.4% and direction of arrow shows the acceptable range

4.3.4. Static bending results

To determine the effect of DDGS loading (25%, 50%, and 75%) and type of DDGS (fractionated and original), a static bending test was conducted to find the modulus of rupture (MOR) and the modulus of elasticity (MOE) of the pressed boards. The average value for each formulation was calculated for MOE and MOR after measuring three samples from each board formulation. ANOVA analysis was used to determine significant factors influencing the MOE and MOR at a 95% confidence interval.

4.3.4.1. Modulus of elasticity (MOE)

Modulus of elasticity represents the stiffness that the board has during initial loading before unrecovered deformation occurs. Figure 4.14 shows the boxplot constructed for the average values of MOE and the general spread of data for each formulation.

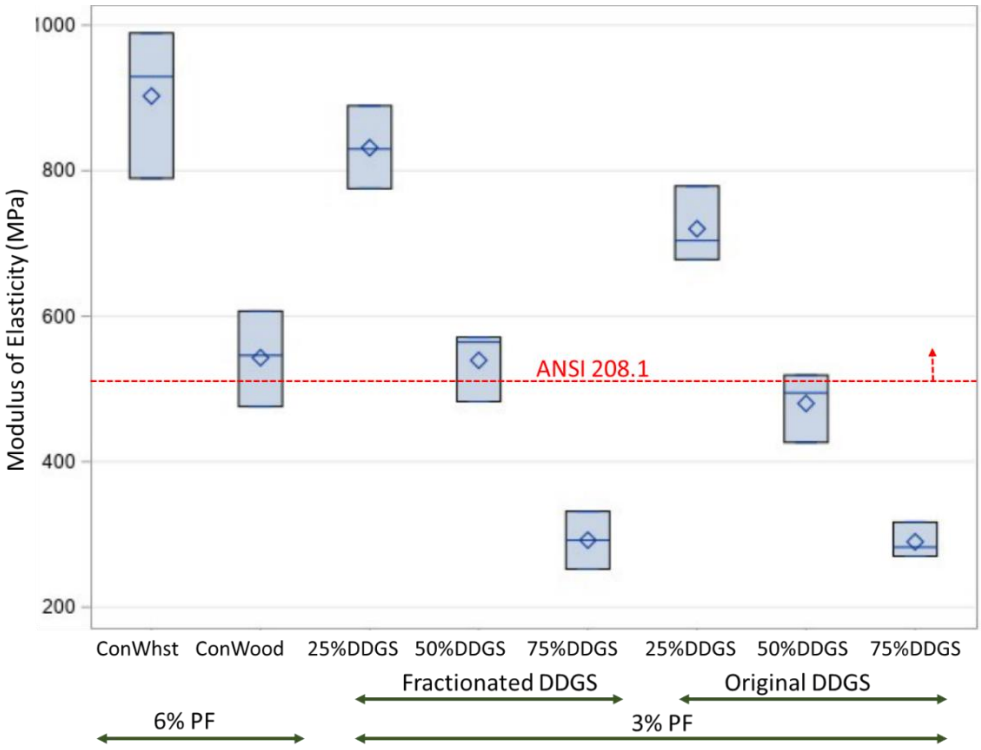

Figure 4.14: Boxplot of modulus of elasticity
PF = Phenol Formaldehyde, ANSI 208.1 standard for low-density particleboards for modulus of elasticity is 500 MPa and direction of arrow shows the acceptable range

The boxplot shows that changes were primarily caused by DDGS loading concentration rather than DDGS type (i.e. high fiber or #20-lighter DDGS and original DDGS). The ANOVA shows that the MOE value for particleboards from the 25% fractionated DDGS loading was not statistically different from the control wheat straw and significantly higher than the control wood. For both the original DDGS and the fractionated DDGS, the MOE values decreased with an increase in DDGS concentration. The MOE values at 50% and 75% DDGS loading were not significantly different for fractionated DDGS and original DDGS. However, the MOE value was

significantly higher for fractionated DDGS boards at 25% DDGS loading compared to original DDGS boards. The high MOE values with wheat straw based particleboards compared to wood based boards are associated with the high aspect ratio (length to diameter of fiber) of the wheat straw fibers making them stiffer (Rowell et al., 1995). The model accuracy was given by R^2 = 95.36%, indicating a good estimator of the variability in the modulus of elasticity (MOE) properties.

4.3.4.2. Modulus of rupture (MOR)

Modulus of rupture represents the maximum flexural strength that the board can experience before failure. Figure 4.15 shows the boxplot constructed for the average values of MOR and the general spread of data for each formulation.

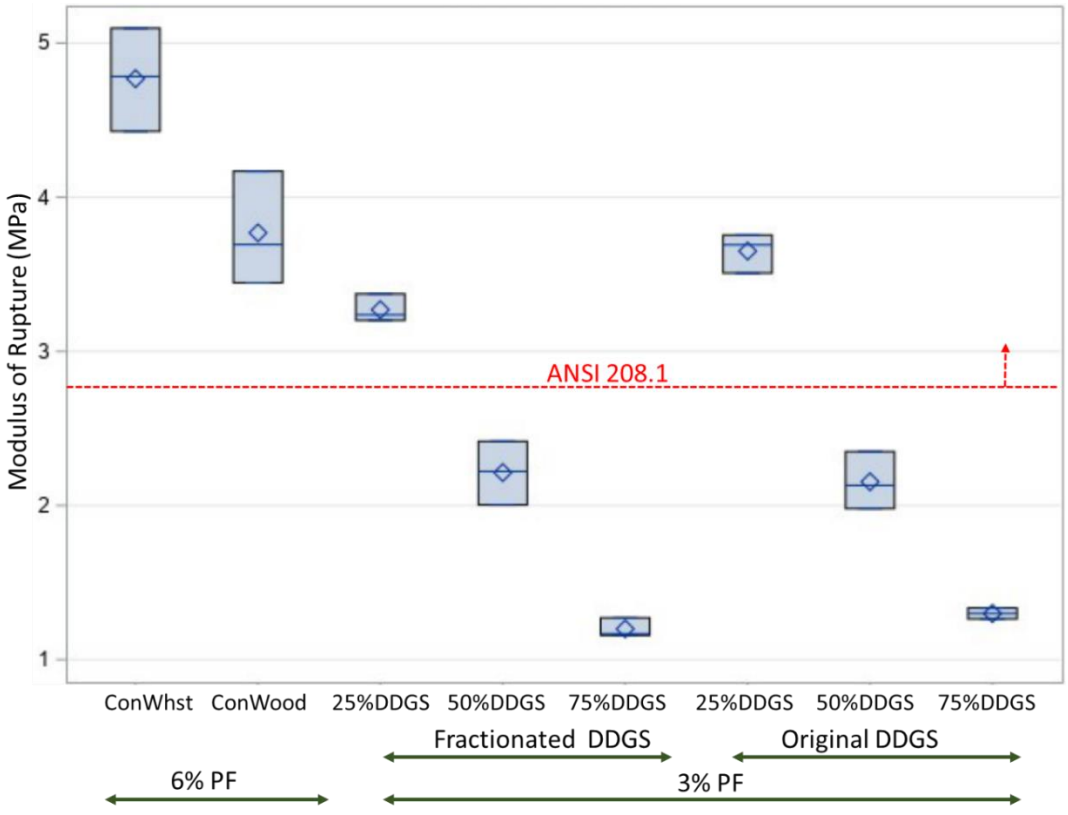

Figure 4.15: Boxplot of modulus of rupture
PF = Phenol Formaldehyde, ANSI 208.1 standard for low-density particleboards for modulus of rupture is 2.8 MPa and direction of arrow shows the acceptable range

The boxplot shows that changes were primarily caused by DDGS loading concentration rather than DDGS fiber content. The MOR value for particleboards from 25% original DDGS loading was not statistically different from control wood. Control wheat straw boards had superior MOR performance than any other treatments. The high MOR values with wheat straw based particleboards are also associated with the high aspect ratio (length to the diameter of fiber) of the wheat straw fibers that make the particleboards stronger and rigid (Rowell et al., 1995). For both original DDGS and fractionated DDGS, the MOR values decreased with an increase in DDGS concentration. Similar to the MOE values, the MOR values at 50% and 75% DDGS loading were not significantly different for fractionated DDGS and original DDGS. The MOR value at 25% DDGS loading, however, was significantly higher for original DDGS boards as compared to fractionated DDGS boards, may be because of particle morphology. The model accuracy was given by R^2 = 98.31%, indicating a good estimator of the variability in the modulus of elasticity (MOE) properties.

4.3.5. Internal bond results

Internal bonding or tension perpendicular to surface was conducted to test the effect of DDGS loading as well as DDGS fiber content on the board's resistance to internal failure. Internal bond strength shows the adhesion of fibers within the boards. Two samples from all the three boards for each treatment were tested and ANOVA was done to determine the significant factors influencing internal bonding with a 95% confidence interval. A boxplot was created to show the average value and deviation for each treatment as show in Figure 4.16.

The drastic decrease in the IB value of control wheat straw boards compared to control wood boards is likely because of the surface wax of wheat straw, which is one of the main adhesion inhibitors in its use as a raw material for particleboard (Zhang et al., 2003). Boquillon

et al. (2004) reported that wheat straw has an outer layer with very low porosity which disrupts resin penetration. Moreover, the rate of resin penetration into straw was recently observed to be several orders of magnitude slower than that into wood (Tabarsa et al., 2011). All the boards with fractionated DDGS and boards with 25% original DDGS had similar IB values compared to control wheat straw, which suggests that the DDGS zein protein can be used as a natural binder, reducing the PF content by 50% in control wheat straw boards. Boards with 50% and 75% DDGS loadings with original DDGS had even better performance as compared to control wheat straw. All the boards with original DDGS had better IB properties compared to boards with fractionated DDGS. This is because of the higher protein content in original DDGS which acted as natural binder during higher temperatures of hot press operations. Besides higher protein, the variable size of particles in original DDGS may have contributed to significant IB values in its 50% and 75% loaded particleboards. During heating, the formation of 'liquid-gel' is easier for smaller particles which upon cooling, transitions back to solid state giving better adhesive properties (Tisserat, et al., 2018). The R-Square value for this model prediction was 98.47%, suggesting that this model is a good estimator of variability in internal bond strength values of the manufactured particleboards.

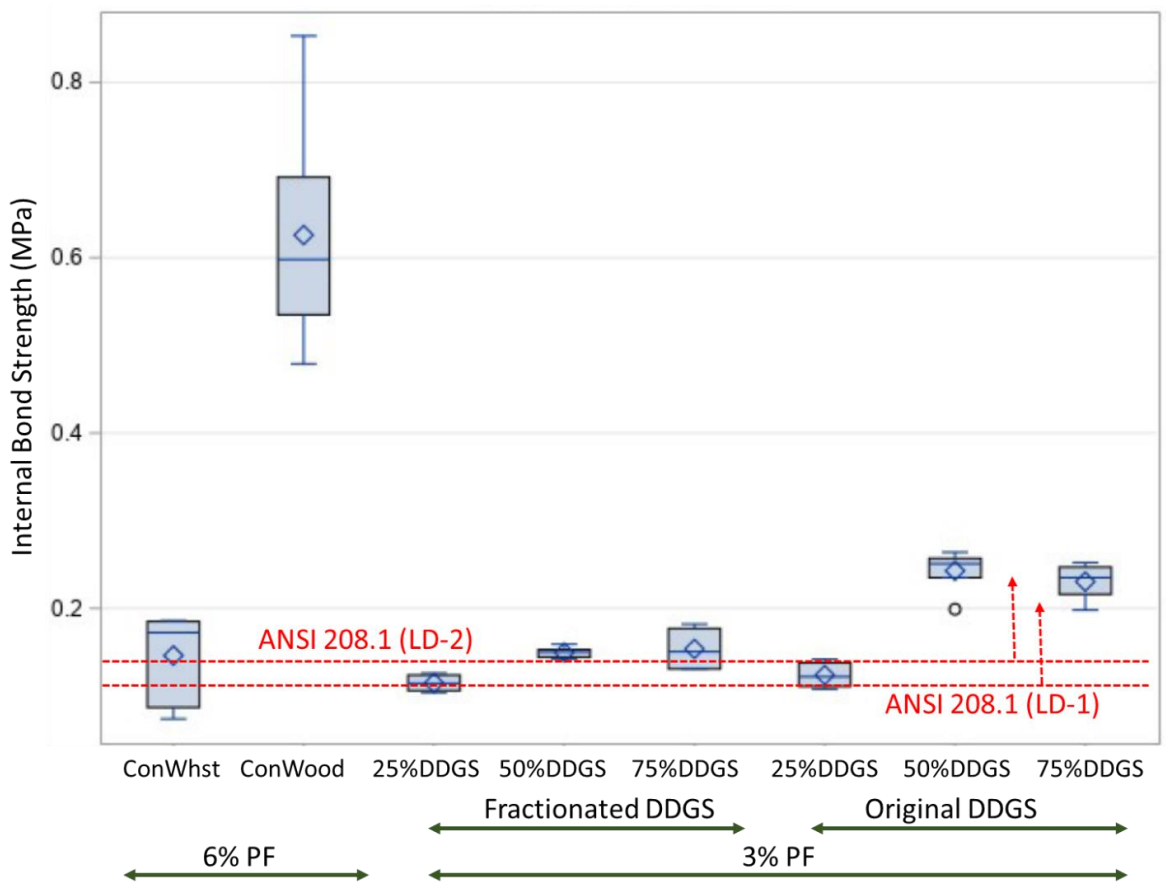

Figure 4.16: Boxplot of internal bond strength

PF = Phenol Formaldehyde, ANSI 208.1 standard for low-density particleboards for internal bonds are 0.1 MPa and 0.14 MPa respectively for LD-1 and LD-2, and direction of arrow shows the acceptable range

4.3.6. Direct screw withdrawal results

Screw withdrawal test shows the resistance to fastener withdrawal from the face of the board. This test was conducted to determine the effect of DDGS loading and fiber content on screw withdrawal resistance. Three samples from each board were tested for screw withdrawal with an average load determined for each formulation. ANOVA analysis was used to determine the significant factors influencing the screw withdrawal resistance at a 95% confidence level. A boxplot was constructed (Figure 4.17) showing the average values for the direct screw withdrawal load and the general spread of data for each formulation.

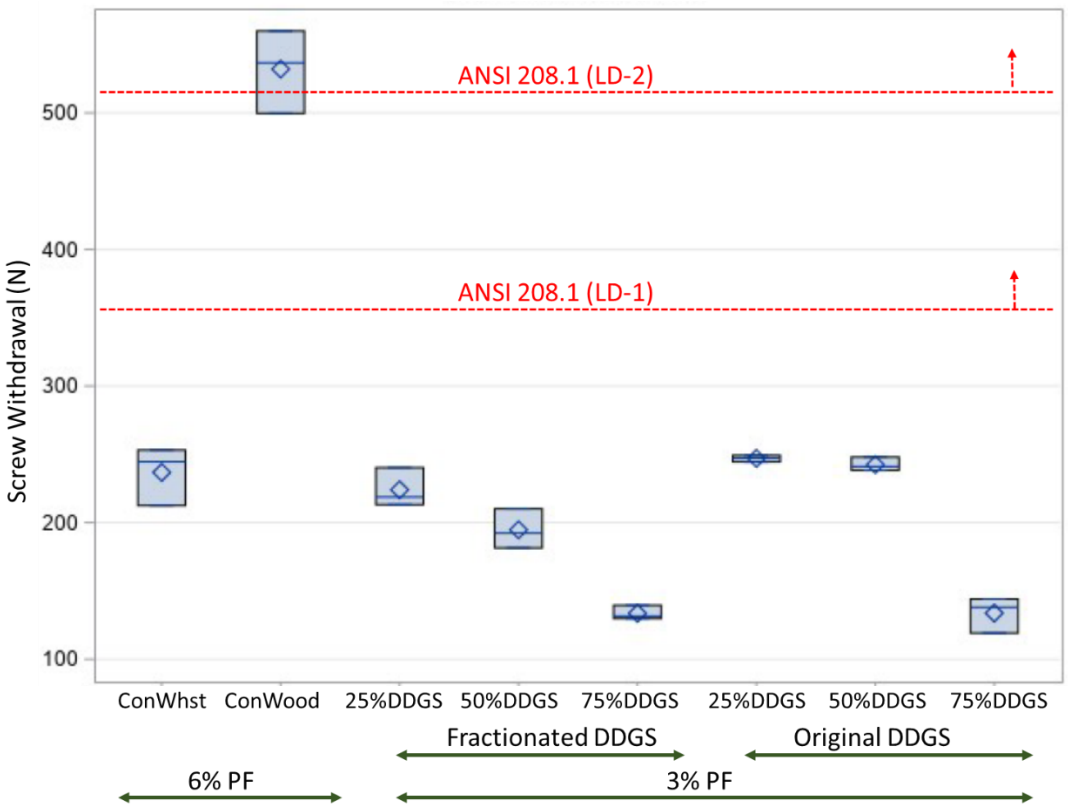

Figure 4.17: Boxplot of screw withdrawal force
PF = Phenol Formaldehyde, ANSI 208.1 standard for low-density particleboards for screw withdraw are 360 N and 520 N respectively for LD-1 and LD-2, and direction of arrow shows the acceptable range

Only control wood boards met the ANSI 208.1 standard for low-density particleboards for screw withdrawal results. However, the boards from both fractionated DDGS and original DDGS at 25% DDGS loading had comparable screw withdrawal properties to control wheat straw boards. At the same concentration level, the means for original DDGS based particleboards and fractionated DDGS based particleboards were not significantly different. This suggests that DDGS loading is a more important factor in screw withdrawal properties, than NDF content on the DDGS. For screw withdrawal, the model accuracy for ANOVA method was R^2 = 98.96%, suggesting that this model is a good estimator of variability in screw withdrawal strength values of the manufactured particleboards.

4.3.7. Hardness results

Hardness testing was conducted to determine the effect of DDGS loading and DDGS types (original DDGS vs high fiber DDGS) on manufactured boards. The hardness test shows the local resistance to deformation for the face of the board. Four samples from each treatment were tested for the hardness load with an average load determined for each formulation. ANOVA analysis was used to determine the significant factors in influencing the hardness with a 95% confidence interval. A boxplot was constructed to show the variation from as well as within each treatment as shown in Figure 4.18.

The hardness value for the boards from original DDGS at 25% DDGS loading had comparable results to both control wheat straw and control wood boards. The boards from the original DDGS had better properties to that of fractionated DDGS at all concentration levels, and this is most likely because of smaller size particles present on the original DDGS going into the wheat straw fibers to avoid the void spaces. In line with other mechanical properties (except IB), hardness values also decreased with an increase in DDGS loading for both original as well as fractionated DDGS. For hardness, the model accuracy for ANOVA method was R^2 = 94.62%, suggesting that this model is a good estimator of variability in hardness values of the manufactured particleboards.

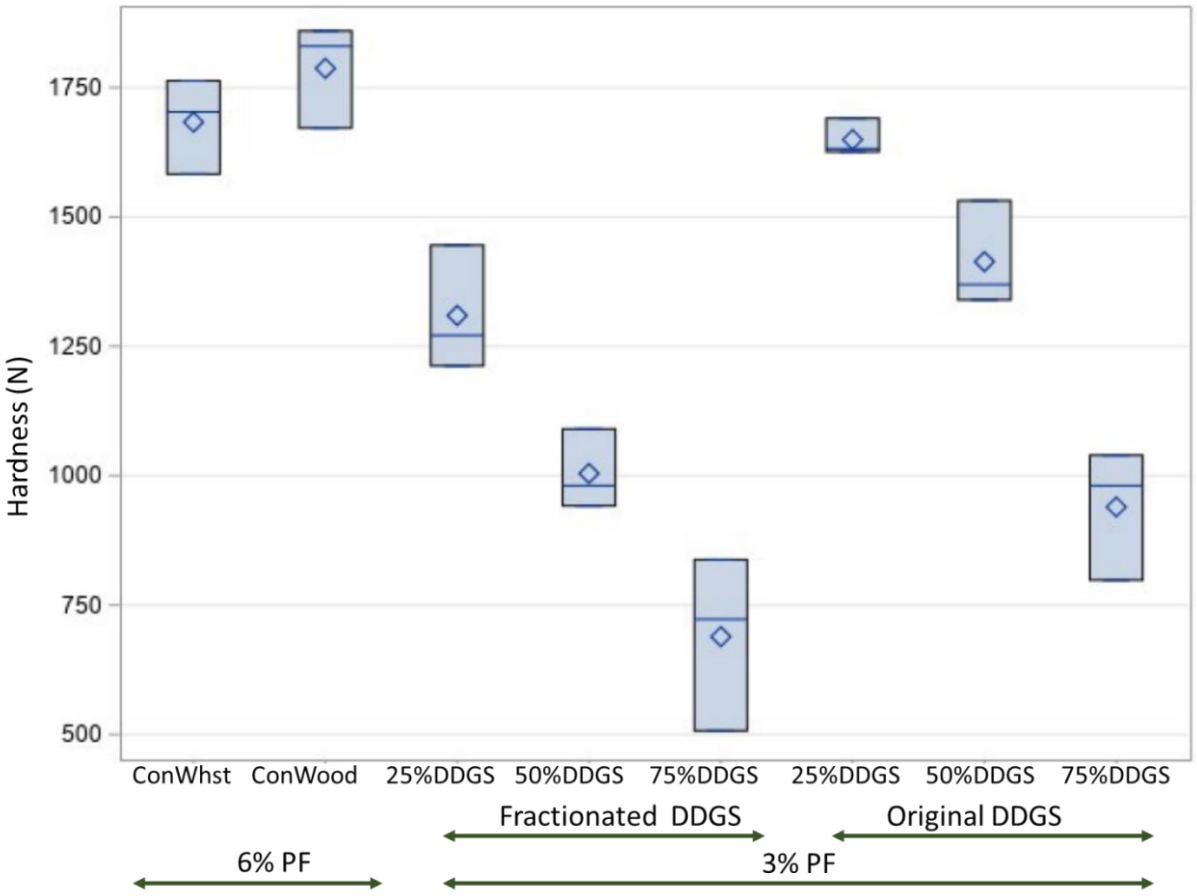

Figure 4.18: Boxplot of hardness
PF = Phenol Formaldehyde, There is no ANSI 208.1 standard for low-density particleboards for hardness

4.4. Effect of pretreatment

Particleboards were manufactured with and without alkaline treatment to study the effect of alkaline pretreatment of DDGS and wheat straw for properties of manufactured particleboards. 25% DDGS loading was applied in all cases, with 75% wheat straw. The amount of phenol-formaldehyde used for the boards (if used) was the same as in the case of fractionated DDGS-based boards (i.e., 3% db.). For all the treatments, density, internal bond strength, screw withdrawal force, modulus of elasticity, and modulus of rupture were calculated.

Table 4.4 below summarizes the properties of boards with different loading of sodium hydroxide pretreatment. Note that the concentration of NaOH used was 2M.

Table 4.4: Properties of particleboards with alkaline pretreated (2M NaOH) DDGS and wheat straw

Treatment	Density(kg/m3)	IB(MPa)	Screw withdrawal(N)	MOE (MPa)	MOR (MPa)
ANSI for LD1,LD2	<640	0.1,0.14	360,520	500	2.8
PF only (no NaOH)	614.92±17.57[a]	0.115±0.008[a]	230.80±15.45[b]	831.53±46.52[a]	3.27±0.07[a]
10% NaOH+PF	603.1±12.12[a]	0.067±0.010[b]	297.03±28.65[a]	463.08±25.64[b]	2.05±0.03[b]
15% NaOH+PF	631.50±19.35[a]	0.051±0.003[c]	248.26±18.48[b]	422.05±5.16[b]	1.60±0.15[c]
20% NaOH+PF	604.49±18.05[a]	0.004±0.005[c]	241.64±22.68[b]	416.11±26.26[b]	1.85±0.06[d]
Only NaOH 20%	622.84±26.35[a]	0.021±0.005[d]	113.98±2.24[c]	249.93±35.13[c]	0.84±0.08[e]

4.4.1. Modulus of elasticity

Modulus of elasticity represents the stiffness that the board has during initial loading before unrecovered deformation occurs. Figure 4.19 shows the boxplot constructed for the average values of MOE and the general spread of data for each formulation.

The boxplot shows that changes were primarily caused by the NaOH loading concentration. The model accuracy was given by R^2 = 98.61%, indicating a good estimator of the variability in the modulus of elasticity (MOE) properties. The modulus of elasticity of the boards decreased with an increase in sodium hydroxide loading. Since the values are decreasing with increasing NaOH loadings, it can be said that NaOH loading deteriorated the performance of the boards. This result is in opposition to the findings of Liaw et al. (2019) where they found that 20% NaOH loading for DDGS and wood improved the mechanical properties. This is most probably because of the different nature of wood and wheat straw. Wheat straw has low levels of cellulose and lignin and high levels of ash content as well as high silica content, which reduces the interactions with polar adhesives (Ndazi et al., 2007).

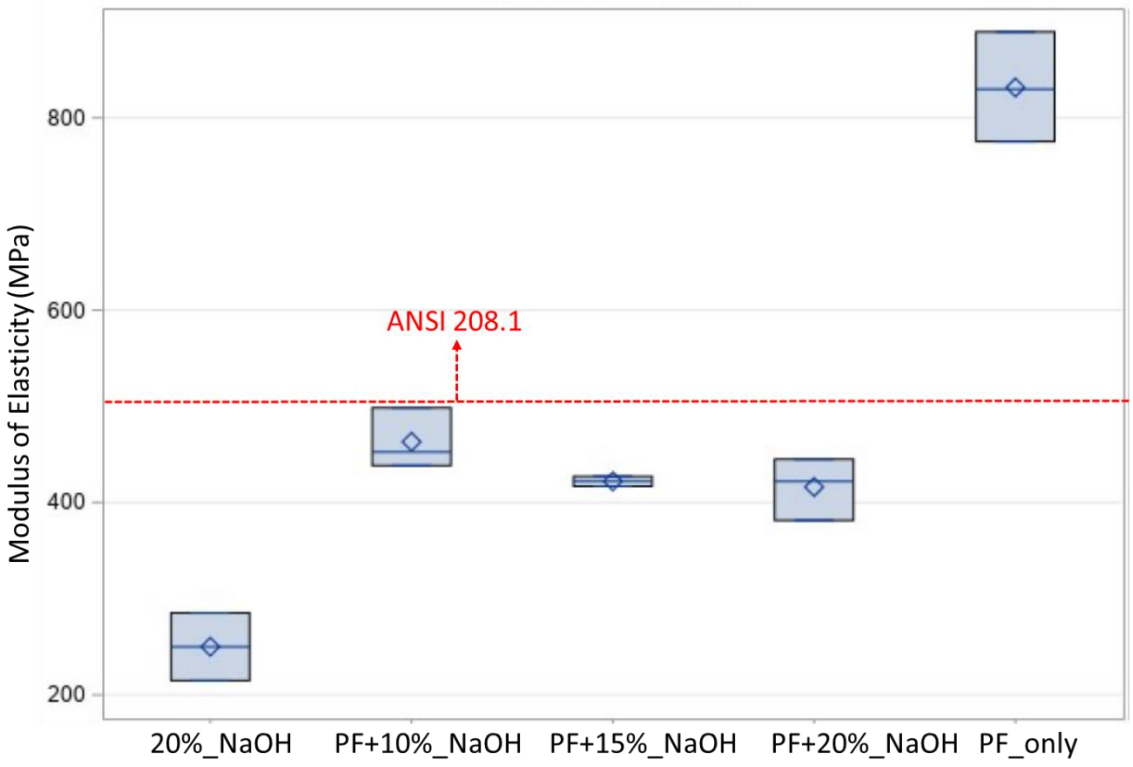

Figure 4.19: Modulus of elasticity of particleboards with pretreated biomass
PF = Phenol Formaldehyde, ANSI 208.1 standard for low-density particleboards for modulus of elasticity is 500 MPa and direction of arrow shows the acceptable range

4.4.2. Modulus of rupture

Modulus of rupture (MOR) represents the maximum flexural strength that the board can experience before failure. Figure 4.20 shows the boxplot constructed for the average values of MOR and the general spread of data for each formulation.

The boxplot shows that changes were caused mostly by the choice of NaOH loading concentration. The model accuracy was given by R^2 = 99.18%, indicating a good estimator of the variability in the modulus of rupture properties. Wheat straw has a high silica and ash content. As the material was not washed after the alkaline pretreatment, this deteriorated performance might be because of the spread of ash and silica over the surface and degradation of lignin, which can also be seen on the SEM-EDX results for pretreated wheatstraw.

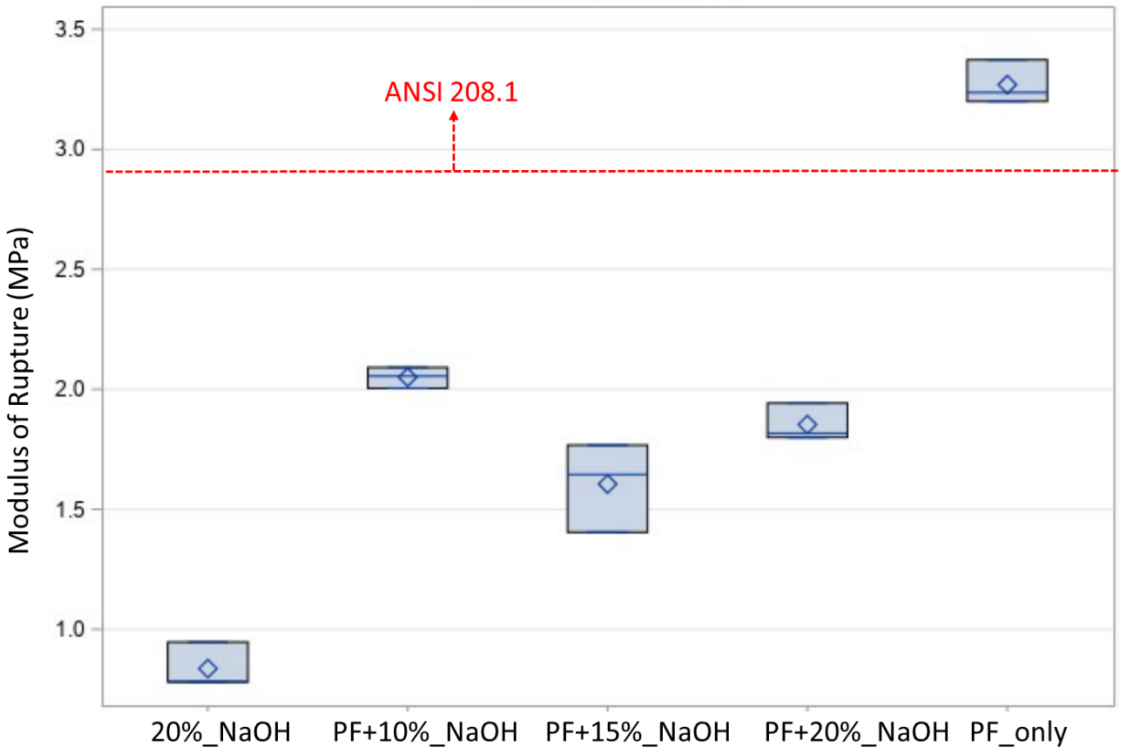

Figure 4.20: Modulus of rupture of boards from pretreated biomass
PF = Phenol Formaldehyde, ANSI 208.1 standard for low-density particleboards for modulus of rupture is 2.8 MPa and direction of arrow shows the acceptable range

4.4.3. Screw withdrawal force

Screw withdrawal test shows the resistance to fastener withdrawal from the face of the board. This test was conducted to determine the effect of pretreatment loading on screw withdrawal resistance. Four samples from each board were tested for screw withdrawal with an average load determined for each formulation. ANOVA analysis was used to determine the significant factors influencing the screw withdrawal resistance at a 95% confidence level. A boxplot was constructed (Figure 4.21) showing the average values for the direct screw withdrawal load and the general spread of data for each formulation.

For screw withdrawal, the model accuracy for ANOVA method was R^2 = 92.26 %, suggesting that this model is a good estimator of variability in screw withdrawal strength values

of the manufactured particleboards. The screw withdrawal properties of boards with sodium hydroxide has a slightly better results, the reasons are not clear at the present moment.

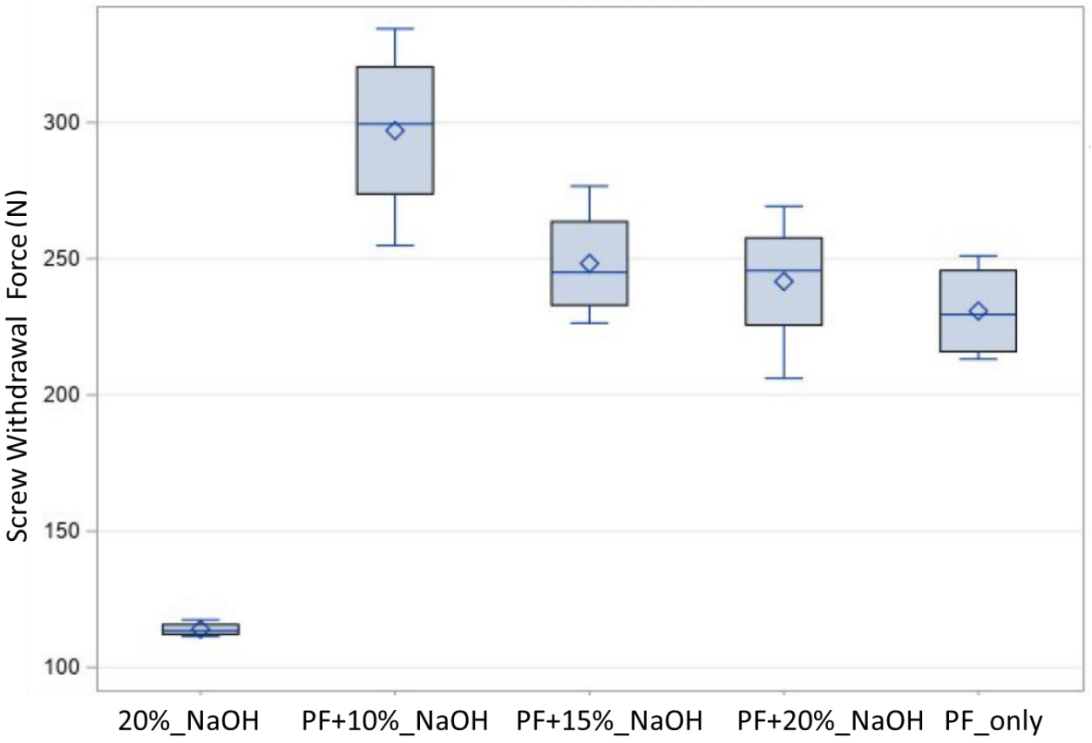

Figure 4.21: Screw withdrawal force of boards with pretreated biomass

4.4.4. Internal bond strength

Internal bonding or tension perpendicular to surface was conducted to test the effect of NaOH loading on the board's resistance to internal failure. Internal bond strength shows the adhesion of fibers within the boards. Two samples from all the three boards for each treatment were tested and ANOVA was done to determine the significant factors influencing internal bonding with a 95% confidence interval. A boxplot was created to show the average value and deviation for each treatment as shown in Figure 4.22.

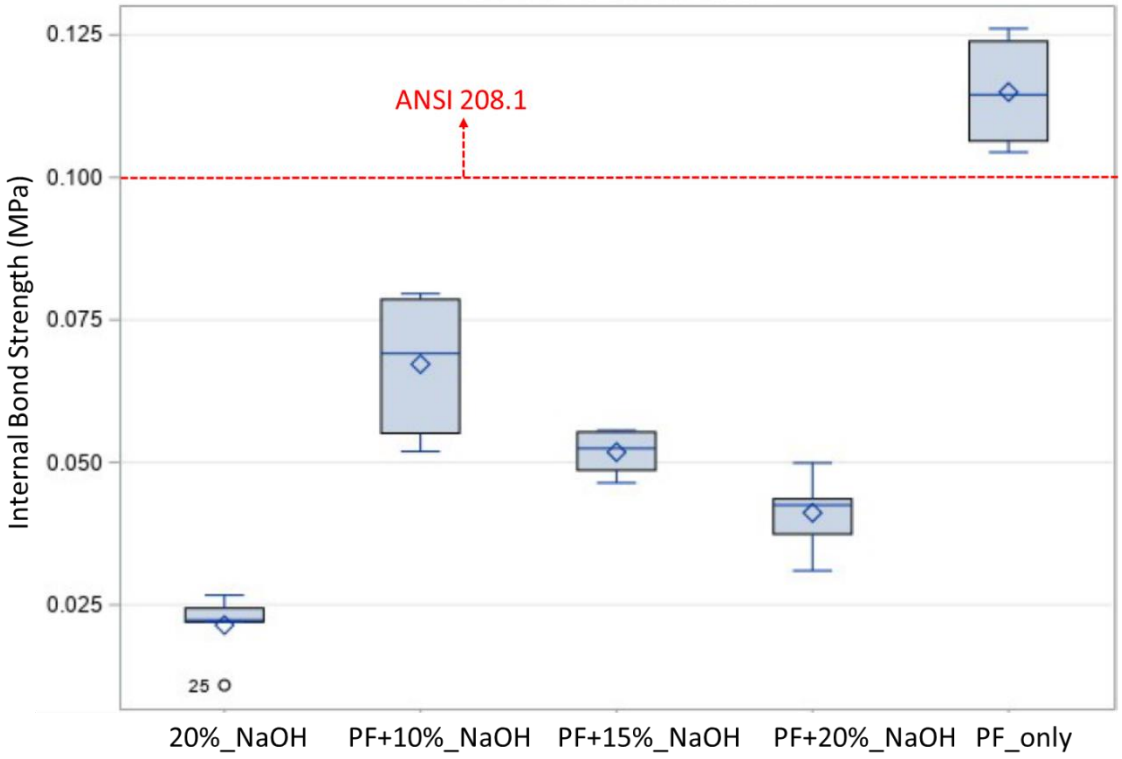

Figure 4.22: Internal bond strength of boards with pretreated biomass

The R-Square value for this model prediction was 98.47%, suggesting that this model is a good estimator of variability in internal bond strength values of the manufactured particleboards. There is a decreasing trend of internal bond strength with the increase in NaOH loading, suggesting that NaOH loading has an obstructive effect on bonding properties. The purpose of NaOH treatment is to expose the abundantly available polar groups for adhesion (Wang and Sun, 2002), but since the biomass was not washed after NaOH spray, the wax, ash, and silica might have been exposed.

In our study, we found that all the mechanical properties of the manufactured particleboards decreased with the use of 2M NaOH pretreatment at the ratio of 4:1 (biomass:NaOH) for only one day. Severity of NaOH pretreatment depends on the concentration of NaOH, loading ratio, pretreatment time, pretreatment condition (i.e., temperature and pressure), and washing off the degraded hemicellulose. In our case, we did not wash the

pretreated biomass, rather, we just sprayed it on the surface of biomass (here the biomass is mixture of DDGS and wheat straw) while the biomass was mixed in a cement mixture. A study by Cao et al., (2017) found that spraying of NaOH in to wheat straw increased the mechanical properties of manufactured particleboards with MDI resin. In their study they used 1 wt%, 2 wt%,a nd 3 wt% NaOH in the ratio of 1 mL NaOH to 1 g wheat straw. Here the severity of NaOH is higher because higher ratio of NaOH to biomass was used. And they used only wheat straw while in our study the biomass was a mixture of DDGS and wheatstraw.

Conventional practices usually use a higher ratio of NaOH (for eg 1:10) and follow by washing to remove the alkali once the soaking is done (Ciannamea et al., 2010). Doing this allows enough time and surface area to facilitate adhesive nature of the fiber surface by removing natural and artificial impurities, and cause the separation of structural linkages between lignin carbohydrate and disruption of lignin structure (Ciannamea et al., 2010; Ndazi et al., 2007). In our case we used biomass to NaOH ratio of 4:1. Lower quantity of NaOH used might be a reason for ineffectiveness of alkaline pretreatment in our study. It does not mean that higher loading of NaOH will necessarily improve the mechanical properties of particleboards. In some studies, higher loading of NaOH has been found to deteriorate the performance of manufactured particleboards. Using 1 M NaOH at the loading rate of 1g biomass to 10 mL NaOH, Zheng et al., (2007) found that particleboards manufactured from Jose Tall Wheatgrass (JTW) with NaOH treated particles had lower qualities than those made from untreated particles for both UF and PMDI resin bonded boards. It was believed that the NaOH may have reacted with some components of JTW and changed surface structure of JTW preventing adhesives from bonding with JTW particles. To figure out the exact reasons for decreasing performance of manufactured particleboards with NaOH pretreatment, material characterization using FTIR and

SEM-EDX can helpful. Also, further study can be done using different severity of NaOH to study the effects.

4.4.5. Fourier transform infrared spectroscopy of pretreated and untreated samples

Fourier transform infrared spectroscopy was used to determine what the functional groups of biomass (i.e. DDGS and wheat straw) are before and after the sodium hydroxide pretreatment. For DDGS, the broad band centered around 3350 cm^{-1} was assigned to the stretching vibration of – OH and – NH from carbohydrates and protein abundantly present in lignocellulosic materials (Li et al., 2014), the peak around 2950 cm^{-1} to the stretching of –CH from lipids, the peak at 1650 cm^{-1} to the amide I absorption of corn protein, and the peaks at the region of 1250 -1000 cm^{-1} to carbohydrates. These results confirm that DDGS is composed of carbohydrates, protein, and lipids. The peak around 2950 cm^{-1} to the stretching of –CH from lipids was smaller for wheat straw compared to DDGS, suggesting that wheat straw has less lipids. All spectra showed characteristic H–bonding and –OH stretching absorption around 3300 to 3500 cm^{-1} and is identified as –OH of carbohydrate overlapping the protein –NHs. For DDGS, a residual ester or lignocellulosic carbonyl and protein bands occur at 1738 cm^{-1} (–C=O, medium carbonyl band either from lignin or uronic esters), and 1656 cm^{-1} (N–C=O, amide I) (Tisserat et. al., 2018).

The FTIR spectra of both the original DDGS and SA#20-L DDGS are similar to their pretreated parts. However, there was a slight change in the peak at 1081 cm^{-1} (–CHO–), the peak being larger for pretreated sample compared to their untreated counterparts. The peaks near 2850 and 2920 cm^{-1}, which can be attributed to the symmetric and asymmetric stretching of C–H bonds, is prominent on DDGS based samples but not in wheat straw based samples. The same phenomenon is observed with the stretching absorption of carbonyl (C=O) bond at

approximately 1740 cm^{-1}, which is associated with the ester group of triglyceride in lipid (fat) (Craig et al., 2012).

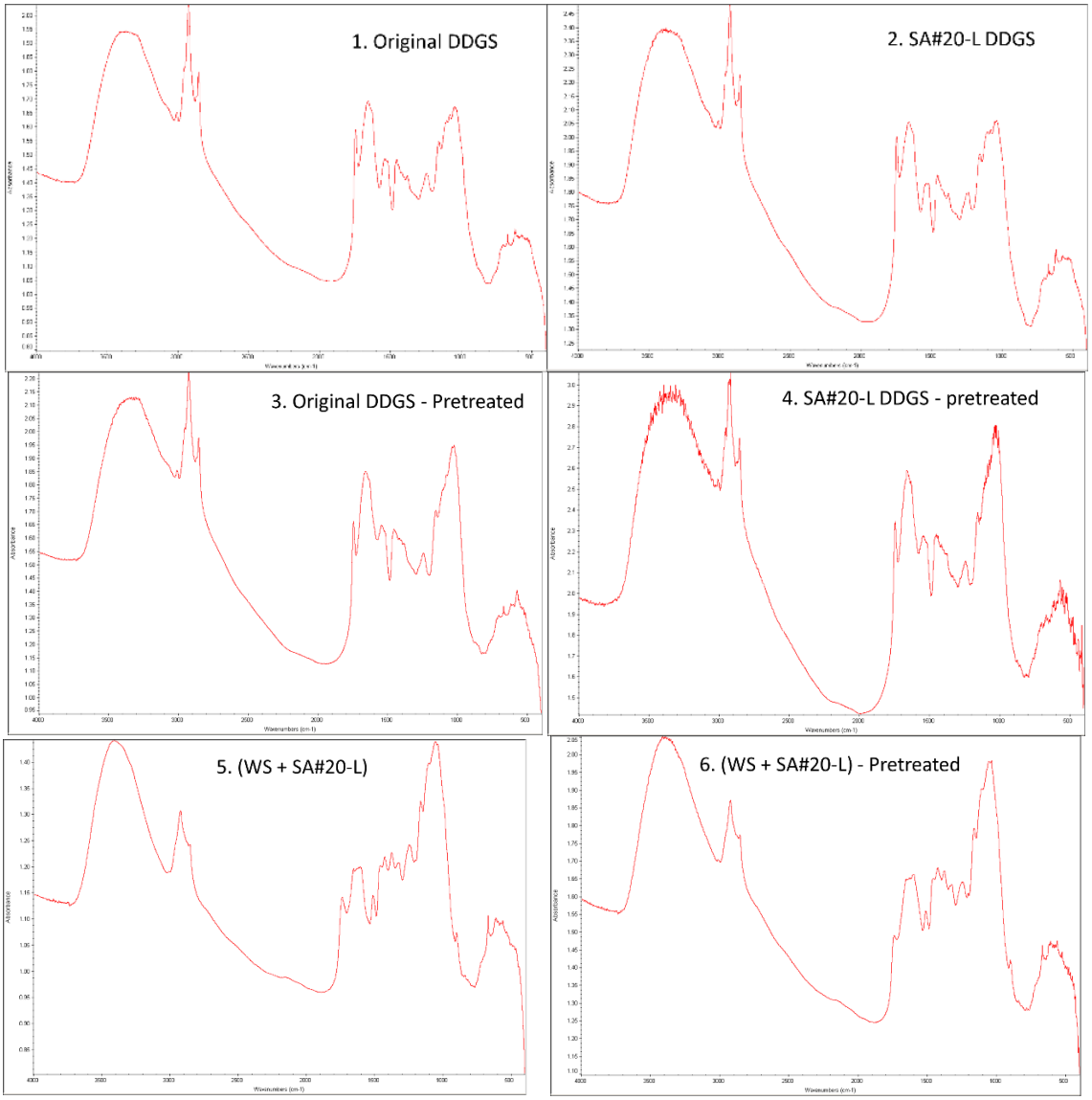

Figure 4.23: FTIR images of different samples
1. untreated orginal DDGS, 2. number 20 sieved lighter fraction of DDGS, 3. untreated orginal DDGS, 4. Pretreated number 20 sieved lighter fraction of DDGS, 5. mixture of aspirated lighter fraction of number 20 sieved DDGS and wheat straw, 6. pretreated (NaOH 2M) mixture of wheat straw and number 20 lighter DDGS

The absorption peaks at 1650 cm^{-1} and 1050 cm^{-1} for original DDGS and sieved and aspirated lighter fraction of number 20 DDGS are different, with original DDGS having a larger

peak (Figure 4.23). Both DDGS samples had increased peaks at these wavenumbers (1650 cm^{-1} and 1050 cm^{-1}) with 2M NaOH pretreatment. Since the peak at 1631 cm^{-1} represents the bands of protein related to C=O absorptions (Zarrinbakhsh et al., 2013), it can be said that more protein of DDGS was exposed after pretreatment with NaOH. However, there was no major difference on peaks between the FTIR images of mixture of wheat straw and SA#20-L DDGS and 2M NaOH pretreated mixture of wheat straw and SA#20-L DDGS (Figure 4.23).

4.4.6. Energy-dispersive X- ray (EDX) and scanning electron microscope (SEM) results

Scanning electron microscopy (SEM) was used to investigate the surface morphology of different biomass particles (wood, wheat straw, and DDGS) and the change in structure caused by sodium hydroxide pretreatment of DDGS and wheat straw. DDGS exists in irregular shapes and various sizes and has coarse surfaces. SEM images suggest that pretreatment did not degrade the surface structure by chemical etching after treatement, because there were not significant changes on the surface morphology of the pretreated biomass. The brighter and smooth surface of pretreated DDGS suggested that there is some peeling effect caused by the 2M NaOH pretreatment on the surface of DDGS (Figure 4.24).

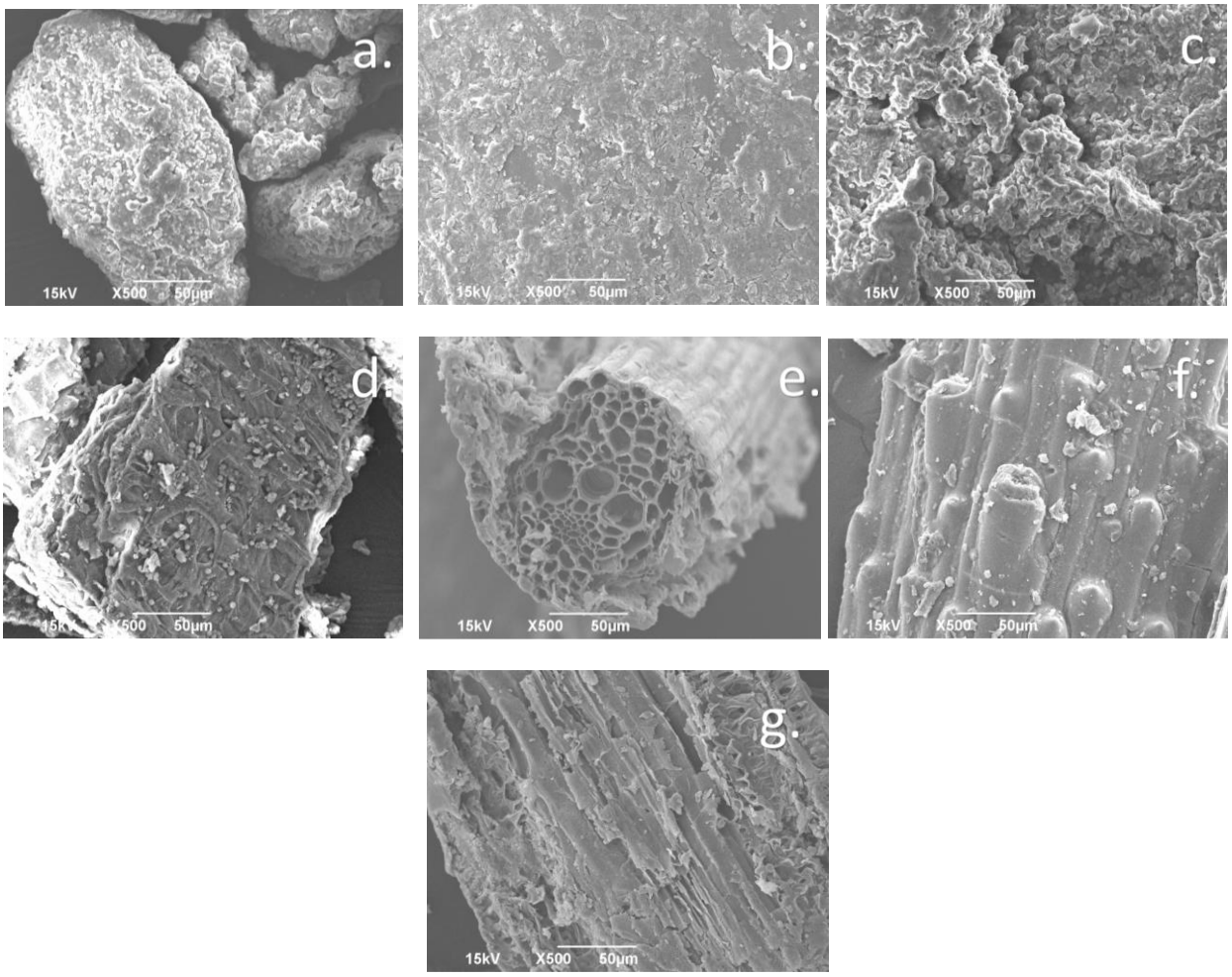

Figure 4.24: Scanning electron microscopy of different particles
a. original DDGS, b. pretreated original DDGS, c. SA#20-L DDGS, d. pretreated SA#20-L DDGS, e. wheat straw, f. mixture of SA#20-L DDGS and wheat straw, g. mixture of pretreated wheat straw and SA#20-L DDGS

Energy-dispersive X-ray (EDX) was used to obtain the elemental spectrum from various spots on the surface of DDGS and wheat straw particles (APPENDIX: B). With respect to the EDX results, it was found that the spectrum obtained was dependent on the spot investigated and that the compositional make-up changed from point to point on the sample. This can be attributed to the inhomogeneity of particles and to the fact that the EDX signal is collected only from the surface of a particular specimen. All DDGS samples showed the presence of carbon, oxygen, potassium, phosphorus, and trace amounts of sodium, magnesium, and sulfur. The wheat

straw samples had carbon, nitrogen, oxygen, sodium, magnesium, silicon , and trace amounts of potassium, phosphorus, and calcium.

The energy-dispersive X-ray (EDX) results for different samples show that wheat straw has some amount of silica attached to its surface. And when this wheat straw is subjected to alkaline pretreatment, the silica layer from the wheat straw fiber get spread into its surface, which hinders the bonding performace of pretreated wheat straw surface with the synthetic resin (Ndazi et al., 2007). Hague et al., (1998) also identified wax and inorganic silica on the surfaces of wheat-straw particles as barriers to conventional water-based resins. Table 4.5 shows the weight percentage of silica present on different wheat straw samples taken at various point of SEM (for more details of individual samples please refer to the Appendix E: Energy-dispersive X-ray (EDX) results).

Except for slight changes in silica and calcium content, there was not any significant changes on elemental composition between untreated and NaOH treated samples. No significant changes on C and O content of the pretreated samples, suggest that the surface of DDGS samples were not changed much by NaOH pretreatment.

Table 4.5: Energy-dispersice X-ray (EDX) results for constituent of different wheat straw samples

Component	Samples	Component content (wt %)							
		Pt (1)	Pt (2)	Pt (3)	Pt (4)	Pt (5)	Pt (6)	Pt (7)	Pt (8)
Silica (Si)	Original DDGS	-	-	-	-	-	-	-	-
	#20-L DDGS	X	X	X	X	0.70	X	-	-
	Prt original DDGS	-	-	-	-	-	-	-	-
	Prt #20-L DDGS	X	5.67	X	X	X	X	X	-
	WS only	2.52	X	1.78	0.78	1.61	7.97	-	-
	WS and #20-L DDGS	X	X	10.86	23.78	0.68	1.45	-	-
	Prt WS and #20-L DDGS	28.39	12.45	4.67	X	28.79	-	-	-
Carbon (C)	Original DDGS	47.29	35.52	44.81	37.21	40.84	-	-	-
	#20-L DDGS	33.77	38.51	34.37	13.52	47.53	39.22	-	-
	Prt original DDGS	36.81	23.80	36.49	37.57	37.30	-	-	-
	Prt #20-L DDGS	33.01	45.02	33.59	26.28	35.89	40.44	35.86	-
	WS only	32.37	18.20	34.66	30.79	29.93	34.66	-	-
	WS and #20-L DDGS	32.31	35.25	35.03	32.77	39.05	37.70	-	-
	Prt WS and #20-L DDGS	21.69	29.46	35.34	24.47	19.21	-	-	-
Oxygen (O)	Original DDGS	38.86	60.30	48.02	46.38	45.70	-	-	-
	#20-L DDGS	38.80	47.31	58.96	36.70	34.71	52.96	-	-
	Prt original DDGS	51.59	42.35	48.37	43.79	45.37	-	-	-
	Prt #20-L DDGS	51.92	46.96	57.44	46.53	53.66	46.69	42.18	-
	WS only	60.89	49.73	61.12	47.33	36.77	48.50	-	-
	WS and #20-L DDGS	59.66	61.53	50.64	38.56	45.25	50.92	-	-
	Prt WS and #20-L DDGS	42.48	53.70	51.25	34.15	43.13	-	-	-
Nitrogen (N)	Original DDGS	-	-	-	-	-	-	-	-
	#20-L DDGS	-	-	-	-	-	-	-	-
	Prt original DDGS	X	3.08	8.34	8.38	8.38	-	-	-
	Prt #20-L DDGS	X	X	X	X	X	10.35	5.87	-
	WS only	X	8.99	X	4.40	4.81	X	-	-
	WS and #20-L DDGS	X	X	X	X	9.84	7.83	-	-
	Prt WS and #20-L DDGS	X	X	X	5.83	4.82	-	-	-
Almunium (Al)	Original DDGS	0.22	X	1.42	0.27	0.50	-	-	-
	#20-L DDGS	0.19	0.44	X	X	X	X	-	-
	Prt original DDGS	X	X	0.29	0.13	0.23	-	-	-
	Prt #20-L DDGS	0.17	0.17	X	0.14	0.28	0.35	0.28	-
	WS only	0.55	X	0.74	0.25	0.33	1.85	-	-
	WS and #20-L DDGS	X	0.83	X	0.85	X	X	-	-
	Prt WS and #20-L DDGS	0.40	0.33	X	1.07	2.34	-	-	-
Potassium (K)	Original DDGS	5.78	2.48	3.81	3.71	1.04	-	-	-
	#20-L DDGS	14.20	5.66	4.27	27.96	7.36	3.49	-	-
	Prt original DDGS	4.51	6.06	2.91	3.05	2.76	-	-	-
	Prt #20-L DDGS	3.83	0.92	1.82	6.51	2.15	0.72	5.51	-
	WS only	3.67	23.08	1.69	3.21	7.32	7.01	-	-
	WS and #20-L DDGS	3.23	2.39	1.98	3.40	1.51	1.57	-	-
	Prt WS and #20-L DDGS	4.49	1.53	3.65	4.45	13.70	-	-	-
Magnesium (Mg)	Original DDGS	1.09	0.69	X	0.68	0.82	-	-	-
	#20-L DDGS	0.84	1.15	0.93	1.45	0.72	1.63	-	-
	Prt original DDGS	0.77	8.73	X	0.50	X	-	-	-
	Prt #20-L DDGS	3.13	0.41	0.40	5.31	X	0.65	2.45	-
	WS only	X	X	X	4.64	5.88	X	-	-
	WS and #20-L DDGS	0.33	X	0.47	0.64	0.43	0.53	-	-
	Prt WS and #20-L DDGS	X	X	0.58	X	2.28	-	-	-
Sodium (Na)	Original DDGS	1.75	1.02	0.94	1.59	0.43	-	-	-
	#20-L DDGS	2.58	1.67	1.47	4.29	1.04	0.88	-	-
	Prt original DDGS	6.32	6.24	3.59	5.05	4.51	-	-	-
	Prt #20-L DDGS	4.89	0.84	6.38	7.02	5.91	0.80	1.24	-
	WS only	X	X	X	1.72	2.51	X	-	-
	WS and #20-L DDGS	4.48	X	1.03	X	1.62	X	-	-
	Prt WS and #20-L DDGS	2.53	2.53	4.51	1.25	0.72	-	-	-

Table 4.5: Energy-dispersice X-ray (EDX) results for constituent of different wheat straw samples (continued)

Component	Samples	Component content (wt %)							
		Pt (1)	Pt (2)	Pt (3)	Pt (4)	Pt (5)	Pt (6)	Pt (7)	Pt (8)
Calcium (Ca)	Original DDGS	-	-	-	-	-	-	-	-
	#20-L DDGS	X	X	X	X	1.38	X	-	-
	Prt original DDGS	-	-	-	-	-	-	-	-
	Prt #20-L DDGS	X	X	X	X	1.71	X	X	-
	Prt #20-H DDGS	0.46	X	X	X	1.10	1.81	X	X
	WS only	X	X	X	2.37	1.82	X	-	-
	WS and #20-L DDGS	X	X	X	X	X	0.31	-	-
	Prt WS and #20-L DDGS	X	X	X	X	6.46	-	-	-

Pt – point, X – element not present at this point, #20-L – Number 20 sieved lighter fraction, #20-H – Number 20 sieved heavier fraction, prt – pretreated with 2M NaOH, WS – Wheat straw

4.5. Economic analysis

It is important to study the economic benefits of using DDGS and wheat straw to reduce the amount of synthetic resins used. The costs of materials used in this experiment are approximated in Table 4.6 and may vary based upon the bulk purchase prices. This study includes the cost of manufacturing $1m^2$ of particleboard for three different treatments: control wood, control wheat straw, and fractionated DDGS loading at 25% concentration. Besides this cost analysis, there are other environmental and health benefits of using a lesser amount of synthetic resins. It is assumed that, with all the treatment, the same manufacturing process and conditions will be used, and the cost of transportation and storage are the same for all the biomass materials (wood, wheat straw, and DDGS). Although, because of the density variation of biomass, transportation and storage can be different. DDGS, having the highest density, can have the least cost of transportation and storage, while wheat straw, having the lowest density, can have the highest cost of transportation and storage. The cost of transportation and storage are, therefore, out of the scope of this study. Also, the economic feasibility of the manufacturing facility was not considered; instead, it was assumed that the existing manufacturing industry could incorporate all different biomass as their raw material. This study did not consider the

fractionation process's cost to separate fiber from DDGS; fractionation of DDGS has been found economical in previous research by Srinivasan et al. (2006).

It should be noted that- to make $1m^2$ boards with a target density of 600 kg/m^3, using a 6 mm thick mold, the approximate mass of the biomass would be 3.77 kg. The prices of all the material were obtained from their respective manufacturers (Tharaldson Ethanol for DDGS, American Wood Fibers for wood flour, Georgia Pacific Resins for phenol-farmaldehyde, and online sellers from farms.com for wheat straw).

Table 4.6: Breakdown of experiment's raw material cost

Component	Cost per kilogram -USD/kg (USD/lb)
DDGS	0.22 (0.10)
Wheat straw	0.18 (0.08)
Wood flour	0.32 (0.15)
Phenol formaldehyde (PF) resin	0.65 (0.30)

Based on these prices, the input material cost to manufacture a control wood panel was calculated at $1.35/square meter, as shown in Table 4.7.

Table 4.7: Input material cost to manufacture a control wood panel

Formulation	Ratio	Cost per meter square (USD)
100% wood	0.88	$0.88 \times 3.77 \times 0.32 = 1.06$
12 % PF	0.12	$0.12 \times 3.77 \times 0.65 = 0.29$
	Total cost (USD/m^2)	1.35

The imput material cost to manufacture a square meter of control wheat straw panel with 12 % phenol formaldehyde (i.e., 6% PF by db.) was calculated at $0.89 per square meter, as shown in Table 4.8.

Table 4.8: Input material cost to manufacture a control wheat straw panel

Formulation	Ratio	Cost per meter square (USD)
100% wheat straw	0.88	0.88 × 3.77 × 0.18 = 0.60
12 % PF	0.12	0.12 × 3.77 × 0.65 = 0.29
	Total cost (USD/m^2)	0.89

The input material cost to manufacture a square meter of preferred panel formulation (25% DDGS loading and 75 % wheat straw) with 6 % phenol formaldehyde (i.e., 3% PF by db.) was calculated at $0.81 per square meter, as shown in Table 4.9.

Table 4.9: Input material cost to manufacture a preferred formulation of particleboard

Formulation	Ratio	Cost per meter square (USD)
25% DDGS	0.235	0.235 × 3.77 × 0.22 = 0.19
75% wheat straw	0.705	0.705 × 3.77 × 0.18 = 0.47
6% PF	0.06	0.06 × 3.77 × 0.65 = 0.15
	Total cost (USD/m^2)	0.81

There is 40% saving on the input material cost of manufacturing a square meter of preferred formulation of particleboard if we shift from 100% wood based particleboard. This saving proves the economic benefits of using DDGS and wheat straw in manufacturing particleboards. Besides the economic benefit, there are health and environmental benefits of using this preferred formulation because of the reduction of phenol-formaldehyde by 50%.

5. CONCLUSION AND RECOMMENDATIONS

5.1. Conclusion

This study investigated the prospects of using DDGS and wheat straw for low-density particleboard production. Fractionation of DDGS in high and low fiber portions was achieved by sieving and air aspiration. Utilizing a high fiber fraction of DDGS in the composite materials showed promising results in this study. At 25% DDGS loading level, boards from high fiber fraction DDGS had better physical properties than those from the original DDGS. However, at higher DDGS loading (50% and 75%) with the high fiber fraction, the physical properties were better for particleboards with the original DDGS. All the mechanical properties were better for particleboards from the original DDGS than from the fractionated DDGS except for modulus of elasticity. These variations are caused by different shapes and sizes of the fractionated DDGS and the oil and NDF content variation. Internal bonding (IB) strength increased significantly for particleboards from both the fractionated and the original DDGS when the DDGS loading was increased from 25% to 50%. However, there was no significant increase in the IB value when DDGS loading increased from 50% to 75%. The higher concentration of the original DDGS resulted in better IB values than the higher concentration of the fractionated DDGS because of the higher protein content on the original DDGS, which was denatured by the high temperature showing its adhesive property. Alkali (NaOH) pretreatment decreased the static bending characteristics and internal bonding strength of the manufactured particleboards, while the screw withdrawal properties were not affected. Overall, particleboards with 25% DDGS loading and 75% wheat straw had comparable properties to wheat straw boards, with a 50% reduced resin. This study suggests that a higher fiber fraction DDGS and wheat straw can be used in low-

density particleboards instead of wood, saving the cost (40 % saving on input raw material cost) and reducing health and environmental harm.

5.2. Recommendation

This research focused on the high fiber portion (lighter fraction) of DDGS from the sieving and aspiration process to manufacture particleboard as a value-added product. Other value-added products can also be produced from the high-oil and high protein fraction (heavier fraction). Further research can be done using p-MDI as the binding agent since better properties are reported with p-MDI for wheat straw boards.

2M NaOH alkali pretreatment in our study had a negative impact on particleboards' properties, and the reasons are not yet clear. Further research can be done by first removing the wax and extractives from wheat straw using hot water and then only using alkaline pretreatment. Also, since the pretreatment effects depends on the severity of pretreatment, further research can be done using higher concentration and/or higher loadings of NaOH. In this research, only three different proportions of DDGS and wheat straw (25%, 50%, and 75% DDGS) were used. DDGS loadings can be increased at a smaller interval (5%) to get a more apparent trend and study DDGS loadings' effect. An industrial trial with high fraction DDGS and wheat straw should also be performed to commercialize DDGS-wheat straw particleboards.

During this research, proper resin mixing was a problem because of several constraints like the inability of the sprayer gun to spray highly viscous phenol-formaldehyde, size of cement mixture to mix the biomass with resin, and continuous spraying. Further research can be done by finding a better way of mixing resin on a small scale. Besides the protein and NDF content, this study did not consider the effect of all the sieve size (i.e, #10, #20, #40, #60, and Pan) on the properties of particleboards. Further research can be done on the impact of lighter fraction from

different sieve size (not only #20). Continuous moisture release during hot pressing is vital to get better results for boards. The release of moisture from the mold's side during the hot pressing procedure was not considered in this study. In future research, mold can be designed in a way that it can let the moisture evaporate from the side.

REFERENCES

Abbott, A. P., Palazuela Conde, J., Davis, S. J., Wise, W. R. (2012). Starch as a replacement for urea-formaldehyde in medium density fibreboard. *Green Chemistry*, *14*(11), 3067–3070. https://doi.org/10.1039/c2gc36194a

Alharbi, M. A. H., Hirai, S., Tuan, H. A., Akioka, S., Shoji, W. (2020). Effects of chemical composition, mild alkaline pretreatment and particle size on mechanical, thermal, and structural properties of binderless lignocellulosic biopolymers prepared by hot-pressing raw microfibrillated Phoenix dactylifera and Cocos nucifera . *Polymer Testing*, *84*, 106384.

Ando, M., Sato, M. (2009). Manufacture of plywood bonded with kenaf core powder. *Journal of Wood Science*, *55*(4), 283–288. https://doi.org/10.1007/s10086-009-1022-8

Ando, M., Sato, M. (2010). Evaluation of the self-bonding ability of sugi and application of sugi powder as a binder for plywood. *Journal of Wood Science*, *56*(3), 194–200. https://doi.org/10.1007/s10086-009-1096-3

Anglès, M. N., Reguant, J., Montané, D., Ferrando, F., Farriol, X., Salvadó, J. (1999). Binderless composites from pretreated residual softwood. *Journal of Applied Polymer Science*, *73*(12), 2485–2491.

Araújo Junior, C. P., Coaquira, C. A. C., Mattos, A. L. A., de Souza Filho, M. de S. M., Feitosa, J. P. de A., Morais, J. P. S. de, de Freitas Rosa, M. (2018). Binderless Fiberboards Made from Unripe Coconut Husks. *Waste and Biomass Valorization*, *9*(11), 2245–2254. https://doi.org/10.1007/s12649-017-9979-9

Arzt, E. (1998). Size Effects in Materials due to Microstructural and Dimensional Constraints: A comparative Review. *Acta Materialia*, *46*(16), 5611–5626. https://doi.org/10.1007/BF00437113

ASTM. (2012). Standard test methods for evaluating Properties of Wood-Based Fiber and Particle Panel Materials. In *D1037-12* (p. 32). https://doi.org/10.1520/D1037-12.1

Beg, M. D. H., Pickering, K. L., Weal, S. J. (2005). Corn gluten meal as a biodegradable matrix material in wood fibre reinforced composites. *Materials Science and Engineering A*, *412*(1–2), 7–11. https://doi.org/10.1016/j.msea.2005.08.015

Bekhta, P., Korkut, S., Hiziroglu, S. (2013). Effect of pretreatment of raw material on properties of particleboard panels made from wheat straw. *BioResources*, *8*(3), 4766–4774. https://doi.org/10.15376/biores.8.3.4766-4774

Belyea, R. L., Rausch, K. D., Tumbleson, M. E. (2004a). Composition of corn and distillers dried grains with solubles from dry grind ethanol processing. *Bioresource Technology*, *94*(3), 293–298. https://doi.org/10.1016/j.biortech.2004.01.001

Belyea, R. L., Rausch, K. D., Tumbleson, M. E. (2004b). Composition of Corn and distillers dried grains with solubles from dry grind ethanol processing. *Bioresource Technology*, (94), 293–298.

Bhadra, R., Rosentrater, K. A., Muthukumarappan, K. (2009). Cross-sectional staining and surface properties of DDGS particles and their influence on flowability. *Cereal Chemistry*, *86*(4), 410–420.

Biagiotti, J., Puglia, D., Kenny, J. M. (2004). A review on natural fibre-based composites-part I: structure, processing and properties of vegetable fibres. *Journal of Natural Fibers*, *1*(2), 37–68.

Boquillon, N., Elbez, G., Schönfeld, U. (2004). Properties of wheat straw particleboards bonded with different types of resin. *Journal of Wood Science*, *50*(3), 230–235. https://doi.org/10.1007/s10086-003-0551-9

Cao, Y., Song, W., Yang, Z., Chen, Z., Zhang, S. (2017). The properties of particleboard made from alkaline-treated wheat straw and methylene diphenyl diisocyanate binder. *BioResources, 12*(2), 3265–3276.

Chatzifragkou, A., Kosik, O., Prabhakumari, P. C., Lovegrove, A., Frazier, R. A., Shewry, P. R., Charalampopoulos, D. (2015). Biorefinery strategies for upgrading Distillers' Dried Grains with Solubles (DDGS). *Process Biochemistry, 50*(12), 2194–2207. https://doi.org/10.1016/j.procbio.2015.09.005

Cheesbrough, V., Rosentrater, K. A., Visser, J. (2008). Properties of distillers grains composites: a preliminary investigation. *Journal of Polymers and the Environment, 16*(1), 40–50.

Cheng, E., Sun, X., Karr, G. S. (2004). Adhesive properties of modified soybean flour in wheat straw particleboard. *Composites Part A: Applied Science and Manufacturing*, *35*(3), 297–302.

Cheng, M.-H., Riess, S., Rosentrater, K. A. (2014). Fractionation of distillers dried grains with solubles (DDGS) by combination of sieving and aspiration. In *2014 Montreal, Quebec Canada July 13–July 16, 2014* (p. 1). American Society of Agricultural and Biological Engineers.

Christiansen, A. W. (1991). How Overdrying Wood Reduces Its Bonding to Phenol-Formaldehyde Adhesives - a Critical-Review of the Literature .2. Chemical-Reactions. *Wood and Fiber Science*, *23*(1), 69–84.

Ciannamea, E. M., Stefani, P. M., Ruseckaite, R. A. (2010). Medium-density particleboards from modified rice husks and soybean protein concentrate-based adhesives. *Bioresource Technology, 101*(2), 818–825.

CIGI. (2013). *Wheat DDGS Feed Guide*. Retrieved from https://cigi.ca/wp-content/uploads/2013/02/DDGS-Feed-Guide_Revised_Jan.-2013.pdf

Council, U. S. G. (2021). DDGS Production and Export. Retrieved from https://grains.org/buying-selling/ddgs/#:~:text=Production and Exports&text=DDGS utilization as a feed,million metric tons of DDGS.

Craig, A. P., Franca, A. S., Oliveira, L. S. (2012). Discrimination between defective and non-defective roasted coffees by diffuse reflectance infrared Fourier transform spectroscopy. *LWT*, *47*(2), 505–511.

Davis, K. S. (2001). Corn Milling, Processing and Generation of Co-products. In *Proceedongs of the 62nd Minnesota Nutirtion Conference and Minnesota Corn Growers Association Technical Symposium* (p. 9). Bloomington, Minnesota: Minnesota Corn Growers Association. Retrieved from https://www.biofuelscoproducts.umn.edu/sites/biodieselfeeds.cfans.umn.edu/files/ddgs-techinfo-pro-20.pdf

De Melo, R. R., Stangerlin, D. M., Campomanes Santana, R. R., Pedrosa, T. D. (2014). Physical and Mechanical Properties of particleboard manufactured from wood, bamboo and rice husk. *Materials Research*, 1–5. https://doi.org/10.4067/s0718-221x2015005000006

Fahmy, T. Y. A., Mobarak, F. (2013). Advanced binderless board-like green nanocomposites from undebarked cotton stalks and mechanism of self-bonding. *Cellulose*, *20*(3), 1453–1457.

Fu, S. Y., Feng, X. Q., Lauke, B., Mai, Y. W. (2008). Effects of particle size, particle/matrix interface adhesion and particle loading on mechanical properties of particulate-polymer

composites. *Composites Part B: Engineering*, *39*(6), 933–961. https://doi.org/10.1016/j.compositesb.2008.01.002

Halvarsson, S. B., Edlund, H., Norgren, M. (2010). Wheat straw as raw material for manufacture of straw MDF. *BioResources*, *5*(2), 1215–1231.

Han, G., Zhang, C., Zhang, D., Umemura, K., Kawai, S. (1998). Upgrading of urea formaldehyde-bonded reed and wheat straw particleboards using silane coupling agents. *Journal of Wood Science*, *44*(4), 282–286.

Harr, M. E. (1977). *Mechanics of particulate media: a probabilistic approach*. McGraw-Hill Companies.

Hemmilä, V., Adamopoulos, S., Karlsson, O., Kumar, A. (2017). Development of sustainable bio-adhesives for engineered wood panels-A Review. *RSC Advances*, *7*(61), 38604–38630. https://doi.org/10.1039/c7ra06598a

Howard, J. L., Liang, S. (2019). U.S. timber production, trade, consumption, and price statistics, 1965-2017. *United States Departmet of Agriculture*, (July), 1–106.

Huda, M. S. (2020). *INCREASED OIL RECOVERY FROM DISTILLERS DRIED GRAINS WITH SOLUBLES AND WHOLE STILLAGE*. *North Dakota State University*. North Dakota State University.

Igathinathane, C., Ulusoy, U., Pordesimo, L. O. (2012). Comparison of particle size distribution of celestite mineral by machine vision ΣVolume approach and mechanical sieving. *Powder Technology*, *215*, 137–146.

Iswanto, A. H., Simarmata, J., Fatriasari, W., Azhar, I., Sucipto, T., Hartono, R. (2017). Physical and mechanical properties of three-layer particleboards bonded with uf and umf adhesives. *Journal of the Korean Wood Science and Technology*, *45*(6), 787–796.

Juliana, A. H., Paridah, M. T., Rahim, S., Azowa, I. N., Anwar, U. M. K. (2012). Properties of particleboard made from kenaf (Hibiscus cannabinus L.) as function of particle geometry. *Materials & Design*, *34*, 406–411.

Julson, J. L., Subbarao, G., Stokke, D. D., Gieselman, H. H., Muthukumarappan, K. (2004). Mechanical properties of biorenewable fiber/plastic composites. *Journal of Applied Polymer Science*, *93*(5), 2484–2493. https://doi.org/10.1002/app.20823

Karr, G. S., Cheng, E., Sun, X. S. (2000). Physical properties of strawboard as affected by processing parameters. *Industrial Crops and Products*, *12*(1), 19–24. https://doi.org/10.1016/S0926-6690(99)00041-2

Kawasaki, T., Kawai, S. (2006). Thermal insulation properties of wood-based sandwich panel for use as structural insulated walls and floors. *Journal of Wood Science*, *52*(1), 75–83.

Keskin, H., Kucuktuvek, M., Guru, M. (2015). The potential of poppy (Papaver somniferum Linnaeus) husk for manufacturing wood-based particleboards. *Construction and Building Materials*, *95*, 224–231.

Khosravi, S., Khabbaz, F., Nordqvist, P., Johansson, M. (2010). Protein-based adhesives for particleboards. *Industrial Crops and Products*, *32*(3), 275–283. https://doi.org/10.1016/j.indcrop.2010.05.001

Kim, S., Xu, J., Liu, S. (2010). Production of biopolymer composites by particle bonding. *Composites Part A: Applied Science and Manufacturing*, *41*(1), 146–153. https://doi.org/10.1016/j.compositesa.2009.09.019

Krueger, R. K; Alexander, R. J. (1976). *3983084*. US. https://doi.org/10.1016/0375-6505(85)90011-2

Kundu, B., Kurland, N. E., Bano, S., Patro, C., Engel, F. B., Yadavalli, V. K., Kundu, S. C. (20014). Silk Proteins for biomedical applications: Bioengineering Perspectives. *Progress in Polymer Science*, *39*(2), 251–267. https://doi.org/10.1007/BF00766784

Lee, S., Shupe, T. F., Hse, C. Y. (2006). Properties of bio-based medium density fiberboard. *In: Recent Developments in Wood Composites: 51-58*.

Li, X., Cai, Z., Winandy, J. E., Basta, A. H. (2011). Effect of oxalic acid and steam pretreatment on the primary properties of UF-bonded rice straw particleboards. *Industrial Crops and Products*, *33*(3), 665–669.

Li, X., Strezov, V., Kan, T. (2014). Energy recovery potential analysis of spent coffee grounds pyrolysis products. *Journal of Analytical and Applied Pyrolysis*, *110*, 79–87.

Li, Y., Sun, S. X. (2011). Mechanical and Thermal Properties of Biocomposites from Poly(lactic acid) and DDGS. *Journal of Applied Polymer Science*, *121*, 589–597. https://doi.org/10.1002/app.33681

Liaw, J. D., Bajwa, D. S., Shojaeiarani, J., Bajwa, S. G. (2019). Corn distiller's dried grains with solubles (DDGS)-A value added functional material for wood composites. *Industrial Crops and Products*, *139*, 111525.

Liu, K. S. (2009). Fractionation of distillers dried grains with solubles (DDGS) by sieving and winnowing. *Bioresource Technology*, *100*(24), 6559–6569. https://doi.org/10.1016/j.biortech.2009.07.053

Liu, K. S. (2008). Particle size distribution of distillers dried grains with solubles (DDGS) and relationships to compositional and color properties. *Bioresource Technology*, *99*(17), 8421–8428. https://doi.org/10.1016/j.biortech.2008.02.060

Liu, K. S., Rosentrater, K. A. (2012). *Distillers Grains: Production, Properties and Utilization*. (KeShun Liu & K. A. Rosentrater, Eds.). CRC Press. https://doi.org/https://doi.org/10.1201/b11047

Luo, P., Yang, C. (2010). Production of particleboard from wheat straw. *2010 4th International Conference on Bioinformatics and Biomedical Engineering, ICBBE 2010*, 1–3. https://doi.org/10.1109/ICBBE.2010.5517323

Maloney, T. M. (1977). *Modern particleboard & dry-process fiberboard manufacturing* (Vol. I). San Francisco: Miller Freeman Publications.

Mancera, C., El Mansouri, N.-E., Ferrando, F., Salvado, J. (2011). The suitability of steam exploded vitis vinifera and alkaline lignin for the manufacture of fiberboard. *BioResources*, *6*(4), 4439–4453.

Martinez-Amezcua, C., Parsons, C. M., Singh, V., Srinivasan, R., Murthy, G. S. (2007). Nutritional characteristics of corn distillers dried grains with solubles as affected by the amounts of grains versus solubles and different processing techniques. *Poultry Science*, *86*(12), 2624–2630. https://doi.org/10.3382/ps.2007-00137

Mo, X., Hu, J., Sun, X. S., Ratto, J. A. (2001). Compression and tensile strength of low-density straw-protein particleboard. *Industrial Crops and Products*, *14*(1), 1–9.

Mobarak, F., Fahmy, Y., Augustin, H. (1982). Binderless lignocellulose composite from bagasse and mechanism of self-bonding. *Holzforschung*, *36*(3), 131–135.

Mohanty, A. K., Misra, M., Drzal, L. T. (2005). *Natural Fibers, Biopolymers, And Biocomposites*. BocaRaton: CRC Press. Retrieved from https://www.crcpress.com/Natural-Fibers-Biopolymers-and-Biocomposites/Mohanty-Misra-Drzal/p/book/9780849317415

Moubarik, A., Allal, A., Pizzi, A., Charrier, F., Charrier, B. (2010). Characterization of a formaldehyde-free cornstarch-tannin wood adhesive for interior plywood. *European Journal of Wood and Wood Products*, *68*(4), 427–433. https://doi.org/10.1007/s00107-009-0379-0

Moubarik, A., Pizzi, A., Allal, A., Charrier, F., Khoukh, A., Charrier, B. (2010). Cornstarch-mimosa tannin-urea formaldehyde resins as adhesives in the particleboard production. *Starch/Staerke*, *62*(3–4), 131–138. https://doi.org/10.1002/star.200900228

Ndazi, B. S., Karlsson, S., Tesha, J. V, Nyahumwa, C. W. (2007). Chemical and physical modifications of rice husks for use as composite panels. *Composites Part A: Applied Science and Manufacturing*, *38*(3), 925–935.

Nikvash, N., Kraft, R., Kharazipour, A., Euring, M. (2010). Comparative properties of bagasse, canola and hemp particle boards. *European Journal of Wood and Wood Products*, *68*(3), 323–327. https://doi.org/10.1007/s00107-010-0465-3

Nonaka, S., Umemura, K., Kawai, S. (2013). Characterization of bagasse binderless particleboard manufactured in high-temperature range. *Journal of Wood Science*, *59*(1), 50–56. https://doi.org/10.1007/s10086-012-1302-6

Nordqvist, P., Nordgren, N., Khabbaz, F., Malmström, E. (2013). Plant proteins as wood adhesives: Bonding performance at the macro- and nanoscale. *Industrial Crops and Products*, *44*, 246–252. https://doi.org/10.1016/j.indcrop.2012.11.021

Palmieri, N., Forleo, M. B., Giannoccaro, G., Suardi, A. (2017). Environmental impact of cereal straw management: An on-farm assessment. *Journal of Cleaner Production*, *142*, 2950–2964.

Pandey, P. (2017). *Hull Fiber from DDGS and Corn grain as Alternative Fillers in Polymer Composites with High Density Polyethylene*. North Dakota State University.

Pandey, P., Bajwa, S., Bajwa, D. (2018). Fiber from DDGS and Corn Grain as Alternative Fillers in Polymer Composites with High Density Polyethylene from Bio-based and Petroleum Sources. *Journal of Polymers and the Environment*, *26*(6), 2311–2322. https://doi.org/10.1007/s10924-017-1108-0

Pandey, P., Bajwa, S. G., Bajwa, D. S., Englund, K. (2017). Performance of UV weathered HDPE composites containing hull fiber from DDGS and corn grain. *Industrial Crops and Products*, *107*(July), 409–419. https://doi.org/10.1016/j.indcrop.2017.06.050

Puettmann, M., Oneil, E., Wilson, J. (2013). *Cradle to Gate Life Cycle Assessment of U.S. Particleboard Production*. *Consortium for Research on Renewable Industrial Materials, USA*.

Quintana, G., Velasquez, J., Betancourt, S., Ganan, P. (2009). Binderless fiberboard from steam exploded banana bunch. *Industrial Crops and Products*, *29*(1), 60–66.

Rausch, K. D., Belyea, R. L., Ellersieck, M. R., Singh, V., Johnston, D. B., Tumbleson, M. E. (2005). Particle size distributions of ground corn and DDGS from dry grind processing. *Transactions of the ASAE*, *48*(1), 273–277.

RFA. (2019). *Powered With Renewed Energy*. Retrieved from https://ethanolrfa.org/wp-content/uploads/2019/05/RFA_outlook_2019_newlogo.pdf

Rowell, R., Kawai, S., Inoue, M. (1995). Dimensionally stabilized, very low density fiberboard. *Wood and Fiber Science*, *27*(4), 428–436.

Rowell, R. M. (2012). *Handbook of wood chemistry and wood composites*. CRC press.

Salam, A., Reddy, N., Yang, Y. (2007). Bleaching of kenaf and cornhusk fibers. *Industrial & Engineering Chemistry Research*, *46*(5), 1452–1458.

Sari, B., Nemli, G., Ayrilmis, N., Baharoğlu, M., Bardak, S. (2013). The Influences of Drying Temperature of Wood Particles on the Quality Properties of Particleboard Composite. *Drying Technology*, *31*(1), 17–23. https://doi.org/10.1080/07373937.2012.711791

Schneider, G. J., Conway, H. D. (1969). Effect of fiber geometry and partial debonding on fiber-matrix bond stresses. *Journal of Composite Materials*, *3*(1), 116–135.

Shukla, R., Cheryan, M. (2001). Zein: The industrial protein from corn. *Industrial Crops and Products*, *13*(3), 171–192. https://doi.org/10.1016/S0926-6690(00)00064-9

Shurson, G. C. (2018). Yeast and yeast derivatives in feed additives and ingredients: Sources, characteristics, animal responses, and quantification methods. *Animal Feed Science and Technology*, *235*(November 2017), 60–76. https://doi.org/10.1016/j.anifeedsci.2017.11.010

Singh, V., Moreau, R. A., Hicks, K. B., Belyea, R. L., Staff, C. H. (2002). Removal of fiber from distillers dried grains with solubles (DDGS) to increase value. *Transactions of the ASAE*, *45*(2), 389.

Sitz, E. D. (2016). *Processing and Manufacture of Soybean and Wheat Straw Medium Density Fiberboard Utilizing Epoxidized Sucrose Soyate Resin*. North Dakota State University. Retrieved from https://library.ndsu.edu/ir/bitstream/handle/10365/27990/Processing and Manufacture of Soybean and Wheat Straw Medium Density Fiberboard Utilizing Epoxidized Sucrose Soyate Resin.pdf?sequence=1&isAllowed=y

Srinivasan, R., Moreau, R. A., Parsons, C., Lane, J. D., Singh, V. (2008). Separation of fiber from distillers dried grains (DDG) using sieving and elutriation. *Biomass and Bioenergy*, *32*(5), 468–472. https://doi.org/10.1016/j.biombioe.2007.10.013

Srinivasan, R., Moreau, R. A., Rausch, K. D., Belyea, R. L., Tumbleson, M. E., Singh, V. (2005). Separation of fiber from distillers dried grains with solubles (DDGS) using sieving and elutriation. *Cereal Chemistry, 82*(5), 528–533. https://doi.org/10.1094/CC-82-0528

Srinivasan, R., Singh, V., Belyea, R. L., Rausch, K. D., Moreau, R. A., Tumbleson, M. E. (2006). Economics of fiber separation from distillers dried grains with solubles (DDGS) using sieving and elutriation. *Cereal Chemistry*, *83*(4), 324–330. https://doi.org/10.1094/CC-83-0324

Srinivasan, R., To, F., Columbus, E. (2009). Pilot scale fiber separation from distillers dried grains with solubles (DDGS) using sieving and air classification. *Bioresource Technology*, *100*(14), 3548–3555. https://doi.org/10.1016/j.biortech.2009.02.049

Sundquist, D. J., Bajwa, D. S. (2016). Dried distillers grains with solubles as a multifunctional filler in low density wood particleboards. *Industrial Crops and Products*, *89*, 21–28. https://doi.org/10.1016/j.indcrop.2016.04.071

Tabarsa, T., Jahanshahi, S., Ashori, A. (2011). Mechanical and physical properties of wheat straw boards bonded with a tannin modified phenol-formaldehyde adhesive. *Composites Part B: Engineering*, *42*(2), 176–180. https://doi.org/10.1016/j.compositesb.2010.09.012

Tatara, R. A., Rosentrater, K. A., Suraparaju, S. (2009). Design properties for molded, corn-based DDGS-filled phenolic resin. *Industrial Crops and Products*, *29*(1), 9–15. https://doi.org/10.1016/j.indcrop.2008.03.002

Tatara, R. A., Suraparaju, S., Rosentrater, K. A. (2007). Compression molding of phenolic resin and corn-based DDGS blends. *Journal of Polymers and the Environment*, *15*(2), 89–95. https://doi.org/10.1007/s10924-007-0052-9

Taylor & Francis Group, L. (2003). *Handbook of Adhesive Technology*. (A. Pizzi & K. L. Mittal, Eds.), *Marcel Dekker, Inc* (Second). New York: MARCEL DEKKER INC.

Thakur, V. K., Thakur, M. K., Gupta, R. K. (2013). Graft Copolymers from Natural Polymers Using Free Radical Polymerization. *International Journal of Polymer Analysis and Characterization*, *18*(7), 495–503. https://doi.org/10.1080/1023666X.2013.814241

Tisserat, B.; Hwang, H. S.; Steven, F. B.; Berhow, M. A.; Peterson, S. C.; Joshee, N.; Vaidya, B. N.; Kuru, R. H. (2018). Fiberboard Created Using the Natural Adhesive Properties of Distillers Dried Grains with Solubles. *BioResources*, *13*(2), 2678–2701.

Tisserat, B., Reifschneider, L., O'Kuru, R. H., Finkenstadt, V. L. (2013). Mechanical and thermal properties of high density polyethylene - dried distillers grains with solubles composites. *BioResources*, *8*(1), 59–75.

USDA-NASS. (2019). *Crop Production 2018 Summary*. Retrieved from https://www.nass.usda.gov/Publications/Todays_Reports/reports/cropan19.pdf

V. Singh, R. A. Moreau, K. B. Hicks, R. L. Belyea, C. H. Staff. (2001). Removal of Fiber From Distillers Dried Grains With Solubles (Ddgs) To Increase Value. *Transactions of the ASAE*, *45*(2), 389–392. https://doi.org/10.13031/2013.8510

Wang, D., Sun, X. S. (2002). Low density particleboard from wheat straw and corn pith. *Industrial Crops and Products*, *15*(1), 43–50. https://doi.org/10.1016/S0926-6690(01)00094-2

Widyorini, R., Xu, J., Umemura, K., Kawai, S. (2005). Manufacture and properties of binderless particleboard from bagasse I: Effects of raw material type, storage methods, and manufacturing process. *Journal of Wood Science*, *51*(6), 648–654. https://doi.org/10.1007/s10086-005-0713-z

Wu, J., Gatewood, B. M. (1998). Bleaching of wheat straw, an alternative cellulosic (hard) fiber for potential industrial application. In *International conference and exhibition of the American association of textile colorist and chemists* (pp. 58–67).

Wu, Y. V., Stringfellow, A. C. (1982). Corn Distillers' Dried Grains with Solubles and Corn Distillers' Dried Grains: Dry Fractionation and Composition. *Journal of Food Science*, *47*(4), 1155–1157.

Xu, J., Widyorini, R., Yamauchi, H., Kawai, S. (2006). Development of binderless fiberboard from kenaf core. *Journal of Wood Science, 52*(3), 236–243. https://doi.org/10.1007/s10086-005-0770-3

Yang, I., Kuo, M., Myers, D. J., Pu, A. (2006). Comparison of protein-based adhesive resins for wood composites. *Journal of Wood Science*, *52*(6), 503–508. https://doi.org/10.1007/s10086-006-0804-5

Zarrinbakhsh, N., Mohanty, A. K., Misra, M. (2013). Fundamental studies on water-washing of the corn ethanol coproduct (DDGS) and its characterization for biocomposite applications. *Biomass and Bioenergy*, *55*, 251–259.

Zhang, Y., Lu, X., Pizzi, A., Delmotte, L. (2003). Wheat straw particleboard bonding improvements by enzyme pretreatment. *Holz Als Roh-Und Werkstoff*, *61*(1), 49–54.

Zhang, Y., Gu, J., Zuo, Y., Di, M., Tan, H., Zhu, L. (2010). Mechanical properties of wheat straw particleboard using Composite adhesives. *Advanced Materials Research*, *113–116*, 2096–2099. https://doi.org/10.4028/www.scientific.net/AMR.113-116.2096

Zheng, Y., Pan, Z., Zhang, R., Jenkins, B. M., Blunk, S. (2007). Particleboard quality characteristics of saline jose tall wheatgrass and chemical treatment effect. *Bioresource Technology*, *98*(6), 1304–1310.

APPENDIX A. SUPPLEMENTAL FIGURES

Class Level Information		
Class	Levels	Values
Rep	3	1 2 3
Sample	2	1 2
Treatment	8	ConWhSt ConWood EluDD25 EluDD50 EluDD75 OriDD25 OriDD50 OriDD75

Number of Observations Read	48
Number of Observations Used	48

The ANOVA Procedure

Dependent Variable: Density

Source	DF	Sum of Squares	Mean Square	F Value	Pr > F
Model	23	28661.60000	1246.15652	3.64	0.0013
Error	24	8223.19205	342.63300		
Corrected Total	47	36884.79205			

R-Square	Coeff Var	Root MSE	Density Mean
0.777057	3.042902	18.51035	608.3123

Source	DF	Anova SS	Mean Square	F Value	Pr > F
Rep	2	514.82120	257.41060	0.75	0.4825
Treatment	7	15393.91696	2199.13099	6.42	0.0003
Rep*Treatment	14	12752.86183	910.91870	2.66	0.0170

Tests of Hypotheses Using the Anova MS for Rep*Treatment as an Error Term					
Source	DF	Anova SS	Mean Square	F Value	Pr > F
Rep	2	514.82120	257.41060	0.28	0.7580
Treatment	7	15393.91696	2199.13099	2.41	0.0760

Figure A1: ANOVA of density of particleboards

Class Level Information		
Class	Levels	Values
Rep	3	1 2 3
Sample	2	1 2
Treatment	8	ConWhSt ConWood EluDD25 EluDD50 EluDD75 OriDD25 OriDD50 OriDD75

Number of Observations Read	48
Number of Observations Used	48

The ANOVA Procedure

Dependent Variable: IB_Test

Source	DF	Sum of Squares	Mean Square	F Value	Pr > F
Model	23	1.29258567	0.05619938	67.24	<.0001
Error	24	0.02006000	0.00083583		
Corrected Total	47	1.31264567			

R-Square	Coeff Var	Root MSE	IB_Test Mean
0.984718	12.94030	0.028911	0.223417

Source	DF	Anova SS	Mean Square	F Value	Pr > F
Rep	2	0.01337267	0.00668633	8.00	0.0022
Treatment	7	1.20207133	0.17172448	205.45	<.0001
Rep*Treatment	14	0.07714167	0.00551012	6.59	<.0001

Tests of Hypotheses Using the Anova MS for Rep*Treatment as an Error Term					
Source	DF	Anova SS	Mean Square	F Value	Pr > F
Rep	2	0.01337267	0.00668633	1.21	0.3266
Treatment	7	1.20207133	0.17172448	31.17	<.0001

Figure A2: ANOVA of internal bond strength of particleboards

Class Level Information		
Class	Levels	Values
Rep	3	1 2 3
Treatment	8	ConWhSt ConWood EluDD25 EluDD50 EluDD75 OriDD25 OriDD50 OriDD75

Number of Observations Read	24
Number of Observations Used	24

The ANOVA Procedure

Dependent Variable: Pmax

Source	DF	Sum of Squares	Mean Square	F Value	Pr > F
Model	9	331190.6540	36798.9616	148.35	<.0001
Error	14	3472.6951	248.0497		
Corrected Total	23	334663.3491			

R-Square	Coeff Var	Root MSE	Pmax Mean
0.989623	6.479991	15.74959	243.0496

Source	DF	Anova SS	Mean Square	F Value	Pr > F
Rep	2	578.6016	289.3008	1.17	0.3400
Treatment	7	330612.0524	47230.2932	190.41	<.0001

Figure A3: ANOVA of screw withdrawal force

Class Level Information		
Class	Levels	Values
Rep	3	1 2 3
Treatment	8	ConWhSt ConWood EluDD25 EluDD50 EluDD75 OriDD25 OriDD50 OriDD75

Number of Observations Read	24
Number of Observations Used	24

Modulus of Elasticity (MPa)

The ANOVA Procedure

Dependent Variable: MOE

Source	DF	Sum of Squares	Mean Square	F Value	Pr > F
Model	9	1102460.567	122495.619	31.97	<.0001
Error	14	53639.852	3831.418		
Corrected Total	23	1156100.419			

R-Square	Coeff Var	Root MSE	MOE Mean
0.953603	10.76861	61.89845	574.8046

Source	DF	Anova SS	Mean Square	F Value	Pr > F
Rep	2	1725.201	862.600	0.23	0.8012
Treatment	7	1100735.366	157247.909	41.04	<.0001

Figure A4: ANOVA of modulus of elasticity

Class Level Information		
Class	Levels	Values
Rep	3	1 2 3
Treatment	8	ConWhSt ConWood EluDD25 EluDD50 EluDD75 OriDD25 OriDD50 OriDD75

Number of Observations Read	24
Number of Observations Used	24

Modulus of Rupture (MPa)

The ANOVA Procedure

Dependent Variable: MOR

Source	DF	Sum of Squares	Mean Square	F Value	Pr > F
Model	9	34.13462058	3.79273562	90.84	<.0001
Error	14	0.58455725	0.04175409		
Corrected Total	23	34.71917783			

R-Square	Coeff Var	Root MSE	MOR Mean
0.983163	7.322418	0.204338	2.790583

Source	DF	Anova SS	Mean Square	F Value	Pr > F
Rep	2	0.12423608	0.06211804	1.49	0.2595
Treatment	7	34.01038450	4.85862636	116.36	<.0001

Figure A5: ANOVA of modulus of rupture

Class Level Information		
Class	Levels	Values
Rep	3	1 2 3
Treatment	8	ConWhSt ConWood EluDD25 EluDD50 EluDD75 OriDD25 OriDD50 OriDD75

Number of Observations Read	24
Number of Observations Used	24

Hardness (N)

The ANOVA Procedure

Dependent Variable: Hardness

Source	DF	Sum of Squares	Mean Square	F Value	Pr > F
Model	9	3328710.646	369856.738	27.38	<.0001
Error	14	189146.217	13510.444		
Corrected Total	23	3517856.862			

R-Square	Coeff Var	Root MSE	Hardness Mean
0.946233	8.876034	116.2344	1309.531

Source	DF	Anova SS	Mean Square	F Value	Pr > F
Rep	2	1234.729	617.365	0.05	0.9555
Treatment	7	3327475.916	475353.702	35.18	<.0001

Figure A6: ANOVA of hardness

Class Level Information		
Class	Levels	Values
Rep	4	1 2 3 4
Treatment	8	ConWhSt ConWood EluDD25 EluDD50 EluDD75 OriDD25 OriDD50 OriDD75

Number of Observations Read	32
Number of Observations Used	32

Thickness Swelling_2hrs(%)

The ANOVA Procedure

Dependent Variable: TS

Source	DF	Sum of Squares	Mean Square	F Value	Pr > F
Model	10	1644.636900	164.463690	28.14	<.0001
Error	21	122.742900	5.844900		
Corrected Total	31	1767.379800			

R-Square	Coeff Var	Root MSE	TS Mean
0.930551	7.773082	2.417623	31.10250

Source	DF	Anova SS	Mean Square	F Value	Pr > F
Rep	3	60.843200	20.281067	3.47	0.0344
Treatment	7	1583.793700	226.256243	38.71	<.0001

Figure A7: ANOVA of 2 hour thickness swelling

Class Level Information		
Class	Levels	Values
Rep	4	1 2 3 4
Treatment	8	ConWhSt ConWood EluDD25 EluDD50 EluDD75 OriDD25 OriDD50 OriDD75

Number of Observations Read	32
Number of Observations Used	32

Thickness Swelling_24hrs(%)

The ANOVA Procedure

Dependent Variable: TS

Source	DF	Sum of Squares	Mean Square	F Value	Pr > F
Model	10	1690.339925	169.033992	24.04	<.0001
Error	21	147.666675	7.031746		
Corrected Total	31	1838.006600			

R-Square	Coeff Var	Root MSE	TS Mean
0.919659	8.214820	2.651744	32.28000

Source	DF	Anova SS	Mean Square	F Value	Pr > F
Rep	3	108.006525	36.002175	5.12	0.0082
Treatment	7	1582.333400	226.047629	32.15	<.0001

Figure A8: ANOVA of 24 hour thickness swelling

Class Level Information		
Class	Levels	Values
Rep	4	1 2 3 4
Treatment	8	ConWhSt ConWood EluDD25 EluDD50 EluDD75 OriDD25 OriDD50 OriDD75

Number of Observations Read	32
Number of Observations Used	32

Water Absorbtion_2hrs(%)

The ANOVA Procedure

Dependent Variable: WA

Source	DF	Sum of Squares	Mean Square	F Value	Pr > F
Model	10	2582.848956	258.284896	10.18	<.0001
Error	21	532.560466	25.360022		
Corrected Total	31	3115.409422			

R-Square	Coeff Var	Root MSE	WA Mean
0.829056	4.206080	5.035874	119.7284

Source	DF	Anova SS	Mean Square	F Value	Pr > F
Rep	3	39.117009	13.039003	0.51	0.6770
Treatment	7	2543.731947	363.390278	14.33	<.0001

Figure A9: ANOVA of 2 hour water absorption

Class Level Information		
Class	Levels	Values
Rep	4	1 2 3 4
Treatment	8	ConWhSt ConWood EluDD25 EluDD50 EluDD75 OriDD25 OriDD50 OriDD75

Number of Observations Read	32
Number of Observations Used	32

Water Absorbtion_24hrs(%)

The ANOVA Procedure

Dependent Variable: WA

Source	DF	Sum of Squares	Mean Square	F Value	Pr > F
Model	10	3250.789956	325.078996	12.72	<.0001
Error	21	536.657491	25.555119		
Corrected Total	31	3787.447447			

R-Square	Coeff Var	Root MSE	WA Mean
0.858306	3.993281	5.055207	126.5928

Source	DF	Anova SS	Mean Square	F Value	Pr > F
Rep	3	93.557184	31.185728	1.22	0.3270
Treatment	7	3157.232772	451.033253	17.65	<.0001

Figure A10: ANOVA of 24 hour water absorption

Class Level Information		
Class	Levels	Values
Rep	3	1 2 3
Treatment	8	ConWhSt ConWood EluDD25 EluDD50 EluDD75 OriDD25 OriDD50 OriDD75

Number of Observations Read	24
Number of Observations Used	24

The ANOVA Procedure

Dependent Variable: LE

Source	DF	Sum of Squares	Mean Square	F Value	Pr > F
Model	9	0.34702158	0.03855795	7.41	0.0005
Error	14	0.07286375	0.00520455		
Corrected Total	23	0.41988533			

R-Square	Coeff Var	Root MSE	LE Mean
0.826468	19.22094	0.072143	0.375333

Source	DF	Anova SS	Mean Square	F Value	Pr > F
Rep	2	0.01776558	0.00888279	1.71	0.2171
Treatment	7	0.32925600	0.04703657	9.04	0.0003

Figure A11: ANOVA of linear expansion

APPENDIX B. ENERGY-DISPERSIVE X-RAY (EDX) RESULTS

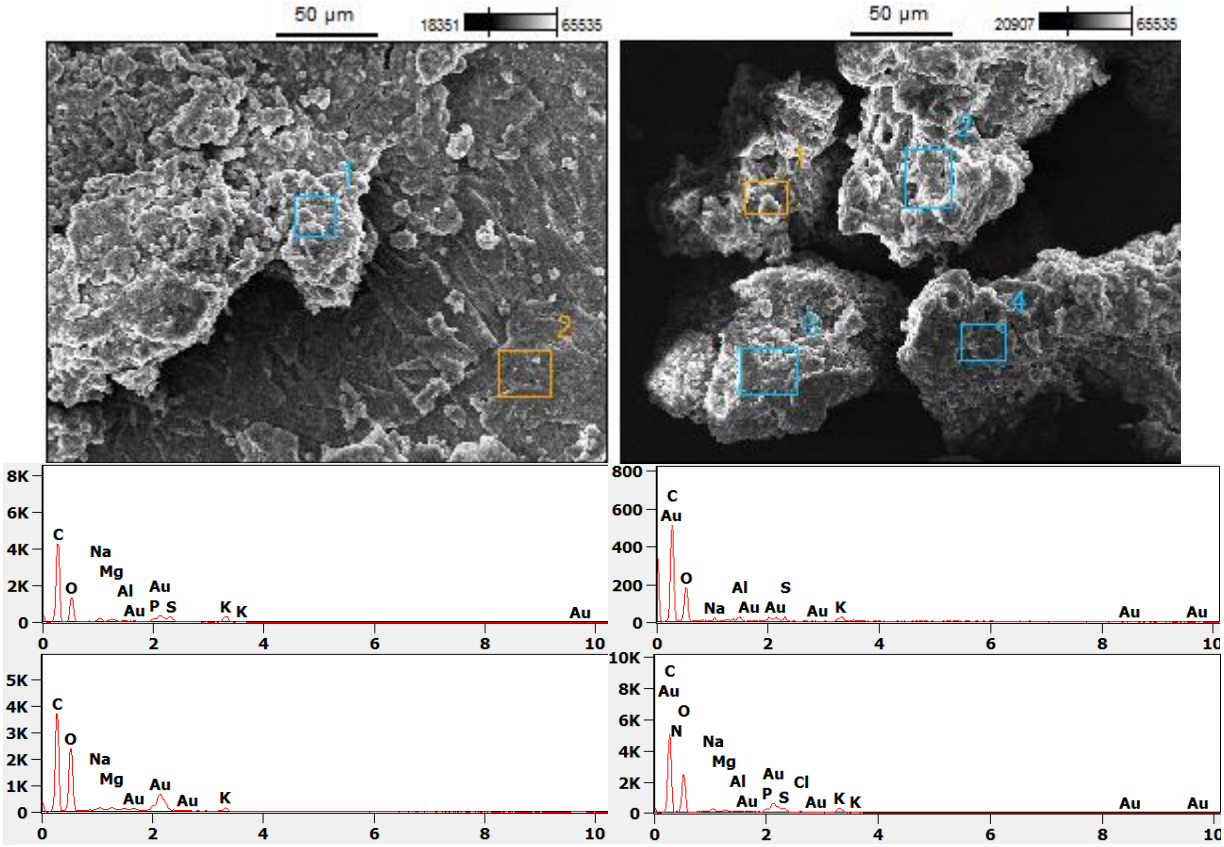

Net Counts

	C-K	O-K	Na-K	Mg-K	Al-K	P-K	S-K	K-K
218688 1(1)_pt1	24830	7494	1141	911	214	1639	3317	3593
218688 1(1)_pt2	20786	14227	499	447				1293

Weight %

	C-K	O-K	Na-K	Mg-K	Al-K	P-K	S-K	K-K
218688 1(1)_pt1	47.29	38.86	1.75	1.09	0.22	1.62	3.38	5.78
218688 1(1)_pt2	35.52	60.30	1.02	0.69				2.48

Net Counts

	C-K	N-K	O-K	Na-K	Mg-K	Al-K	P-K	S-K	Cl-K	K-K
218688 1(2)_pt1	2855		1018	56		128		93		227
218688 1(2)_pt2	29023	822	14048	1417	789	359	1955	3120	484	3315
218688 1(2)_pt3-No Data.										
218688 1(2)_pt4	22653	790	6859	195	496	349				484

Weight %

	C-K	N-K	O-K	Na-K	Mg-K	Al-K	P-K	S-K	Cl-K	K-K
218688 1(2)_pt1	44.81		48.02	0.94		1.42		0.99		3.81
218688 1(2)_pt2	37.21	6.15	46.38	1.59	0.68	0.27	1.36	2.22	0.44	3.71
218688 1(2)_pt3-No Data.										
218688 1(2)_pt4	40.84	10.63	45.74	0.43	0.82	0.50				1.04

Figure B1: Energy-dispersive X-ray results for original DDGS

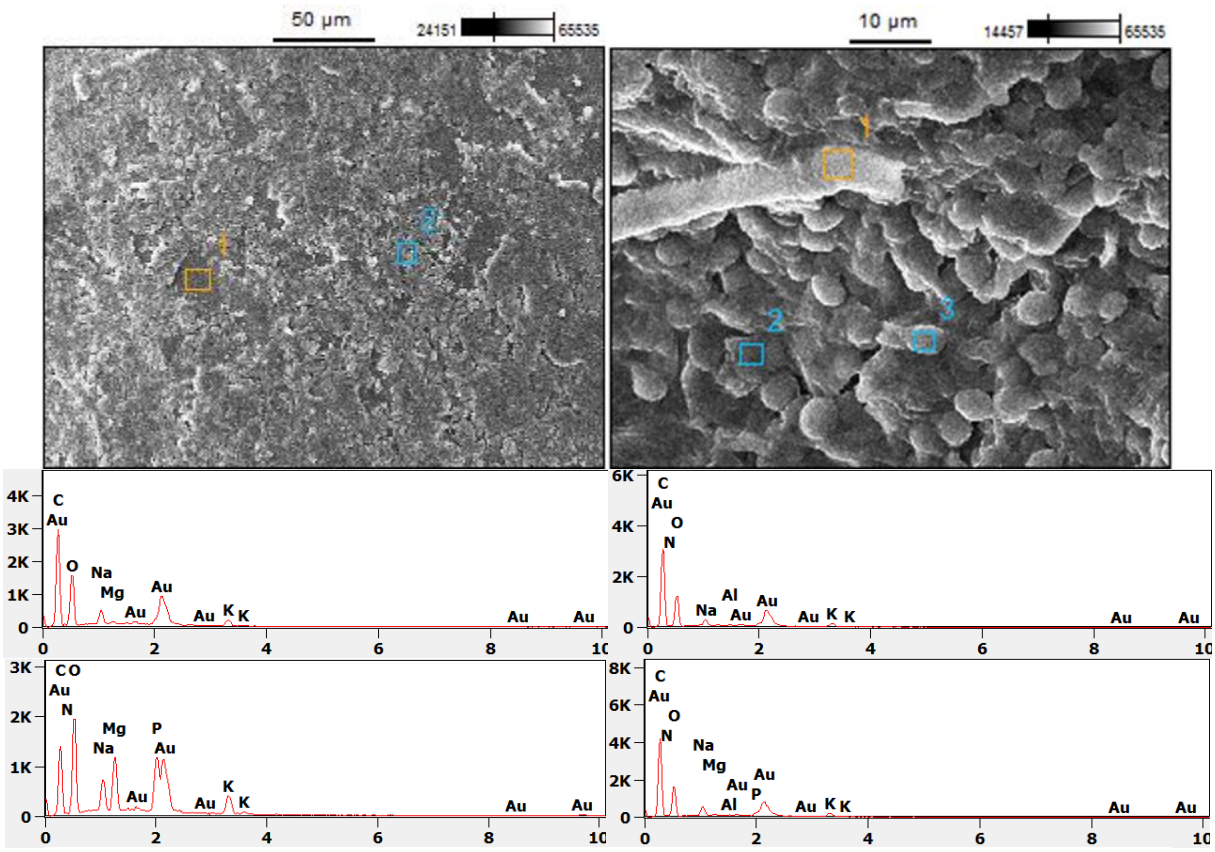

Net Counts

	C-K	N-K	O-K	Na-K	Mg-K	P-K	K-K
218689 2(1)_pt1	16662		9495	2850	427		2070
218689 2(1)_pt2	8269	346	11446	4777	7999	10659	4236

Weight %

	C-K	N-K	O-K	Na-K	Mg-K	P-K	K-K
218689 2(1)_pt1	36.81		51.59	6.32	0.77		4.51
218689 2(1)_pt2	23.80	3.08	42.35	6.24	8.73	9.73	6.06

Net Counts

	C-K	N-K	O-K	Na-K	Mg-K	Al-K	P-K	K-K
218689 2(2)_pt1	18035	615	7505	1571		191		1306
218689 2(2)_pt2	24000	857	9571	3366	414	122	1600	2010
218689 2(2)_pt3	30281	1083	12463	3683		280	1876	2254

Weight %

	C-K	N-K	O-K	Na-K	Mg-K	Al-K	P-K	K-K
218689 2(2)_pt1	36.49	8.34	48.37	3.59		0.29		2.91
218689 2(2)_pt2	37.57	8.38	43.79	5.05	0.50	0.13	1.53	3.05
218689 2(2)_pt3	37.30	8.38	45.37	4.51		0.23	1.45	2.76

Figure B2: Energy-dispersive X-ray results for pretreated original DDGS

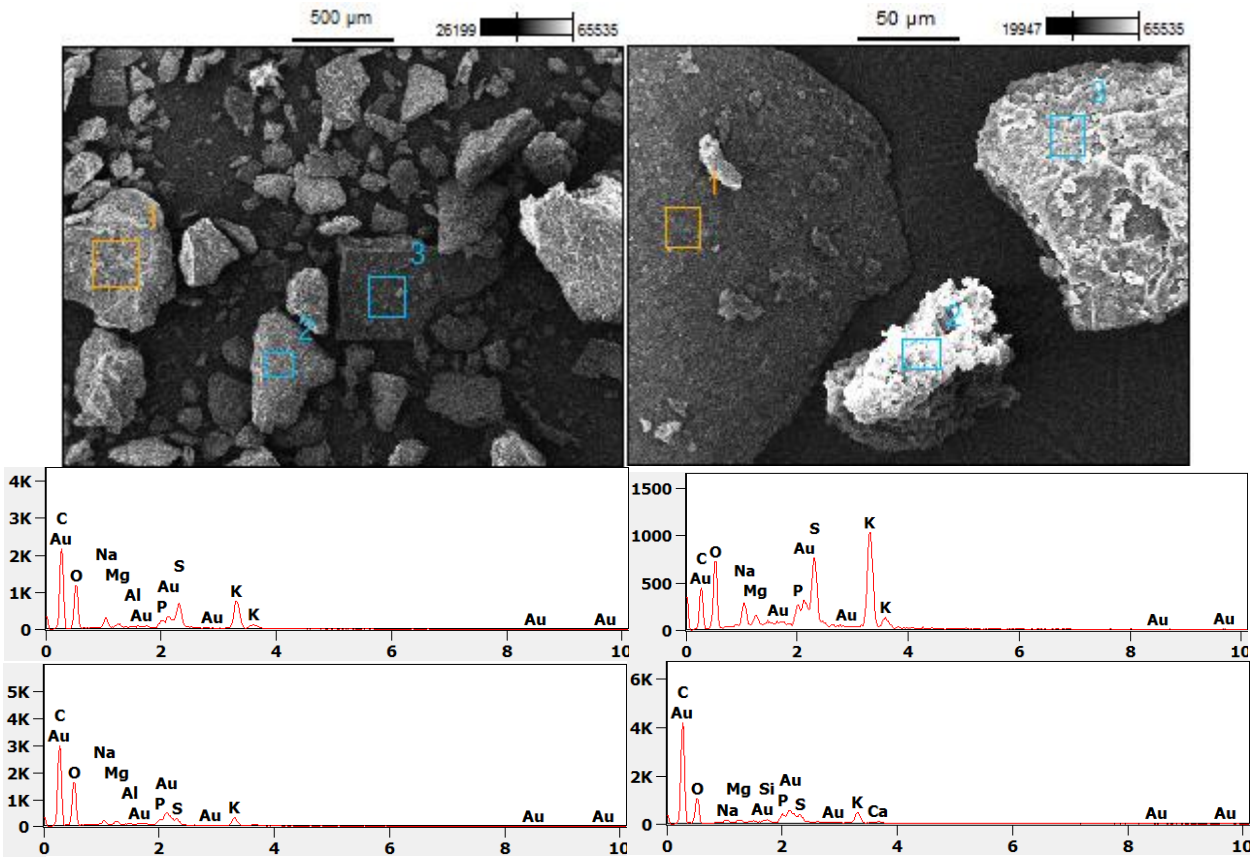

Net Counts

	C-K	O-K	Na-K	Mg-K	Al-K	P-K	S-K	K-K
218690 3(1)_pt1	12652	6928	1614	671	179	1975	7361	8588
218690 3(1)_pt2	17167	9589	956	855	375	1914	2845	3229
218690 3(1)_pt3	12351	8443	455	382				1415

Weight %

	C-K	O-K	Na-K	Mg-K	Al-K	P-K	S-K	K-K
218690 3(1)_pt1	33.77	38.80	2.58	0.84	0.19	1.98	7.62	14.20
218690 3(1)_pt2	38.51	47.31	1.67	1.15	0.44	2.08	3.19	5.66
218690 3(1)_pt3	34.37	58.96	1.47	0.93				4.27

Net Counts

	C-K	O-K	Na-K	Mg-K	Si-K	P-K	S-K	K-K	Ca-K
218690 3(2)_pt1	2544	4246	1847	782		2274	8509	11575	
218690 3(2)_pt2	23225	6125	687	615	688	3024	3497	4571	740
218690 3(2)_pt3	27273	14620	598	1455		2006		2418	

Weight %

	C-K	O-K	Na-K	Mg-K	Si-K	P-K	S-K	K-K	Ca-K
218690 3(2)_pt1	13.52	36.70	4.29	1.45		3.30	12.79	27.96	
218690 3(2)_pt2	47.53	34.71	1.04	0.72	0.70	2.97	3.58	7.36	1.38
218690 3(2)_pt3	39.22	52.96	0.88	1.63		1.82		3.49	

Figure B3: Energy-dispersive X-ray results for aspirated lighter fraction of number 20 sieved DDGS

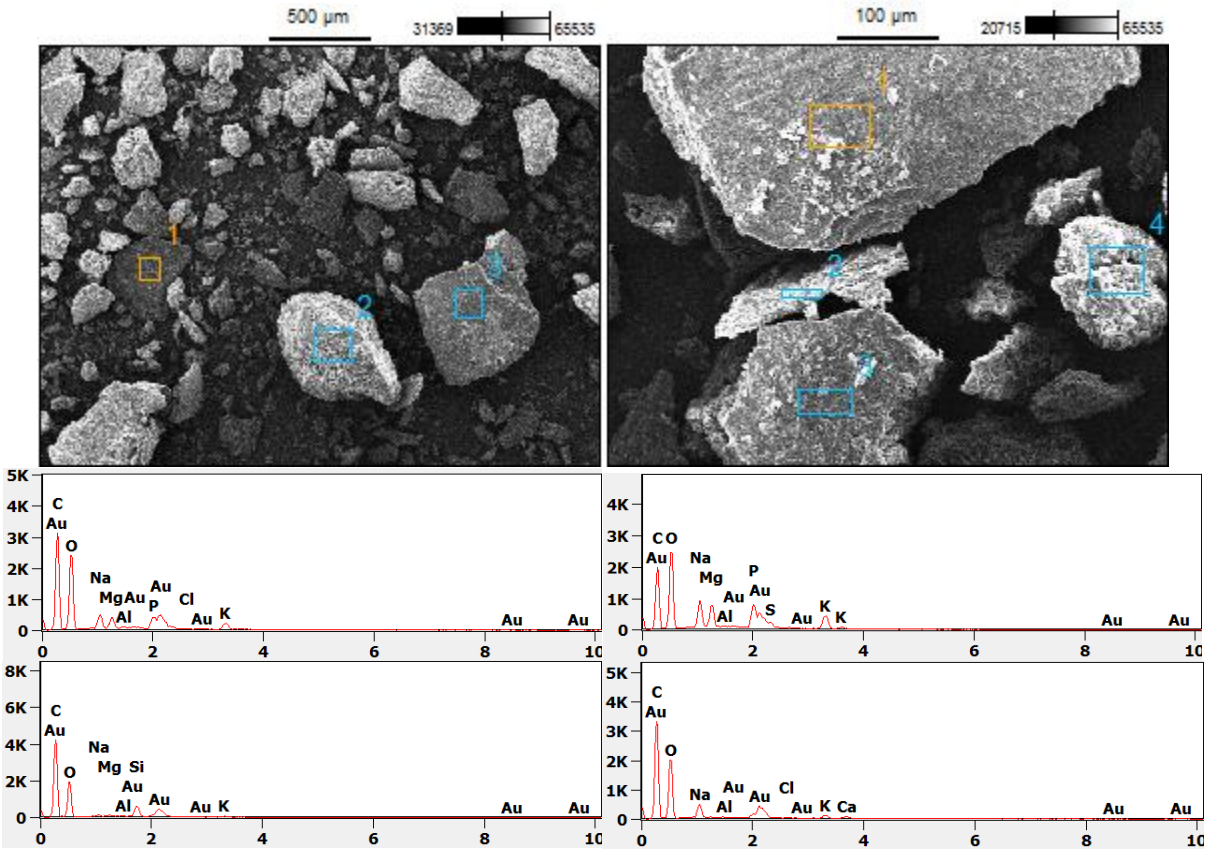

Net Counts

	C-K	O-K	Na-K	Mg-K	Al-K	Si-K	P-K	Cl-K	K-K
218691 4(1)_pt1	16896	14375	3211	2545	160		2763	263	2476
218691 4(1)_pt2	24083	10575	519	334	158	5354			557
218691 4(1)_pt3	19402	16167	3725	286				279	1089

Weight %

	C-K	O-K	Na-K	Mg-K	Al-K	Si-K	P-K	Cl-K	K-K
218691 4(1)_pt1	33.01	51.92	4.89	3.13	0.17		2.72	0.33	3.83
218691 4(1)_pt2	45.02	46.96	0.84	0.41	0.17	5.67			0.92
218691 4(1)_pt3	33.59	57.44	6.38	0.40				0.37	1.82

Net Counts

	C-K	N-K	O-K	Na-K	Mg-K	Al-K	P-K	S-K	Cl-K	K-K	Ca-K
218691 4(2)_pt1	11079		14445	5663	5108	150	7234	2434		4906	
218691 4(2)_pt2	18877		11935	3084		215			264	1147	797
218691 4(2)_pt3	29240	1024	9336	473	510	317				436	
218691 4(2)_pt4	13623	428	7087	663	1704	223	3232	1948	226	2862	

Weight %

	C-K	N-K	O-K	Na-K	Mg-K	Al-K	P-K	S-K	Cl-K	K-K	Ca-K
218691 4(2)_pt1	26.28		46.53	7.02	5.31	0.14	6.07	2.14		6.51	
218691 4(2)_pt2	35.89		53.66	5.91		0.28			0.40	2.15	1.71
218691 4(2)_pt3	40.44	10.35	46.69	0.80	0.65	0.35				0.72	
218691 4(2)_pt4	35.86	5.87	42.18	1.24	2.45	0.28	3.84	2.41	0.35	5.51	

Figure B4: Energy-dispersive X-ray results for pretreated aspirated lighter fraction of number 20 sieved DDGS

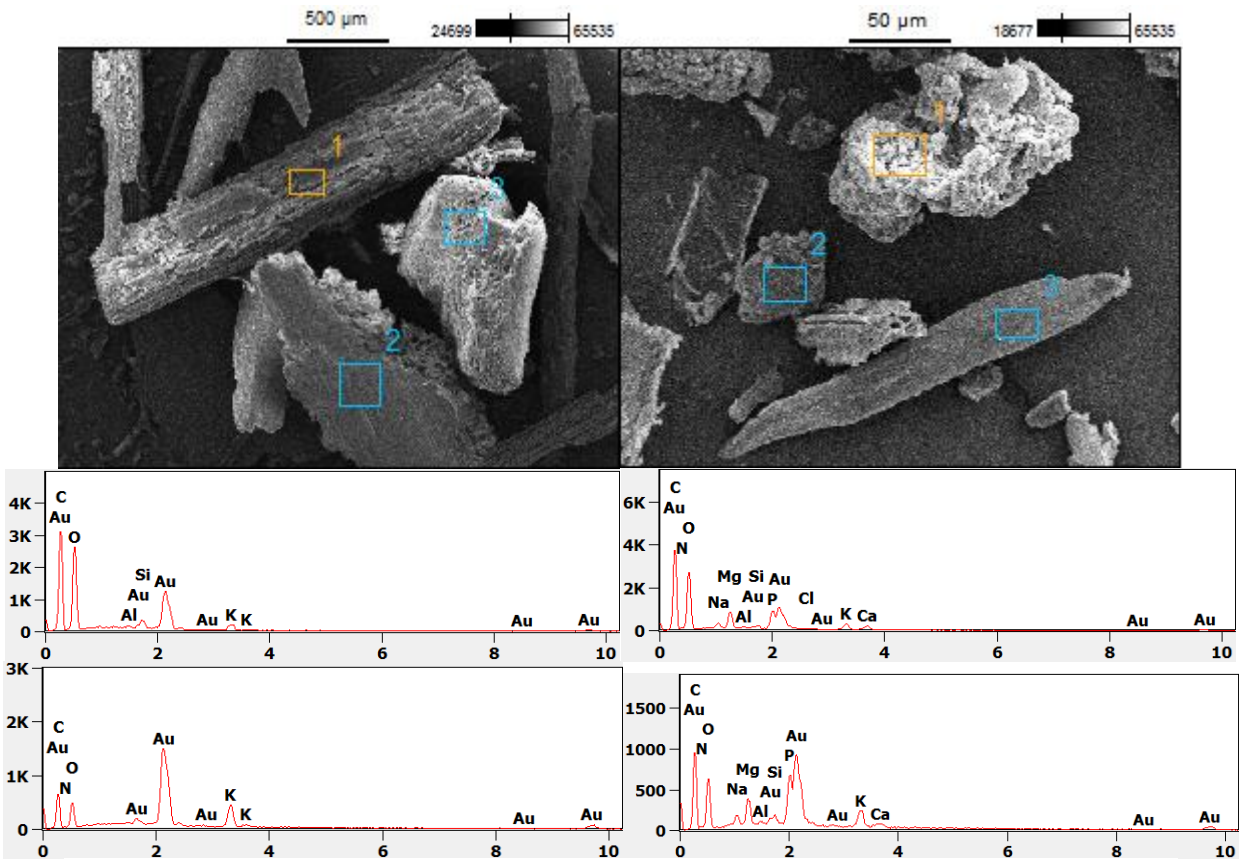

Net Counts

	C-K	N-K	O-K	Al-K	Si-K	K-K
218696-9(1)_pt1	17878		15546	471	2196	2111
218696-9(1)_pt2	3764	226	2590			4295
218696-9(1)_pt3	15819		12642	498	1232	774

Weight %

	C-K	N-K	O-K	Al-K	Si-K	K-K
218696-9(1)_pt1	32.37		60.89	0.55	2.52	3.67
218696-9(1)_pt2	18.20	8.99	49.73			23.08
218696-9(1)_pt3	34.66		61.12	0.74	1.78	1.69

Net Counts

	C-K	N-K	O-K	Na-K	Mg-K	Al-K	Si-K	P-K	Cl-K	K-K	Ca-K
218696-9(2)_pt1	20240	631	15733	1604	5600	331	1092	6274	218	2987	1924
218696-9(2)_pt2	5305	206	3689	872	2577	158	797	4606		2366	510
218696-9(2)_pt3	2464		1727			281	1211			686	

Weight %

	C-K	N-K	O-K	Na-K	Mg-K	Al-K	Si-K	P-K	Cl-K	K-K	Ca-K
218696-9(2)_pt1	30.79	4.40	47.33	1.72	4.64	0.25	0.78	4.31	0.19	3.21	2.37
218696-9(2)_pt2	29.93	4.81	36.77	2.51	5.88	0.33	1.61	9.01		7.32	1.82
218696-9(2)_pt3	34.66		48.50			1.85	7.97			7.01	

Figure B5: Energy-dispersive X-ray results for wheat straw

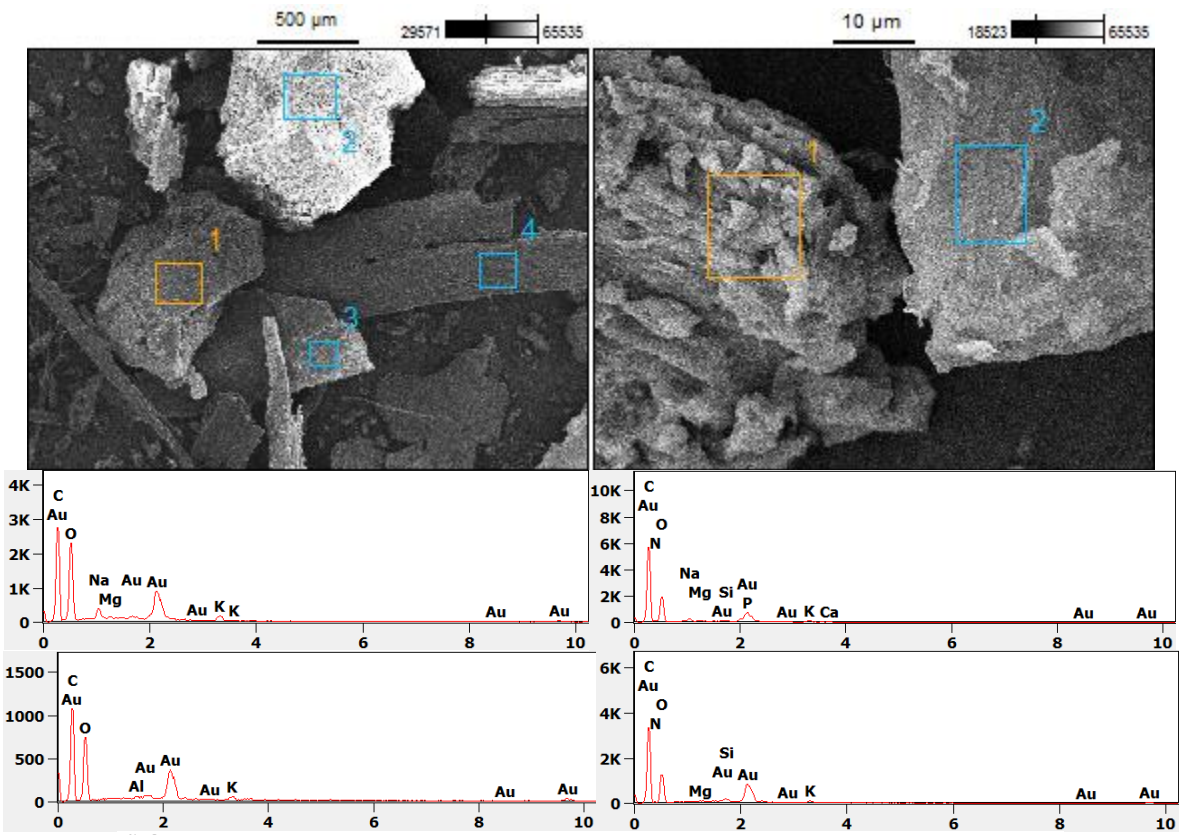

Net Counts

	C-K	O-K	Na-K	Mg-K	Al-K	Si-K	K-K
2186967-10(1)_pt1	15970	13435	2064	194			1590
2186967-10(1)_pt2	6436	4529			201		394
2186967-10(1)_pt3	9757	8709	442	262		7244	838
2186967-10(1)_pt4	2627	2601		176	267	7391	638

Weight %

	C-K	O-K	Na-K	Mg-K	Al-K	Si-K	K-K
2186967-10(1)_pt1	32.31	59.66	4.48	0.33			3.23
2186967-10(1)_pt2	35.25	61.53			0.83		2.39
2186967-10(1)_pt3	35.03	50.64	1.03	0.47		10.86	1.98
2186967-10(1)_pt4	32.77	38.56		0.64	0.85	23.78	3.40

Net Counts

	C-K	N-K	O-K	Na-K	Mg-K	Si-K	P-K	K-K	Ca-K
2186967-10(2)_pt1	32854	1249	11821	1298	451	849	1709	1232	224
2186967-10(2)_pt2	18968	593	8225		314	1022		725	

Weight %

	C-K	N-K	O-K	Na-K	Mg-K	Si-K	P-K	K-K	Ca-K
2186967-10(2)_pt1	39.05	9.84	45.25	1.62	0.43	0.68	1.32	1.51	0.31
2186967-10(2)_pt2	37.70	7.83	50.92		0.53	1.45		1.57	

Figure B6: Energy-dispersive X-ray results for mixture of wheat straw and DDGS

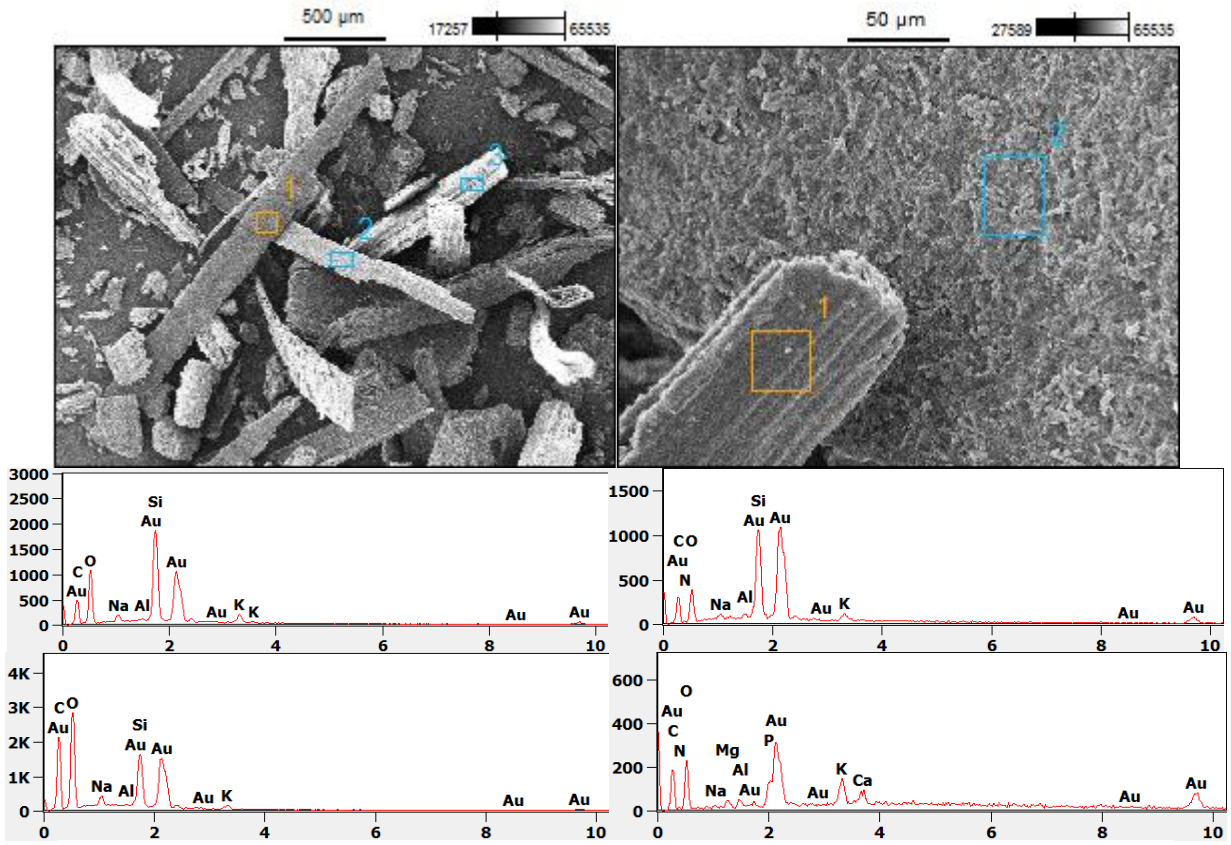

Net Counts

	C-K	O-K	Na-K	Mg-K	Al-K	Si-K	K-K
218694 7(1)_pt1	2738	5935	986		229	16211	1549
218694 7(1)_pt2	12214	16974	1807		352	13771	1084
218694 7(1)_pt3	9317	6792	1475	236		2336	1205

Weight %

	C-K	O-K	Na-K	Mg-K	Al-K	Si-K	K-K
218694 7(1)_pt1	21.69	42.48	2.53		0.40	28.39	4.49
218694 7(1)_pt2	29.46	53.70	2.53		0.33	12.45	1.53
218694 7(1)_pt3	35.34	51.25	4.51	0.58		4.67	3.65

Net Counts

	C-K	N-K	O-K	Na-K	Mg-K	Al-K	Si-K	P-K	K-K	Ca-K
218694 7(2)_pt1	1729	164	2187	278		347	9265		856	
218694 7(2)_pt2	1142	58	1169	65	277	326		1102	1311	520

Weight %

	C-K	N-K	O-K	Na-K	Mg-K	Al-K	Si-K	P-K	K-K	Ca-K
218694 7(2)_pt1	24.47	5.83	34.15	1.25		1.07	28.79		4.45	
218694 7(2)_pt2	19.21	4.82	43.13	0.72	2.28	2.34		7.34	13.70	6.46

Figure B7: Energy-dispersive X-ray results for pretreated mixture of wheat straw and DDGS

APPENDIX C. SAS CODE FOR INTERNAL BOND STRENGTH OF PARTICLEBOARDS WITH PRETREATED SAMPLES

```
options pageno=1;
data RCBDSAMP;
INPUT Treatment $ Rep      SampleIB_Test;
datalines;
25%DDGS    1       1       0.0425
25%DDGS    1       2       0.0437
25%DDGS    2       1       0.0235
25%DDGS    2       2       0.0201
25%DDGS    3       1       0.0123
25%DDGS    3       2       0.0251
50%DDGS    1       1       0.0110
50%DDGS    1       2       0.0128
50%DDGS    2       1       0.0143
50%DDGS    2       2       0.0267
50%DDGS    3       1       0.0141
50%DDGS    3       2       0.0124
75%DDGS    1       1       0.0635
75%DDGS    1       2       0.0701
75%DDGS    2       1       0.0350
75%DDGS    2       2       0.0381
75%DDGS    3       1       0.0147
75%DDGS    3       2       0.0412
Cn-Wood    1       1       0.1018
Cn-Wood    1       2       0.1432
Cn-Wood    2       1       0.1853
Cn-Wood    2       2       0.1524
Cn-Wood    3       1       0.1907
Cn-Wood    3       2       0.1739
Cn-WhSt    1       1       0.0539
Cn-WhSt    1       2       0.0307
Cn-WhSt    2       1       0.0374
Cn-WhSt    2       2       0.0356
Cn-WhSt    3       1       0.0407
Cn-WhSt    3       2       0.0508
;;
proc print;
title 'Internal Bond Strength test';
run;
proc anova;
classes REP SAMPLE TREATMENT;
model IB_Test=rep TREATMENT REP*TREATMENT;
TEST H=REP TREATMENT E=REP*TREATMENT;
```

```
means TREATMENT/lsd E=REP*TREATMENT;
title 'Internal Bond Strength Of Particleboards';
run;
```

APPENDIX D. SAS CODE FOR LINEAR EXPANSION OF PARTICLEBOARDS WITH PRETREATED SAMPLES

```
options pageno=1;
data RCBD;
INPUT Treatment $ Rep       LE;
datalines;
25%DDGS     1       0.552
25%DDGS     2       0.565
25%DDGS     3       0.481
50%DDGS     1       0.494
50%DDGS     2       0.584
50%DDGS     3       0.519
75%DDGS     1       0.480
75%DDGS     2       0.786
75%DDGS     3       0.338
old50%D     1       0.539
old50%D     2       0.461
old50%D     3       0.689
Cn-Wood     1       0.435
Cn-Wood     2       0.383
Cn-Wood     3       0.377
Cn-WhSt     1       0.338
Cn-WhSt     2       0.422
Cn-WhSt     3       0.318
;;
proc print;
title 'Linear Expansion (%)';
run;
proc anova;
classes rep Treatment;
model LE=rep Treatment;
means Treatment/lsd;
title 'Linear Expansion (%)';
run;
```

APPENDIX E. SAS CODE FOR MODULUS OF ELASTICITY OF PARTICLEBOARDS WITH PRETREATED SAMPLES

```
options pageno=1;
data RCBD;
INPUT Treatment $ Rep       MOE;
datalines;
25%DDGS     1       269.28
25%DDGS     2       253.76
25%DDGS     3       284.80
50%DDGS     1       16.80
50%DDGS     2       20.92
50%DDGS     3       12.68
75%DDGS     1       98.36
75%DDGS     2       134.25
75%DDGS     3       326.1
Cn-Wood     1       271.59
Cn-Wood     2       426.34
Cn-Wood     3       251.47
Cn-WhSt     1       534.58
Cn-WhSt     2       612.63
Cn-WhSt     3       781.89
;;
proc print;
title 'Modulus of Elasticity (MPa)';
run;
proc anova;
classes rep Treatment;
model MOE=rep Treatment;
means Treatment/lsd;
title 'Modulus of Elasticity (MPa)';
run;
```